GEORGIA INSTITUTE OF TECHNOLOGY
OFFICE OF CONTRACT ADMINISTRATION
SPONSORED PROJECT INITIATION

Date: March 11, 1980

Project Title: Interaction of Energetic Hydrogen with Surfaces

Project No: G-41-603

Project Director: Dr. E. W. Thomas

Sponsor: Union Carbide Corporation; Nuclear Division; Oak Ridge, Tennessee 37830

Agreement Period: From March 1, 1980 Until ~~February~~ 28, 1981 ~~9/30~~ 9/30/81

Type Agreement: Project Authorization No. X05 under Basic Agreement No. 7802 (under DOE Prime No. W-7405-eng-26)

Amount: $51,960 (UCC-ND)
12,990 (GIT: G-41-335)
$64,950 TOTAL

Reports Required: Final Report

Sponsor Contact Person (s):

Technical Matters

Mr. R. A. Langley / J. B. Roberto
Fusion Energy Division
Union Carbide Corporation
Nuclear Division
P. O. Box X
Oak Ridge, Tennessee 37830

Contractual Matters
(thru OCA)

Mr. W. R. Osborn, Contract Administra
Purchasing Division
Union Carbide Corporation
Nuclear Division
P. O. Box X
Oak Ridge, Tennessee 37830

Defense Priority Rating: None

Assigned to: Physics (School/Laboratory)

COPIES TO:

- Project Director
- Division Chief (EES)
- School/Laboratory Director
- Dean/Director—EES
- Accounting Office
- Procurement Office
- Security Coordinator (OCA)
- Reports Coordinator (OCA)
- Library, Technical Reports Section
- EES Information Office
- EES Reports & Procedures
- Project File (OCA)
- Project Code (GTRI)
- Other C. E. Smith

GEORGIA INSTITUTE OF TECHNOLOGY OFFICE OF CONTRACT ADMINISTRATION

SPONSORED PROJECT TERMINATION SHEET

Date 8/16/83

Project Title: Interaction of Energetic Hydrogen with Surfaces

Project No: G-41-603 (continued by G-41-627)

Project Director: Dr. E. W. Thomas

Sponsor: Union Carbide Corp., Nuclear Div., Oak Ridge, TN (DOE Prime)

Effective Termination Date: 9/30/81

Clearance of Accounting Charges: N/A (Permission received to carry balance over to continuing project G-41-627)

Grant/Contract Closeout Actions Remaining:

None - Contract continued under project G-41-627

- ☐ Final Invoice and Closing Documents
- ☐ Final Fiscal Report
- ☐ Final Report of Inventions
- ☐ Govt. Property Inventory & Related Certificate
- ☐ Classified Material Certificate
- ☐ Other _____

Assigned to: Physics (School/laboratory)

COPIES TO:

Administrative Coordinator	Research Security Services	EES Public Relations (2)
Research Property Management	Reports Coordinator (OCA)	Computer Input
Accounting	Legal Services (OCA)	Project File
Procurement/EES Supply Services	Library	Other Thomas

FORM OCA 10:781

GEORGIA TECH RESEARCH INSTITUTE
ADMINISTRATION BUILDING
GEORGIA INSTITUTE OF TECHNOLOGY
ATLANTA, GEORGIA 30332

Telex: 542507 GTRIOCAATL
Fax: (404) 894-3120

Phone: (404) 894-4814

7 August 1981

Union Carbide Corporation
Nuclear Division
P.O. Box M
Oak Ridge, Tennessee 37830

Attention: Mr. W. R. Osborne
Purchasing Division

Subject: Continuation of Research Under
Project Authorization No. X05
Basic Agreement 7802 entitled,
"Interaction of Energetic Hydrogen
with Surfaces"

Gentlemen:

The GEORGIA TECH RESEARCH INSTITUTE desires to submit for your consideration the subject continuation proposal prepared by Dr. E. W. Thomas of the School of Physics, Georgia Institute of Technology. The attached proposal was prepared for the attention of Dr. R. A. Langley. We understand that Dr. Langley is out of the country at the present time and that Dr. J. B. Roberto of the Solid State Division is temporarily handling this matter.

The report on the work to date under the subject agreement has been prepared and is being forwarded separately, in accordance with the provision of the contract, to Laboratory Records Department (ORNL).

Any questions regarding the technical content of this proposal should be addressed to Dr. Thomas 404/894-5215, while information of a business or contractual nature may be directed to the undersigned, 404/894-4814. In this connection, we assume that any award resulting from this proposal will take the form of a project authorization under existing Basic Agreement 7802.

We look forward to continuing work with you on this project.

Cordially,

Carol A. Cook
GEORGIA TECH RESEARCH INSTITUTE

CAC/jme

Addressee: In triplicate
Enclosure: Proposal - in triplicate

INTERACTION OF ENERGETIC HYDROGEN WITH SURFACES

Proposal for an R & D Subcontract

Interaction of Energetic Hydrogen with Surfaces

Submitted to the

Union Carbide Corporation

Nuclear Division

to follow

Project Authorization No. X05

Under Basic Ordering Agreement 7802

(Under DOE Prime No. W-7405-eng-26)

August 1, 1981

Georgia Institute of Technology

Atlanta, Georgia 30332

Contents

F. Technical Progress

(a) Progress to Date (period 10/1/80 to 9/30/81)

A study of recycling in ISX-B was performed by monitoring the relative amounts of H and D in the plasma edge as the machine was changed from operation with H_2 and later from H_2 back to D_2. The experimental technique was to monitor the intensities of the Balmer alpha lines of H and of D. While close in wavelength these lines may be resolved by use of a Fabry Perot interferometer. By repetitive scanning of the Fabry Perot one can monitor the ratio of H and D line intensities at a number of times during any particular Tokamak discharge. The whole technique was originally developed by McCracken et al.[1], and used first for similar studies on DITE. Following McCracken[1] one argues that the hydrogen emission arises as hydrogen emerging from the wall enters the plasma edge and is excited by electron impact. The ratio of H and D line intensities gives the ratio of H and D fluxes emerging from the wall. In the first shot using H_2, after operation on D_2, the residual D signal indicates the quantity of hydrogen in the discharge that arises from the walls. After repetitive operation on H_2 the D signal should eventually disappear. The reverse holds true as one goes from H_2 operation to D_2. Our observations implied that 60% of the hydrogen in the plasma edge comes from the wall and not from the filling gas. Moreover, isotopic changeover was largely complete in four shots. The work was carried out in a high density plasma with no neutral beam heating. These results are largely consistent with experience

---

1. G. M. McCracken et al., Nuclear Fusion 18, 35 (1978).

on TFR[2] and on Alcator[3] and can be roughly modelled using well established laboratory data on trapping and re-emission.[4] Suprisingly, other experiments[5] performed simultaneously in ISX-B suggest that only 20% of the hydrogen comes from the wall implying that almost complete isotopic changeover occurs in the first discharge in the new gas. This apparent discrepancy may be related to the different viewing positions employed by the experiments and on the face of it implies a poloidal asymmetry in recycling. The matter remains under investigation.

By placing a number of H_α detectors (detecting Balmer alpha emissions from H atoms) at various positions around the torus we plan to study the toroidal asymmetry of hydrogen density in the plasma edge which in turn is related to asymmetries in recycling rate. As an initial step two detectors have been placed on ISX-B and certain preliminary data obtained. The hydrogen density does not appear to differ significantly from one toroidal position to another except at the limiter where H densities are a factor of 20 higher than elsewhere. At all positions the H density rises rapidly to a plateau which is maintained till the injectors are fired. Then the density increases by a factor of ten and remains high until the discharge terminates. Disruptions cause immediate changes to the hydrogen signal. Further studies are necessary using a greater number of detectors; progress in equipment fabrications is well in hand.

We have undertaken design and fabrication of a rotating collector probe

---

2. P. Platz, J. Nucl. Mater. 93 and 94, 173 (1980).

3. E. S. Marmar, J. Nucl. Mater. 76 and 77, 59 (1978).

4. E. W. Thomas, J. Appl. Phys. 51, 1176 (1980).

5. J. B. Roberto et al., to be published.

to be attached to the ISX sample transport system. This cylindrical probe, rotating behind a slit, is exposed to the plasma and receives impacting atoms and ions. The probe may be removed for analysis of the density and nature of the deposited material. This is a well established technique used previously on ISX-A, by this author on DITE[6], and on almost all other present Tokamaks. Analysis of the deposited material allows a measure of the time dependence of impurity and fuel flux to the probe at the limiter radius and at points in the limiter shadow. Novel provisions will be made to permit assessment of the arriving particles energy. When using a small aperture for exposure the lateral spread of deposit density beyond the aperture shadow is related to gyromagnetic radius and hence to velocity. Furthermore, by applying electric fields between probe and sampling aperture one can perform a crude energy separation. This equipment is now constructed and will shortly be assembled at ISX-B.

We have developed equipment to study re-emission of hydrogen from surfaces following the general lines of work performed previously by one of us.[4] A novel feature is that we can study not only re-emission from the bombarded surface of a target but also from the back side of thin film targets. This permits study of permeation by implanted hydrogen, a matter where theory and preliminary experiments are in disagreement.[7] Of particular interest to us is the basic understanding of the process whereby hydrogen recombines on a surface prior to re-emission as a molecule. Direct measurements of this will be performed in association with Emmoth and Braun in Stockholm.

---

6. E. W. Thomas, J. Partridge and J. Vince, J. Nucl. Mater. 89, 182 (1980).

7. H. K. Perkins and T. Noda, J. Nucl. Mater 71, 349 (1978).

We have completed, terminated and published[8] a brief study of oxygen desorption from Fe and Ti by impact of hydrogen ions. Desorption by H^+ appears to be a simple sputtering effect exhibiting cross sections of the order 10^{-18} cm^2 at energies from 20 to 200 keV. However, for H_2^+ and H_3^+ impact cross sections show sharp rises of one order of magnitude or more at 40 Kev/amu for H_2^+ (and H_3^+) on Fe + 0 and at 75 Kev/amu for H_2^+ (and H_3^+) on Ti + 0. These rises have been identified as due to inner shell excitations caused by the electrons stripped from the projectile and are consistent with mechanisms described by Knotek and Feibelman for electron induced desorption.

Within this reporting period we have also completed, terminated and published[9] the results of an extended program to study backscattering of hydrogen from polycrystalline copper, carbon, stainless steel, and other metals. The data includes charge state ratios, energy distributions and angular distributions. In general terms the data on backscattered flux agrees with computer simulations by the TRIM and MARLOWE codes.

(b) Proposed Work (period 10/1/81 to 9/30/82)

Facilities for study of toroidal asymmetry in the ISX-B Tokamak will be completed by providing a total of six H_α detectors located one each close to the limiters and injector port plus four others at non specific positions. The signals received represent the local density of neutral hydrogen at the plasma edge in the region viewed. It is anticipated that hydrogen density at the limiter will be one order of magnitude greater than that elsewhere due to the greater number of particle surface interactions. We shall attempt

---

8. K. O. Legg, R. S. Whaley and E. W. Thomas, Surface Sci. (to be published).
9. J. E. Harriss, R. P. Young and E. W. Thomas, J. Nucl. Mater. 93, 524 (1980).

to understand the toroidal asymmetries using model values of particle flux and known laboratory data on re-emission. Also the time development of density must be understood particularly the ten fold rise in limiter signal on neutral beam injection, but negligible rise elsewhere. The general result of this procedure should be availability of a continuous monitor of gas recycling to compare with other parameters, and with models of the device. We propose specifically to monitor density changes as the machine is re-started after shutdown to study how hydrogen builds back up in the walls.

With the H_α detectors we plan also a limited study of poloidal asymmetries in the hydrogen density. There are indications of differences in recycling studied at the mid plane compared with studies in a vertical direction (parallel to the major axis). This at first sight seems unreasonable and requires exploration.

The rotating probe collector system will be assembled onto the sample transport system and used to follow time development of impurities. Of particular interest will be the initial operation after the shutdown period where we would anticipate a high impurity level due to arcing and desorption that will decrease as the machine is conditioned. Energies of impurities in the plasma edge will be measured for the first time. The anticipated reduction of impurities due to divertor operation will be studied. A very desireable experiment will be a study of impurity lifetime by injecting a pulse of impurities (in the form of a short gas puff or by laser ablation of a metal film) and determining the time it takes to disappear from the collector probe. In analyzing such probes it is assumed only that material deposits on the probe; the possibility of probe erosion is neglected. We propose to expose probes with a depth marker or thin (few monolayer) coating that on subsequent analysis should disclose any significant erosion.

Laboratory experiments to monitor hydrogen re-emission and permeation will be continued. A significant experiment is to implant hydrogen to the center of a thin sample and monitor hydrogen re-emission from both front and back surfaces. In principle behavior should be the same and should be predictable. In practice radiation damage at the front surface may cause enhanced re-emission on the bombarded face. Re-emission will be studied for stainless steel and carbon, as a function of temperature, including regimes where chemical sputtering is anticipated. Direct measurements of surface recombination will be performed by monitoring gas re-emission (essentially by pressure rise) and deuterium density in the surface (by a nuclear reaction technique). The two parameters are related by the recombination coefficient. Again this will be attempted for carbon at temperatures where chemical sputtering is anticipated.

The above plans are in certain measure tentative and subject to changes dictated by the ISX-B operating schedule. Our objective is to accept responsibility for providing certain diagnostic capabilities and then to use these in concert with other diagnostic facilities to pursue the major experimental thrusts on ISX-B.

G. Future Accomplishments (period 10/1/82 to 9/30/83)

Continuing routine studies of hydrogen density and impurity fluxes will be performed. We would anticipate improving the turn-around time of the sample transport system so that a preliminary analysis of impurity flux can be made within five to ten minutes of exposure. This will permit the surface scientist to provide real-time instructions for controlling the Tokamak and minimizing impurities.

H. Relationship to Other Projects

The proposed work is justified entirely by its contribution to the

Impurity Study Program at ORNL. Most of the completed and continuing projects were identified first by personnel at ORNL and undertaken after detailed discussions between ORNL staff and the principal investigator of this program.

The probe collector system for impurity analysis is an integral part of the sample transfer and surface analysis station that has evolved as a major component of ISX-B. Such probe collectors are to be found on almost all contemporary Tokomaks and are a standard diagnostic tool. Data from these various machines may be compared without ambiguity.

The H_α detector system has been shown of value on Macrotor but appears not to have been used elsewhere. The detection systems are sufficiently simple that they could be applied to any other machines, if needed, with minimal mechanical or electrical preparations.

The Principal Investigator is undertaking significant activity in the matter of data assessment, collection and publication. He attended a workshop on "Data for Modelling Plasma-Wall Interactions" held at IAEA Vienna that is designed to produce a standard set of data for modelling use. Also he is organizing a workshop under the US-Japan Personnel Exchange Program to be held in December in Nagoya. This "Surface Data Review Workshop" will be concerned with the continuing processing of published data and assessments of algebraic representations for use in modelling codes.

E. W. Thomas will spend some months at the "Atomic Physics Institute" (A.F.I.) in Stockholm performing studies of surface recombination and hydrogen permeation. While in Stockholm he will also contribute to designs of rotating probe collectors for use in TEXTOR. While Dr. Thomas is away we will have working on the Ga. Tech program Dr. Birger Emmoth who works on the Euratom Fusion program in Stockholm. It should be clearly noted that this personnel

exchange is a matter entirely between Ga. Tech and AFI involving no financial support at all from the funds of this subcontract. However, these temporary moves are clearly designed to benefit the progress of work in this subcontract.

PROGRESS REPORT NO. 1

ORNL/Sub–7802/X05/1

INTERACTION OF ENERGETIC HYDROGEN WITH SURFACES

By

E. W. Thomas
K. O. Legg
W. A. Metz
R. P. Young

Prepared for

OAK RIDGE NATIONAL LABORATORY
OAK RIDGE, TENNESSEE 37830

Operated by

UNION CARBIDE CORPORATION

For the

DEPARTMENT OF ENERGY

Contract No. W–7405–eng–26
Sub Contract No.–7802

1 November 1980

GEORGIA INSTITUTE OF TECHNOLOGY
SCHOOL OF PHYSICS
ATLANTA, GEORGIA 30332

1980

INTERACTION OF ENERGETIC HYDROGEN WITH SURFACES

PROGRESS REPORT NO. 1

Covering the Period

November 1, 1979 to November 1, 1980

by

E. W. Thomas

K. O. Legg

W. A. Metz

R. P. Young

Report prepared by:

The Georgia Institute of Technology

School of Physics

Atlanta, Georgia 30332

Under subcontract number 7802 for

Oak Ridge National Laboratory

Oak Ridge, Tennessee 37830

operated by

Union Carbide Corporation

for the

Department of Energy

Contract No. W-7405-eng-26

1 November 1980

TABLE OF CONTENTS.

I. Title

Interaction of Energetic Hydrogen with Surfaces.

II. Contract Number

This report covers work performed on particle-surface interactions under a contract between Union Carbide Corp with the Georgia Tech Research Institute. The work is covered by Project Authorization No. X05 under Basic Ordering Agreement No. 7802 (under DOE Prime No. W-7405-eng-26).

The work is an extension of studies performed earlier under contract AT-(40-1)-2591 for the U.S. Department of Energy. This direct contract was terminated on 29 February 1980 and superseded on 1 March 1980 by the contract with Union Carbide.

This report covers the period 1 November 1979 to 1 November 1980 the last four months of the DOE contract and the first eight months of the Union Carbide Contract.

III. Abstract

The program studies particle-surface collision phenomena relevant to plasma-wall interactions in Tokamak devices. A study of hydrogen recycling in ISX-B discloses that some 50% of the hydrogen present during the stable part of the discharge has come from the walls and is the result of earlier operation. In changing from a D_2 to an H_2 filling gas it takes some three shots before the discharge is entirely in the new gas. We have shown that sputtering of adsorbed gases by 20-100 keV H^+ has a cross section of the order 10^{-18} cm^2; entirely as expected. For H_2^+ and H_3^+ impact, however, the cross section for removal of O from Ti and Fe is three orders of magnitude higher at some energies; a feature which we ascribe to a quantum desorption mechanism. We describe also data on energy and charge state distribution in backscattering of 5-30 keV H^+, H_2^+, D^+ and D_2^+ from surfaces; we find the backscattered fluxes to be in good agreement with computations by the TRIM computer code.

IV. Discussion of Progress

A. Introduction

The topics from the proposed "Technical Program" of our previous proposal were as follows:

Project (a) Continuation of an existing project to measure sputtering of adsorbed C, O and CO from targets of Be, C, Fe, Cu and stainless steel by impact of H^+, D^+, He^+, Ne^+ and Ar^+. Projectile energies to be in the range 0.5 to 200 keV. Percentage of time devoted to study 25%; target date 29 February 1981.

Project (b) Study of implanted deuterium permeation through stainless steel foils Deuterium to be implanted at 20 keV. Measurement of diffusion and surface recombination coefficients. Percentage of time devoted to study 25%; target date 29 February 1981.

Project (c) Optical spectroscopy of the limiter shadow in ISX-B to correlate impurity line intensities with arcing, neutral beam injection, and other machine operating parameters. Measurement of hydrogen atom speed from Doppler broadened line shapes. Percentage of time devoted to study 25%; target date 29 February 1979.

Project (d) Study of C, Aℓ and stainless steel probes exposed to a Tokamak plasma to determine surface erosion as well as density and penetration depth of deposited material. Percentage of time devoted to study 25%, target date 29 February 1981.

Project (a) is on schedule and will be completed on time.

Project (b) required some equipment construction which is well under way. Preliminary measurements will be commenced befor the end of the contract period.

Project (c) was not fully implemented due to delays in purchasing equipment for our use by the ISX-B group. We did use a simplified system to perform an optical study of the recycling of hydrogen from the wall of ISX-B and that work is reported here. The necessary equipment for fully implementing this task should be delivered before the end of the present contract year but detailed studies must be delayed until the upcoming contract period.

Project (d) is not yet implemented due to a need for designing additional equipment for the ISX-B sample transfer system. The fabrication should be completed by 2/28/80 and experiments are being re-scheduled for the upcoming contract period.

In addition we have performed some basic studies of ion induced Auger spectra from surfaces and devoted a little time to completing a rather detailed study of backscattering of ions from surfaces.

A discussion follows of progress on these various tasks. The narrative of this report is limited to important highlights and relevance of the results to the Magnetic Fusion Energy Program; for details of results we shall refer to a series of Appendixes which largely represent articles destined for publication.

B. Plasma-Wall Diagnostic Experiments on ISX.

(1) H/D Changeover Experiment.

It is well known that a substantial fraction of the hydrogen taking part in any one Tokamak discharge comes from the walls where it has been adsorbed (or implanted) during previous shots. Knowledge of this fraction provides important information for a model of recycling. The amount of fuel retained in the wall is also relevant to questions of Tritium inventory in future machines. A relatively simple way of studying this factor is to perform a series of machine discharges starting first with a D_2 filling gas, then changing to H_2 and monitoring the ratio of D to H in the succeeding discharges by optical spectroscopy.

Clearly for the first discharge in H_2 the signal from H represents the contribution of fuel from the filling gas and the signal from D represents the contribution of fuel desorbed from the wall.

We have performed such an experiment on ISX-B, the details of which are recorded in Appendix i. The significant conclusions are as follows. Some 50 to 60% of the hydrogen participating in the steady part of the ISX-B discharge comes from the walls and is the result of earlier discharges. It takes about three shots to change completely from one isotope to the other. These results are consistent with experience on TFR and in qualitative terms can be explained with recourse to information on scattering, re-emission and trapping. The data are substantially different from work on DITE where changeover takes 15 to 20 shots.

(2) Erosion and Deposition on Probes Exposed to the Plasma.

Surface analysis of probes exposed to the plasma can reveal the flux of impurities to the wall (monitored by the density of deposited atoms) and the rate of erosion due to bombardment (monitored by the material removed from the probe). Based on past experience of DITE, ISX and PLT we believe that such studies are of value only when performed in a time resolved manner so that the effect of different regimes involving arcing, instability, injection and stable plasma can be separately explored. No adequate time resolved exposure facility exists on ISX and we have been designing such equipment to be added to the sample transfer system that is already in place. We propose to depart from the normal practice of spinning a disc or cylinder behind an aperture; this presents many difficulties if the collector is to be rapidly changed with reliable registration of rotary position. We are considering instead a stationary collector with a moving shutter. Designs have been laid out and are currently being detailed. If approved by the ISX team the required equipment will be fabricated at Georgia Tech.

(3) Analysis of Optical Spectra from the Plasma Edge.

We proposed to perform routine spectroscopy of the plasma edge using an Optical Multichannel Analyzer (OMA) which permits a record of a complete spectrum (as opposed to a conventional optical monochromator that records only emission at a single wavelength). In principle a complete spectrum may be recorded in 10m.sec permitting time resolved studies. There has been delay in implementing this facility due to a technical problem with available OMA's. While spectra can be recorded in 10 m sec the decay constant of the phosphors is sufficiently long that the OMA cannot be used for a succeeding spectrum without an excessive time delay for recovery. This technical problem has apparently now been overcome with new phosphors. An OMA has been aquired (by ORNL) for our use and recently delivered. Attachment to ISX is a trivial matter and we would anticipate performing preliminary studies within eight weeks

C. Sputtering of Adsorbates.

We have engaged in a study of the cross sections for sputter removal of adsorbed oxygen from metals by impact of hydrogen ions. Conventional sputtering theory suggests that the mechanism is simply transfer of kinematic energy to the adsorbate and that cross sections should be of the order $10^{-18} cm^2$. We performed experiments that show this to be generally the case. However for molecular ions (H_2^+ , H_3^+) incident at high energies (40 to 100 keV/amu) there are some cases where the cross section rises very rapidly to the remarkable value of 10^{-16} cms^2 (e.g. for removal of 0 from Fe by H_2^+ the threshold is about 50 keV/amu). We ascribe these high cross sections to onset of desorption by a quantum process. The threshold velocity is the same as that where electrons exhibit a threshold for desorption in the same system. For electrons the desorption mechanism is believed to involve excitation of an

inner shell electron in a metal substrate atom followed by Auger decay involving electrons of the adsorbed species; as a result the adsorbate loses two outer shell electrons placing it in a repulsive state so that it desorbs with some energy. We believe that when H_2^+ (or H_3^+) is incident on the surface, an electron is stripped from the projectile and then acts as a free electron with essentially the projectile (H_2^+ or H_3^+) velocity and causing desorption by the excitation process mentioned above.

This work is being prepared for publication and a preliminary draft of a paper is attached as Appendix ii. An implication for the fusion program is that while coefficients for light ion sputtering of bulk materials are of the order 10^{-3} there are some (very limited) circumstances where coefficients for light ion sputtering of adsorbed materials may reach unity.

D. Permeation of Hydrogen through Foils.

Numerous experiments have been performed on the reflection of hydrogen from surfaces, on the retention of implanted hydrogen and on the re-emission of implanted hydrogen. There are however few studies of how implanted hydrogen diffuses into and through a target to emerge from the backside. One might imagine that this is a simple diffusion problem the result of which could be readily predicted with a diffusion equation using known coefficients. However in the one published experiment the rate at which implanted hydrogen diffused through the target was an order of magnitude different from calculated values. There are numerous differences between permeation under a pressure differential and diffusion after implantation. There may be effects of damage, the implant density exceeds conventional solubility limits and the necessity for dissociation is avoided if hydrogen is introduced as H^+.

We are constructing a system to measure the permeation of ion implanted D^+ through a foil. In essence the transmitted D emits into a small volume where it is

monitored by the rise of D_2 partial pressure. We have concluded that the target should be capable of operation from -173°C to 400°C, and should be reversible so that implantation is possible into either face. Finally we have arranged the experiment so that we may detect not only permeation through the back surface but also reflection and re-emission from the front. The equipment is under construction, and will be used initially with a low energy ion beam from our 1 to 30 keV accelerator. Initial measurements should be commenced before the end of the present contract period.

E. Backscattering of Hydrogen from Surfaces.

During the present reporting period we have completed (and terminated) a study of energy and charge state distributions of scattered particles when 5 to 30 keV H^+, H_2^+, D^+ and D_2^+ are incident on various metal surfaces. The work is in course of publication, a pre-print is included as Appendix iii, and we shall simply reproduce the abstract here.

Scattering of 5 to 30 keV Hydrogen from Surfaces

by J. E. Harriss, R. Young and E.W. Thomas

J. Appl. Phys. 51, 5344 (1980)

Studies have been performed of the energy distribution exhibited by recoil H^+ and H^- resulting from impact of 7.5 to 15 keV H^+ on targets of Be, C, Cu, Nb, Au and stainless steel. The scattering geometry involves near grazing incidence and emergence with a scattering angle of 30.4 degrees. Peak flux occurs at higher recoil energies than in previously published studies with large angle (135 degree) scattering. The energy spectrum has been shown to be in excellent agreement with the TRIM computer simulation for one case. The charge state distribution of recoils appears to be governed by charge transfer and ionization events in bi-particle collisions occuring as the recoil emerges through the surface monolayer. In the study of recoil H^+ fragments produced by H_2^+ impact there is evidence that the collision processes experienced by the fragments are in some way correlated. Recoil spectra due to D^+ impact are not the same as for equal energy nor equal velocity H^+ impact. The difference is explained and a simple scaling procedure suggested to relate energy spectra for the two isotopes.

F. Auger Spectra Induced by Ion Impact on Solids.

During the present reporting period we completed (and terminated) a study of Auger spectra induced by ion impact on solids. We were led to the study as a by-product of our attempts to measure sputtering of adsorbates (Section C above) when we discovered that the ion beam induces a clear Auger spectrum that is dissimilar from that due to electron impact. The results are published and included as Appendix iv. For reference we include below the abstract to our major publication on the subject that summarizes many of our findings.

Auger Spectra Induced by 100 keV Ar^+ Impact on Be, Aℓ and Si.

by W. A. Metz, K. O. Legg and E. W. Thomas

J. Appl. Phys. 51, 2888 (1980)

The Auger electron spectrum induced by the impact of 100 keV Ar^+ on metallic aluminum is shown to be consistent with the source of Auger electrons being ejected target particles. The principal spectral line has been identified as being due to ejected Aℓ atoms with a single 2p vacancy. Subsidiary peaks are due to ejected atoms and $A\ell^+$ ions with one or two 2p vacancies. The ion-induced Auger spectrum of silicon is similar. By contrast the spectrum induced by Ar^+ impact on Be exhibits a rather broad peak characteristic of a K-shell vacancy and is similar to that induced by the impact of electrons. By considering the lifetime of the Be K-shell vacancy we conclude that the Auger decay occurs while the Be atoms are either in the solid or interacting with the surface.

V. Related Work in this Laboratory

Within the same laboratories and utilizing certain common facilities there is a NSF funded project to study excited state formation induced by ion impact on surfaces; this also has Professor E. W. Thomas as Principal Investigator. Study of ion induced Auger spectra represents a major component of this effort and is a continuation of work that in part was initiated during the DOE funded contract (see Section IV-F). The program includes also a study of ion induced optical spectra of molecules on surfaces which, it is hoped, will lead to an

understanding of dimer formation in sputtering . While these NSF funded studies have no direct bearing on the work covered by this report they do help to maintain the breadth and comprehensiveness of the research performed by this group.

VI. Conferences and Travel.

During the period covered by this report, Dr. Thomas attended to following conferences:

(a) "Fourth Interantional Conference on Plasma Surface Interactions", Garmisch-Partenkirchen, Germany, 21-25 April 1980.

(b) "SOS 80, Symposium on Sputtering", Pechtolsdorf/Vienna, Austria, 28-30 April 1980.

(c) "Gordon Research Conference on Particle Solid Interactions", Andover N.H. 21-25 July 1980.

(d) "U.S.-Japan Workshop on Atomic Data for Fusion", Boulder, Colorado, 27-31 Oct. 1980.

The Project Director also made visits to the following establishments:

(i) Culham Laboratory U.K.

(ii) MPI fur Plasmafysik, Garching.

(iii) Argonne National Laboratory.

(iv) Joint Institute for Laboratory Astrophysics.

in addition Dr. Thomas, Dr. Legg, Mr. Young, and Mr.Whaley made a total of fourteen man-trips to the Oak Ridge National Laboratory to discuss, set-up and perform experiments on ISX-B.

VII. Personnel

Professor E. W. Thomas has been Project Director and Principal Investigator devoting approximately 27.5% of his full time to this project.

Dr. K. O. Legg, Research Scientist, occupies the position of Co-Principal Investigator and devotes approximately 30% of his full time to this project.

Dr. J. E. Harriss attained his Ph.D. based on work carried out under this and preceding contracts. Mr. R. P. Young has been the principal graduate student on this work during the present reporting period. In addition Mr. W. A. Metz and R. A. Whaley, both graduate students, have participated to a limited extent on these projects.

VIII. Publications.

Eight articles have been published in this period, one is in preparation. All are listed on the final page of this report and some are included also as appendixes.

IX. Appendixes.

(i) H/D changeover Experiment on ISX-B (An interim report).

(ii) Oxygen Desorption from Transition Metals by Hydrogen Ion Bombardment.

(iii) Scattering of 5 to 30 keV Hydrogen from Surfaces.

(iv) Auger Spectra Induced by 100 keV Ar^+ Impact on Be, Aℓ and Si.

(v) Listing of Publications.

Appendix i

H/D Changeover Experiment on ISX-B

(An interim report)

The hydrogen in a Tokamak discharge arises from two sources. First there is hydrogen deliberately introduced as a filling gas or during neutral beam injection. Secondly there is hydrogen liberated in an uncontrolled manner from the walls by the discharge itself. This latter component arises from hydrogen implanted into (or adsorbed on) the walls during previous discharges; in certain cases this component can represent half the hydrogen present during the stable period of the discharge. Its study provides information on fuel recycling. We participated in experiments to study this recycling by monitoring the ratio of D to H emission in the plasma when the machine was changed from operation on deuterium gas to operation on hydrogen. The residual signal of D after commencing use of a H_2 filling gas is a measure of the fuel coming from the wall. The general experimental procedure followed the previous work of McCracken et al.,[1] on the DITE Tokamak.

The diagnostic technique is to record the Balmer alpha radiation from H and D which are separated in wavelength by about 1.78 Å. A Fabry Perot interferometer operating at an interference order of about 1830 provides adequate resolution to separate these lines. Such an interferometer can be rapidly scanned in wavelength using Piezo-electric crystals to move one mirror so that the H and D lines can be traversed as rapidly as once every 20m sec. A Burleigh Instruments type RC40 Fabry Perot was utilized with a photomultiplier as a detector. The photomultiplier output was monitored on a storage oscilloscope and the trace recorded photographically. The interferometer was placed in sector 13 of ISX-B viewing vertically downward through a port at a major radius of 93 cm. Thus the viewing direction is along a chord through the

Dee shaped plasma in ISX. The emission of Balmer spectral lines certainly occurs from the relatively cool edge of the plasma, perhaps from a region no more than 1 cm thick. The emission is therefore detected from two regions, the two intersections of the chord, along which we view, with the plasma.

The experiments were performed on October 24, 1980 employing an ohmically heated plasma with observations of shots 28836 through 28915. Companion experiments performed at the same time included:

(a) Measurements of cumulative hydrogen dose to silicon samples near the wall (Zure and Withrow).

(b) measurements of Balmer α line intensity for H and D on alternate shots (Isler)

(c) measurements of H_2 and D_2 density with a residual gas analyzer (Simpkins)

The discharges showed severe MHD instability at 160m sec; we attempted to determine intensities of H and D at about 100m sec where the plasma was relatively stable. As an example of the traces produced by the detection system we show in Fig. 1 the record of a shot entirely in deuterium after extensive operation on deuterium. The peaks of the Dα line are clearly visible. In mixed H/D operation we observe an Hα peak approximately mid-way between the Dα peaks.

The results of the experiment are displayed in Fig. 2 where we plot the $D/_{H+D}$ ratio, derived from the Balmer alpha line intensities at 100m sec, as a function of the number of discharges. The figure shows first a change from extensive operation on D_2 to operation on an H_2 filling, followed later by return to a D_2 filling. For each case the changeover from one gas to the other was largely completed in three discharges. In particular for the change from D to H the first shot after changing filling gas showed that about 40% of the active fuel was of the new filling gas (H_2). The remaining

60% of the active fuel was of the previous gas and therefore emanates from the wall. These results are similar to experience on TFR where the changeover is somewhat more rapid with the wall adsorbed gas accounting for only 18% of the discharge (c.f. 60% in the present work) on the first shot after changeover. TFR is an inconel wall machine. By contrast a changeover in DITE[1] required at least 14 to 20 shots and was never complete with the wall adsorbed isotope persisting at a level of about 20% almost indefinitely. During these studies on DITE the machine wall was stainless steel and titanium gettering was not yet in use. It is not clear why the changeover occurs at different speeds in three major Tokamaks. While the experiences on ISX and TFR are similar, both would appear inconsistent with the data on DITE. Platz[2] suggests that the changeover is largely governed by oxide layers in which case the results of an experiment would be governed by the preparation of the machine surface.

McCracken et al.,[1] interpret the Balmer alpha line emission as coming from H(and D) atoms entering the plasma from the wall and being excited as they traverse the plasma edge. This flux of atom has two parts. There are slow atoms liberated from adsorbed and implanted gases in the wall. There are fast atoms resulting from reflection of ions that have left the plasma and collided with the wall. The interpretation of shot 28875 on Fig. 2 would be that 60% of the hydrogen is D liberated from the wall (and therefore of thermal energy) while 40% is H from the filling gas and therefore results from reflection of fast particles. Zure and Withrow[3] conclude that about 3×10^{16} hydrogen atoms were incident per cm^2 during the discharges of the present experiment. The work of Thomas[4] suggests that for 1 keV ions (the approximate ion temperature of the present ISX discharges) incident on stainless steel at a dose of 3×10^{16} atoms cm^{-2} the re-emitted flux is about 60% of the incident flux and approximately one half of this is reflected (fast) atoms and one half

is re-emitted (slow) atoms ejected from the solid. This is roughly consistent with the data of shot 28874 Fig. 2 which implies $4/_{10}$ of the hydrogen is reflected (fast) H and $6/_{10}$ is ejected (slow) D from the wall. Study of the spectral line shapes in this shot also leads to the conclusion that the observed H is fast and the observed D is slow.

The records of H and D intensity disclose a number of other general features. One finds for example that during severe MHD instability the signal intensities increase (see Fig. 1) and there may be substantial fluxes of both H and D even when the $H/_D$ ratio during the stable region (at $\approx$ 100m sec) shows only one isotope to be present. This suggests that there are appreciable concentrations of H and D in the wall at all times and that these are liberated by the substantial interactions of the unstable plasma with the wall. Similar phenomena are reported on TFR[3].

Further analysis of these data are planned, perhaps along the lines used by McCracken et al.,[1] for analysis of the DITE changeover experiment. For the moment it is our interim conclusion that about one half of the hydrogen participating in the discharge is liberated from the wall and only one half is from the filling gas. This is consistent with recent data on reflection and re-emission.

References

1. G. M. McCracken, S. J. Fielding, S. K. Erents, A. Pospieszczyk and P. E. Stott. Nucl. Fusion. 18, 35 (1978).

2. P. Platz, "Isotope Exchange Experiments on TFR". Abstracts of papers for the 4th International Conference on Plasma-Surface Interactions, in Controlled Fusion Devices, Garmisch-Partenkirchen, FRG, 21-25 April 1980. (To be published in J. Nucl. Mat.).

3. R. Zure and S. Withrow, Private Communication.

4. E. W. Thomas, J. Appl. Phys. 51, 1176 (1980).

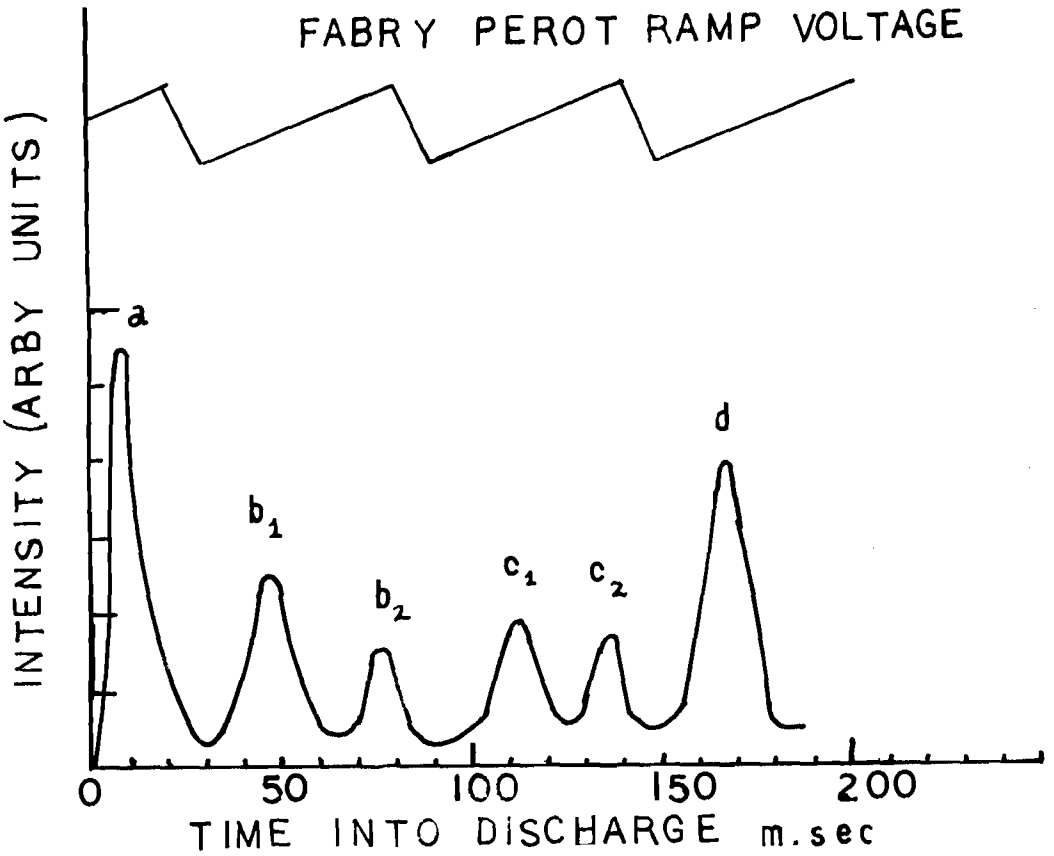

Fig. 1. Facsimile of trace showing intensity as a function of time in shot 28871 on a D_2 filling after extended operation on D_2 and before the changeover experiment was commenced. Shown also is the ramp voltage driving the Fabry Perot at 50m sec per sweep with a 10m sec flyback. Each peak is a scan of the Balmer alpha line of D. Peaks b_1 and b_2 occur in one sweep as do peaks c_1 and c_2. Peaks a and d occur at respectively the end and beginning of scans. Peak d occurs during MHD instability. During changeover the H signal shows up as an additional peak between the D peaks on each sweep.

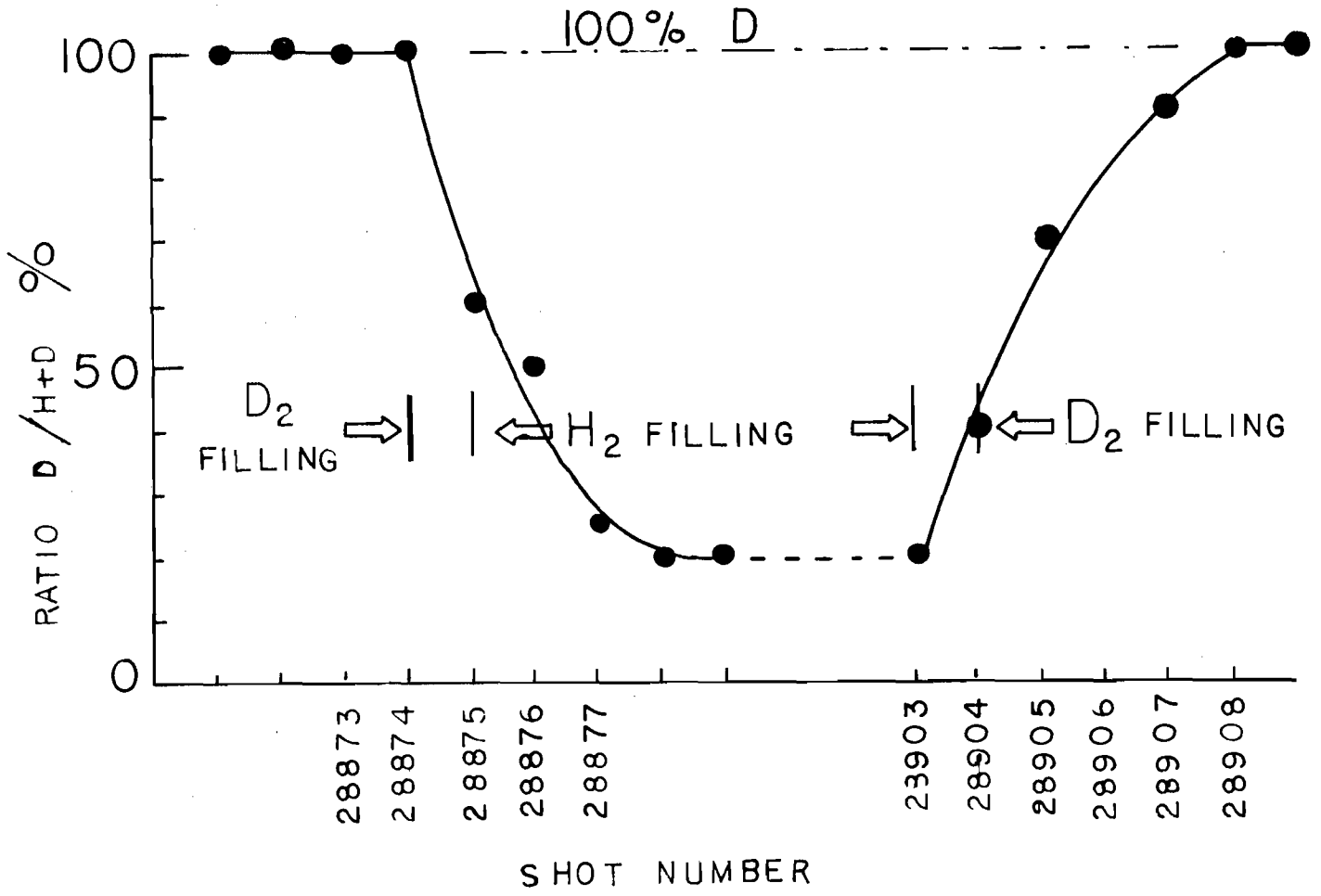

Fig. 2. Ratio of D line intensity to sum of H and D line intensities at 100m sec during changeover from a D_2 filling to H_2 and back to D_2 again. The data shows that interchange of H and D is largely complete three shots after changeover of the filling gas.

Appendix ii

Oxygen Desorption from Transition Metals by Hydrogen Ion Bombardment

K. O. Legg, R. Whaley and E. W. Thomas

School of Physics

Georgia Institute of Technology

Atlanta, GA 30332

Abstract

Measurements are reported of the cross sections for sputtering oxygen from polycrystalline Ti, Cr, Fe and Co by H^+, H_2^+ and H_3^+ in the energy range 20 keV to 200 keV. While no uniform mechanism explains all the cases, there is some evidence for desorption promoted by Auger decay in the manner suggested by Knotek and Feibelman.

Sputtering from solids has usually been modelled in terms of dynamical interactions between the incoming particle and the lattice or in terms of the creation of thermal spikes. However, desorption is not necessarily dependent only on direct energy transfer between the beam and the lattice. For example, electron stimulated desorption (ESD) experiments have shown sharp increases in the desorption yield occuring at beam energies just sufficient to create inner shell holes in surface atoms. The theory put forward by Knotek and Feibelman[1,2,3] to explain this type of effect accounts for the desorption of O^+ from TiO_2, WO_3 and V_2O_5 as the result of an inner shell hole created in the metal ion, which is filled by an interatomic Auger decay from the oxygen ion. This leaves the oxygen in a repulsive well from which it desorbs. While this theory was originally put forward to account for positive ion production, its authors note[1] that O^o should be produced at the O 2s ionization threshold.

We report here measurements of the total oxygen sputtering cross section as a function of ion energy between 20 keV and 200 keV from a number of 3d transition metals under hydrogen ion bombardment, which in some cases shows evidence of desorption caused by electronic excitations.

Polycrystalline samples of Ti, Cr, Fe and Co were cleaned by argon ion sputtering while monitoring with Auger spectroscopy, and about one monolayer of oxygen was adsorbed at room temperature and at a pressure of 10^{-6} Torr. The approximate coverage was determined by continuous Auger monitoring and comparing the O-KLL peak height with the data of Palmberg.[4] The adsorbate was sputtered by a broad H^+, H_2^+ or H_3^+ beam centered about the Auger electron gun beam . The ion current density at the electron impact point was measured with a small aperture faraday cup. During sputtering, the O-KLL Auger signal was continuously monitored using 3 keV electron excitation. In order to check

readsorption rates and to ensure that there was negligible electron beam desorption, the same experiment was run with no ion beam. It should be noted that, because only the oxygen remaining on the surface was measured, only the total desorption cross section was determined.

For sputtering with readsorption from the ambient the surface coverage at time t (in any arbitrary units) is given by:

$$N(t) = \left[N(0) - \frac{N^{o}\,\alpha Ps}{\frac{J}{e}\sigma + \alpha Ps} \right] \exp - \left(\frac{J}{e}\sigma + \alpha Ps \right) t + N^{o} \frac{\alpha Ps}{\frac{J}{e}\sigma + \alpha Ps} \qquad (1)$$

where N^{o} is monolayer coverage, J the ion current density, σ the sputtering cross section, P the partial pressure of oxygen and oxide molecules, s the average sticking coefficient and α the constant of proportionality between arrival rate and pressure ($\alpha = 1/\sqrt{2}\pi mkT$ in ideal gas theory).

$$\text{As} \quad t \to \infty \qquad N(t) \to N(0) - \frac{N^{o}\,\alpha Ps}{\frac{J}{e}\sigma + \alpha Ps} . \qquad (2)$$

Thus a plot of ln $(N(t) - N(\infty))$ vs. t yields a straight line of slope $-\left(\frac{J}{e}\sigma + \alpha Ps\right)$, in which αPs can be determined from the rise of N(t) with time when no ion beam is present.

In reality only the initial portion of the graph was linear because of errors in measuring $N(\infty)$ and αPs and probably also because of the presence of some underlayer oxygen. All data were taken with the ion beam incident at 60^{o} to the normal.

Plots of the sputtering cross section as a function of ion energy for H_2^+ on Fe and Ti and for H_3^+ on Fe are shown in Fig. 1. It can be seen that σ increases rapidly at about 45 keV/proton on Fe, while for Ti a rapid increase is seen at about 84 keV/proton. The cross sections of H_2^+ on Cr and Co and H^+

on Fe, shown in Fig. 2, exhibit no such changes.

In order to examine their electronic structure, electron energy loss curves were taken from clean and oxygen-covered Ti and Fe.

Discussion

In Fig. 1 the curve for iron under H_2^+ bombardment is the most spectacular, showing a sharp increase in yield between 40 and 60 keV/proton. Clearly such a result is not explicable in terms of conventional sputtering theory. The data fit neither existing measurements[5] nor theoretical predictions[6] of the oxygen L-shell ionization cross section. This, together with the absence of the effect when H^+ is used excludes the possibility of direct core or valence level ionization by the protons. In fact, the existence of a high sputtering yield only for H_2^+ and H_3^+ bombardment suggests that the effect is caused by the electrons associated with the incoming ions, rather than the protons themselves.

It is known[7] that electrons are stripped from a nucleus at is enters a solid. In fact, the cross section for loss of the electron from a hydrogen atom colliding with an oxygen atom is expected[8] to be at least 2×10^{-16} cm^2. This means that for our angle of incidence 50% of incoming H^o atoms would be expected to lose their electrons in the surface oxygen monolayer alone. The corresponding numbers for an H_2^+ molecule are not known, but might well be expected to be higher because of the electron's extended wave function. Electrons stripped in this way either from the projectile or the target nuclei tend to travel through the solid at the ion velocity and in the direction of ion travel.[9] Furthermore, the electron yield per proton is 17 times greater for H_2^+ than for H^+ in collisions with He,[9] and it would be reasonable to expect a similar result in our case. This is in accord with our finding that H^+ does not give rise to enhanced desorption.

At the ion energies corresponding to the points where the cross section begins to rise rapidly in Fe and Ti (40 and 80 keV/proton respectiviely),

these stripped electrons would have energies of 22 and 44 eV respectively. At 22 eV the electrons would be capable of ionizing the O-2s level, causing Auger decay and desorption of the oxygen in a charge state determined by its initial bonding arrangement at the surface. Since this is not the maximal valence configuration for iron oxide, we should not expect large O^+ fluxes, but rather a predominant desorption of O^o.[1]

For oxidized Ti, the sputtering cross section threshold is in broad agreement with features found for O^+ desorption in the ESD work of Knotek and Feibelman, which appear to be due to the Auger decay mechanism proposed by those authors.

Neither Cr nor Co show any similar effect. This is not too surprising since the data is the literature for electron beam desorption show great variability, presumably depending on such factors as the density, and coordination of the system. The sputtering rate for oxygen on chromium is uniformly low, as would be expected for a purely dynamical interaction between the ion beam and the adsorbate. On cobalt, the cross section actually rises as the primary energy falls and is far higher than one would expect dynamically. This could be due to an electronic excitation, in which electrons are lost directly from the valence band in the manner suggested by Menzel and Gomer[11] and Redhead.[12] It is however, difficult to see why this should occur only for Co.

Conclusion

It is clear that each of the cases we have studied is different and that no single unifying mechanism appears to underlie the data, even though the targets are all 3d transition metals. Although the data on iron and titanium fit quite well with the theory of Knotek and Feibelman, none of the other elements behave in this way. One point which is somewhat surprising, however, is that the sputtering appears (at least for oxygen on iron) to be due to the electrons associated with the projectile rather than the nucleus itself.

References

1. P. J. Feibelman and M. L. Knotek, Phys. Rev. B18, 6531 (1978).
2. M. L. Knotek and P. J. Feibelman, Phys. Rev. Lett. 40, 964 (1978).
3. M. L. Knotek and P. J. Feibelman, Surf. Sci 90, 78 (1979).
4. L. E. Davis et. al., "Handbook of Auger Electron Spectroscopy" 2nd ed., Physical Electronics Industries Inc. (1976).
5. F. J. De Heer, J. Schutten and H. Moustafa, Physica 32, 1766 (1966).
6. B. -H. Choi, E. Merzbacher and G. S. Khandelwal, Atomic Data 5, 291 (1973).
7. See, for example, N. Cue et al., Phys. Rev. Lett. 45, 613 (1980).
8. D. W. Rule, Phys. Rev. A16, 19 (1977).
9. M. M. Duncon and M. G. Menendez, Phys. Lett. 56A, 177 (1976).
10. K. O. Legg and M. W. Ribarsky, to be published.
11. D. Menzel and R. Gomer, J. Chem. Phys. 41, 3311 (1964).
12. P. A. Redhead, Can. J. Phys. 42, 886 (1964).

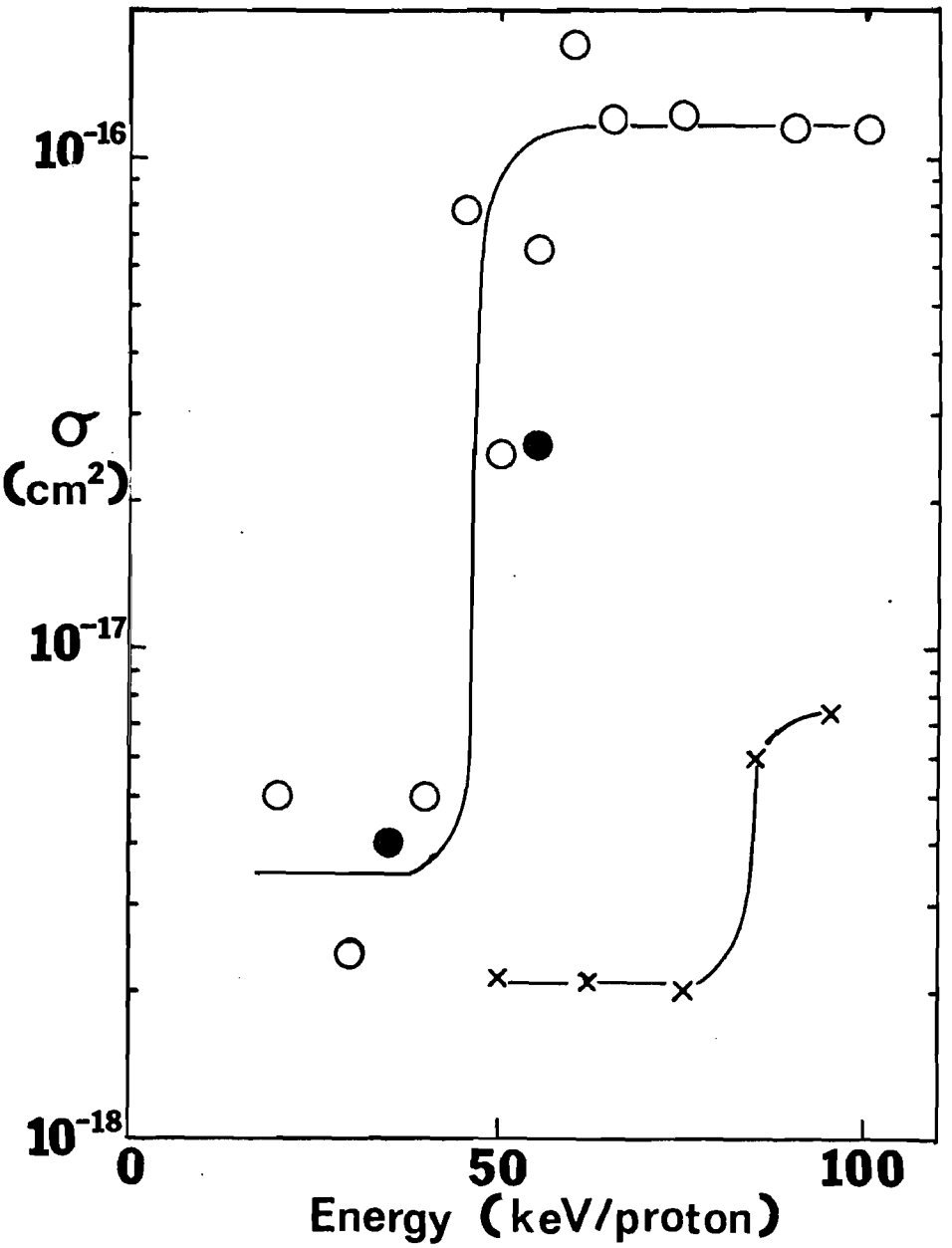

Fig. 1. Sputtering cross section per proton for oxygen desorption. Open circles $H_2^+ \rightarrow$ Fe; filled circles $H_3^+ \rightarrow$ Fe; crosses $H_2^+ \rightarrow$ Ti.

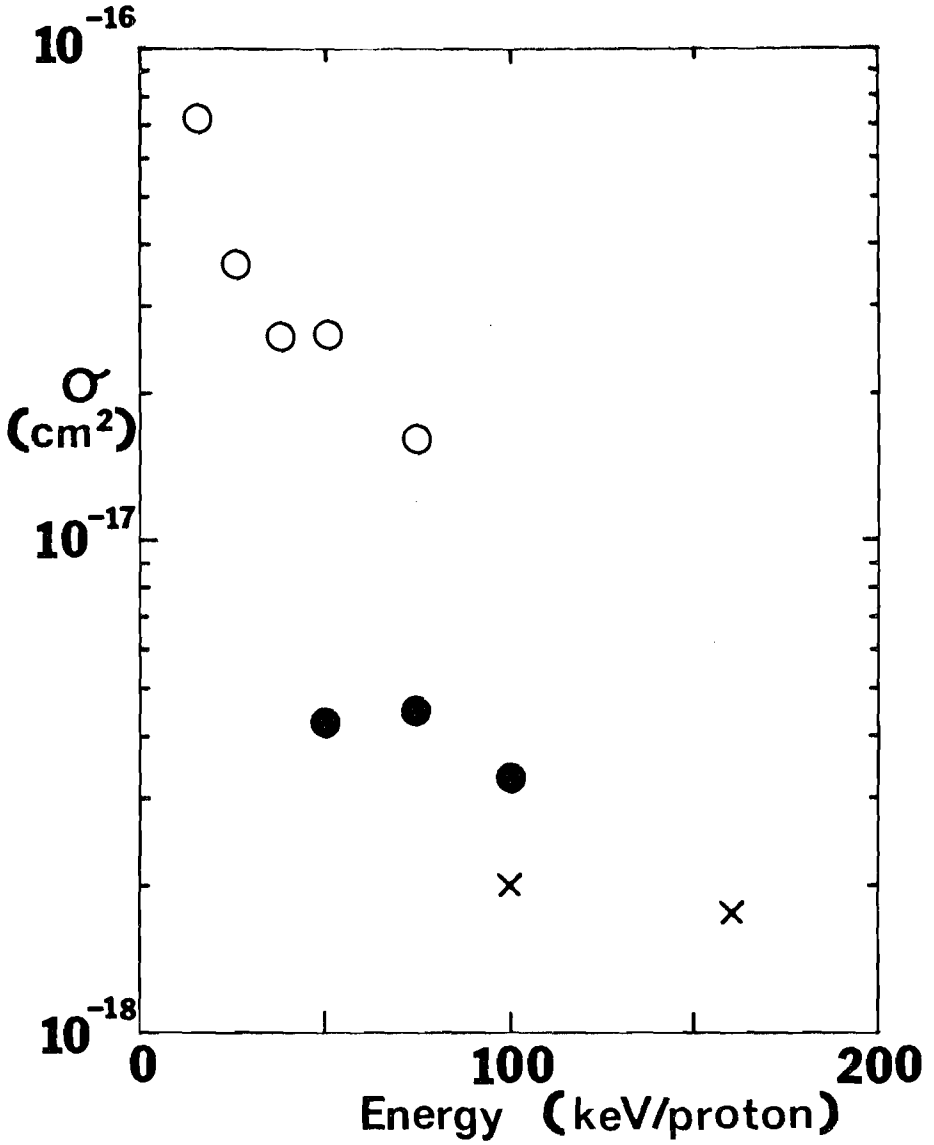

Fig. 2. Sputtering cross section per proton for oxygen desorption.
Open circles $H_2^+ \rightarrow$ Co; filled circles $H_2^+ \rightarrow$ Cr; crosses $H^+ \rightarrow$ Fe.

JAPIA,801000R0K050 (proof copy of article)

Scattering of 5- to 30-keV hydrogen from surfaces

J. E. Harriss,[a] R. Young, and E. W. Thomas
School of Physics, Georgia Institute of Technology, Atlanta, Georgia 30332

(Received 31 March 1980; accepted for publication 2 July 1980)

Studies have been performed of the energy distribution exhibited by recoil H^+ and H^- resulting from the impact of 7.5- to 15-keV H^+ on targets of Be, C, Cu, Nb, Au, and stainless steel. The scattering geometry involves near grazing incidence and emergence with a scattering angle of 30.4°. Peak flux occurs at higher recoil energies than in previously published studies with large-angle (135°) scattering. The energy spectrum has been shown to be in excellent agreement with the TRIM computer simulation for one case. The charge state distribution of recoils appears to be governed by charge transfer and ionization events in biparticle collisions occurring as the recoil emerges through the surface monolayer. In the study of recoil H^+ fragments produced by H_2^+ impact there is evidence that the collision processes experienced by the fragments are in some way correlated. Recoil spectra due to D^+ impact are not the same as for equal energy nor equal velocity H^+ impact. The difference is explained and a simple scaling procedure suggested to relate energy spectra for the two isotopes.

PACS numbers: 61.80.Jh, 61.80.Mk, 34.70. + e, 79.20.Nc

I. INTRODUCTION

Hydrogen ions or atoms incident at keV energies on a solid target will penetrate and undergo a series of collision events. Interaction with electrons will cause energy loss but no deviation while collisions with nuclei may cause large-angle deviations as well as energy loss. As a result of large-angle scattering a certain fraction of the projectiles return to the surface and emerge with an appreciable fraction of their incident kinetic energy. The emergent particles undergo various charge changing events and can emerge as stripped nuclei (H^+), neutral atoms (H^0), or negative ions (H^-). The present work seeks to study these reflected particles with measurements of charge state distribution, energy distribution, and variation of flux with recoil angle. Impetus for the work comes in part from the need to understand recycling of hydrogen fuel from the walls of a Tokamak fusion reactor. Energetic hydrogen escaping from the confinement region will scatter from the device walls and return to the confinement region with some loss of energy. This recycling of the hydrogen contributes to energy loss and must be taken into account in the modeling of the power balance in the device.

Extensive experimental measurements of reflection from polycrystalline metals have been performed by the Garching group.[1–6] Projectiles in the energy range 1–15 keV were incident on the samples at 0–45° from the surface normal; reflected particles were observed at 135° from the intial direction. This scattering geometry represents a rather large-angle scattering event. Robinson and Jackson[7] have also presented similar large-angle scattering studies. The published information on small-angle scattering (15–60°) from surfaces seems to be confined to the paper by Morita *et al.*[8]

A simple theory which accurately predicts effects of the ion-solid collision is useful if one is to obtain an understanding of the important parameters of the interaction. One approach which provides qualitative agreement with several large-scale studies was proposed by McCracken and Freeman[9] to predict a distribution in angle and in energy for particles scattered from an amorphous solid. The principle assumptions are that the projectiles are scattered in a single collision event and that the only other energy loss is due to electron stopping in the solid. Ishitani *et al.*[10] sought to improve on the above theory by dealing with the attenuation of the beam along its path through the solid, which McCracken and Freeman had ignored, and distinguishing between the center-of-mass and laboratory scattering angles, which were assumed equal in the first theory. The single-collision approaches to the scattering problem depend upon the probes having sufficient energy so that the cross section for a projectile's undergoing more than one collision is negligible. For low-energy particles one must allow for multiple colisions. Firsov[11] developed an analytical treatment of the many-collision problem for hydrogen projectiles with energy greater than 25 keV. Littmark and Gras-Marti[12] describe a method of calculating the energy spectra of ions scattered from random solids when ion-energy probes are incident and multiple collisions dominate. Both of these theories require the numerical solution of equations and are, therefore, less tractable, although perhaps more accurate than the single-collision models. Monte-Carlo-type computer simulations, MARLOWE (Robinson and Torrens,[13] Oen and Robinson[14]) and TRIM (Eckstein *et al.*[15]), have been developed to mimic the ion-solid scattering problem. Both programs assume basically a Moliere potential for the interaction. MARLOWE assumes a single-crystal structure, although amorphous materials are approximated by randomly rotating the lattice between collisions. TRIM works with a random solid. Such programs require considerable computation to provide any useful information.

The principal thrust of the present research is to measure experimentally what happens to protons which strike

[a] Present address: Rockwell International, 4311 Jamboree Road, Newport Beach, Calif. 92660.

polycrystalline materials as might be used on the inner wall of a fusion device. We have studied the scattering of hydrogen from surfaces of Au, Be, C, Cu, Nb, and stainless steel (type 302) when 5–15-keV proton beams struck each material at 69° from the target's surface normal. Scattered hydrogen was monitored at angles up to 45° from the initial direction of the projectiles, although most of the data presented here is for 30.4° scattering. The measurements of primary interest were (1) the absolute magnitude of the flux of scattered particles, (2) the angular distributions of the scattered flux, (3) the distribution in energy of ions scattered at particular angles, and (4) the charge-state distribution of the charged and neutral scattered flux.

II. EXPERIMENTAL ARRANGEMENT

The experimental arrangement is shown schematically in Fig. 1 and is a modification of equipment used earlier to study scattering of hydrogen in gases.[16,17] A mass-analyzed ion beam from an rf source is directed into the chamber shown in Fig. 1. Steering plates are used to position the beam with respect to two collimating apertures and an electrostatic analyzer may be used to measure projectile energy. Two targets are mounted on a manipulator which allows each to be separately presented to the beam.

A pair of collimating apertures selects the range of angles for which scattered particles are to be detected and beyond this are various arrangements to analyze the scattered flux. In Fig. 1 we show an energy analyzer to permit analysis of the energy spectrum of scattered ions; detection is with a channel electron multiplier (or channeltron) operated in a pulse-counting mode. Beyond the analyzer we show three Faraday cups; the central cup can be used to monitor the ion flux when the electrostatic energy analyzer is turned off. For certain measurements we removed the electrostatic analyzer and replaced it with a simple deflection plate assembly to allow separation of the charged and neutral particles. To measure the flux of ions incident on a target we had a Faraday cup before the target; the end of the cup could be opened remotely to permit the ion beam to strike the target.

The various beam preparation components (steering plates, energy analyzer, collimating apertures, and Faraday cup) are located on a rigid rail. The components for scattered particle analysis (collimating apertures, energy analyzer, and Faraday cups) were placed on a second rail that can rotate through an angle θ about a hub which also carries at its center the target manipulator. For all the present experiments the targets were set so that the beam was incident at 69° from the surface normal. The detection system could be set at any chosen angle θ from 21 (i.e., detection parallel to the surface) to 45° (detection at 24° from the surface). The whole arrangement is placed in a single vacuum system pumped with silicon oil diffusion pumps and with titanium sublimation; base pressures as low as 1×10^{-9} Torr were achieved.

Targets used in this work were Be, C, Cu, Nb, Au, and type 302 stainless steel. The elemental metals were high-purity (99.99 + %) cold-rolled polycrystalline foils. The stainless steel was a piece of commercial shim-stock. The carbon was a graphite sheet. All materials were 0.025–0.050 cm in thickness. With the exception of Be and C all targets were mechanically polished; before use all targets were washed in distilled water and methanol. Some copper targets were also electropolished but no significant difference was seen in comparison with the mechanically polished targets. In general, all targets were sputter cleaned with a 0.15–0.35-μA/cm^2 beam of 3.5-keV Ne$^+$ before measurements were commenced. In all cases except C we bombarded for a time which we estimate (from the sputtering data of Sigmund[18]) should ensure removal of ten monolayers of target material; for carbon only 2.7 monolayers were removed. By analyzing the energy spectrum of a scattered Ne$^+$ beam during sputtering, we are able to detect the presence of impurities by peaks corresponding to scattering from atoms of different masses on the surface; in essence this is the technique of ion scattering spectroscopy (ISS). Principal surface impurities were C and O. The targets could be heated to 400 °C *in situ*; temperature cycling was not found to change the scattering measurements. Grain size on the targets was found to be about 10^{-1} mm, about one order of magnitude smaller than the beam diameter. Scattering measurements from many different samples of the same material gave results that varied within the estimated limits of reliability; we believe there is no evidence that crystal structure has any bearing on the data presented here. Measured recoil fluxes were shown to vary linearly with projectile beam current for variations of current over one order of magnitude.

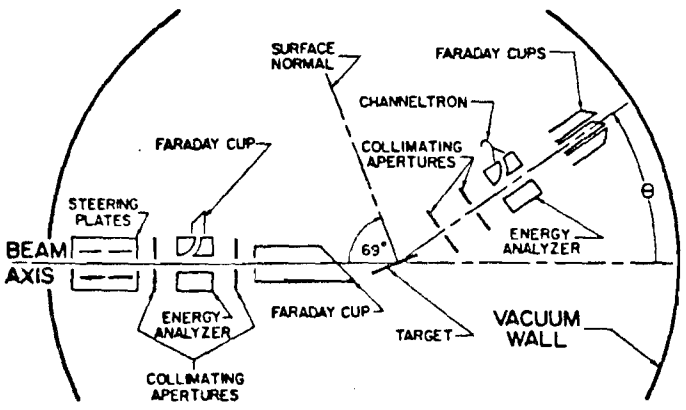

FIG. 1. Schematic diagram of the apparatus as used to measure energy spectra of ions.

III. ESTABLISHING ABSOLUTE MAGNITUDES OF SCATTERED FLUXES

As a first step we determined the scattered ion energy distribution, using the experimental configuration of Fig. 1. A typical result is shown in Fig. 2, where we have the scattered H$^+$ and scattered H$^-$ for 15-keV H$^+$ incident on Au, with the scattering angle θ being 30.4°. The change from H$^+$ to H$^-$ detection is carried out simply by reversing the polarity on the energy analyzer. For H$^-$ detection we did operate the channeltron with −1600 V on the front surface to accelerate ions so that all were incident at 1600 eV or greater energies. For the negative ions no predetection acceleration was used. Our previous study of channeltron response[19] has

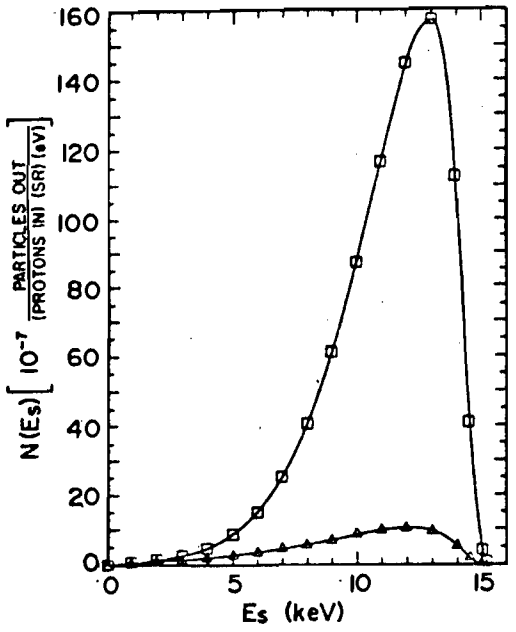

FIG. 2. Energy distribution of recoil protons (squares) and recoil H^- (triangles) measured at a scattering angle θ of 30.4° for 15-keV H^+ incident on Au at an angle of 69° from the surface normal.

shown that detection efficiency for protons is 100% for energies above 2 keV and drops below 80% only for energies less than 1 keV. We can conclude therefore that the H^+ spectrum of Fig. 2 is not significantly distorted by the channeltron response and that the H^- spectrum may be distorted only below 2 keV. These distributions have been corrected for the resolution of the energy analyzer so that the ordinate scale is in terms of signal per eV of energy interval. The relative accuracy of the data points is high, since the only substantial source of errors is the counting statistics of the channeltron. We estimate the reliability of the relative magnitudes to be $\pm 4\%$, this being the reproducibility of the measurements. We calculate the areas under the two curves by a cubic spline fit to the data, and find the ratio of the area under the H^- curve to that under the H^+ curve to be 0.089. This is the ratio of scattered H^- and H^+ fluxes for this particular experimental situation.

To establish the absolute magnitudes of the scattered fluxes, the energy analyzer is removed and replaced with a pair of parallel plates. The scattered flux for the same conditions as used above is measured as a current on the center Faraday cup. By applying a deflecting field to the plates the ions are removed and the background signal to the cup determined; thus the net scattered ion current is determined which is equal to the sum of the positive and negative currents of the H^+ and H^- fluxes. Knowing the ratio of positive and negative fluxes from the energy distributions, we can compute the net current I^+ of H^+ and I^- of H^-. Dividing these by the beam current incident on the target and by the solid angle the detector's collimator subtends at the target (1.75×10^{-4} sr), we arrive at scattered flux per ion incident, integrated over all recoil energies. These values represent the areas under the curves of Fig. 2 and allow us to assign the absolute magnitudes to the ordinates of Fig. 2. During these current measurements there is an appreciable background current caused, we believe, by stray slow electrons within the experimental chamber. By comparing background signals to the three Faraday cups on the detector system (which are all nominally the same) we can estimate a reliability for the determination of these stray currents. Taking into account reproducibility and the limited accuracy of the metering system we arrive at a figure of $\pm 20\%$ for the accuracy of these absolute figures. By contrast, the reliability of relative values in these and all other energy spectra is estimated to be $\pm 4\%$.

An estimate was also made of the scattered neutral flux, integrated over all recoil energies. The central Faraday cup on the detector system was connected so that secondary electrons from the base of the cup could be measured. This allowed detection of ions and neutrals by the ejected secondary electrons, in the manner of Fitzwilson and Thomas.[17] Again, with the energy analyzer replaced by deflection plates we can measure a secondary electron current in the center cup produced by H^+, H^-, and H^0 together; then, with the ions deflected, a signal due to H^+ alone. Since we have already determined the ratio of H^- to H^+ fluxes we can determine the H^0 flux if we know the ratios of the coefficients for secondary electron ejection by H^+, H^0, and H^-. The ratio γ^+/γ^0 of coefficients for H^+ and H^0 has been measured by Fitzwilson and Thomas[17]; it appears that the ratio is independent of material for "dirty surfaces, and is not greatly variant with energy. We assume a value of 0.85 for γ^+/γ^0 which is the measured value[17] at the energy (11.2 keV) for the peak recoil H^+ flux in Fig. 2. In the absence of any direct information on the ratio γ^-/γ^0 we have arbitrarily assumed this to equal γ^+/γ^0. Recent work by Ray *et al.*[20] suggests that γ^- may in fact be twice γ^0 at 2-keV energy; if this difference were to persist for the higher recoil energies, where the majority of the recoil flux occurs, then our estimate of H^0 recoil flux might be too low by 10%. Rather than make a correction we include this uncertainty in γ^- with the uncertainty in other factors contributing to the estimate of H^0 flux and conclude that the overall accuracy does not exceed $\pm 50\%$.

In summary then for 15-keV H^+ incident on Au at 69° to the surface normal, the scattered fluxes at 30.4° scattering angle were determined to be

$$\text{Scattered } H^+ \quad 0.081 \frac{(\text{particles out})}{(\text{protons in})(\text{sr})} \pm 20\%,$$

$$\text{Scattered } H^- \quad 0.0072 \frac{(\text{particles out})}{(\text{protons in})(\text{sr})} \pm 20\%,$$

$$\text{Scattered } H^0 \quad 0.263 \frac{(\text{particles out})}{(\text{protons in})(\text{sr})} \pm 50\%.$$

These results are used to establish all other absolute magnitudes in this paper.

IV. ANGULAR DISTRIBUTIONS OF SCATTERED PARTICLES

Using the technique outlined above we have measured the total recoil flux (H^+, H^0, and H^- together) integrated over all recoil energies, as a function of recoil direction. Figure 3 shows the data for various targets, all for 15-keV H^+ incident at 69° from the surface normal. The recoil angle for peak flux

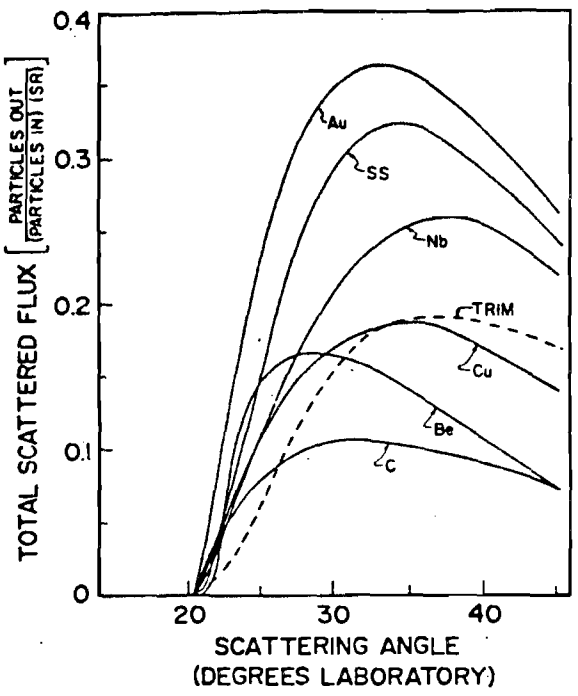

FIG. 3. Angular distribution of total recoil flux (H^+,H^0, and H^-, together) for 15-keV H^+ incident at 69° from the surface normal; targets are Be, C, Cu, Nb, Au, and stainless steel (type 302) as indicated. Also shown is result for a copper target from the TRIM computer simulation[21]; it is normalized to experiment at 35.0°.

increases with the atomic mass of the target material from 29° for Be to 36° for Nb; all peaks are closer to the surface than the specular reflection angle which would be 42°. We have been provided with a computed angular distribution performed by Haggmark,[21] using the TRIM code[15] for the case of copper. This code assumes a random structure of the target. The calculation employs a Moliere potential with Firsov screening length to describe the atomic interactions, and describes energy loss by a nonlocal Lindhard-Scharft formulation; the algebraic expressions used for these factors are as given in the paper by Eckstein *et al.*[15] This simulation is shown on Fig. 3 normalized to the experimental data. There is a fair agreement between experiment and simulation. The simulation produces a magnitude of the flux at 35° which is 20% higher than experiment. This represents an acceptable agreement, since the magnitude of the experimental data may be uncertain by as much as 50% owing to the errors involved in estimating the detection sensitivity for recoil H^0.

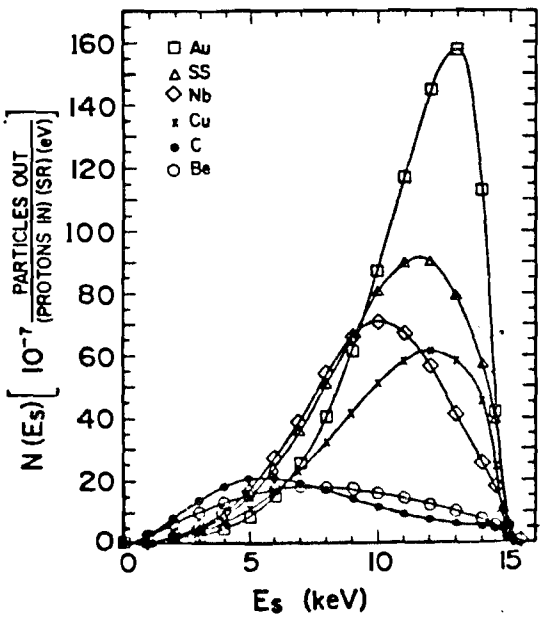

FIG. 4. Energy distributions of recoil H^+ for 15-keV H^+ incident on Be, C, Cu, Nb, Au, and stainless steel at 69° from the surface normal; scattering

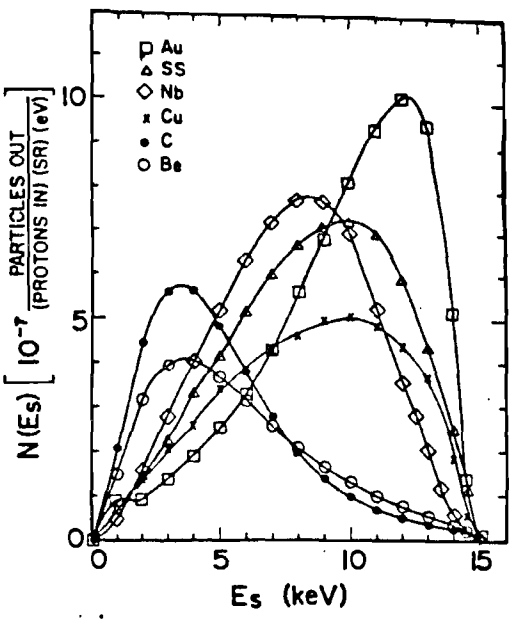

FIG. 5. Energy distributions of recoil H^- for 15-keV H^+ incident on Be, C, Cu, Nb, Au, and stainless steel at 69° from the surface normal; scattering angle θ is 30.4°.

V. ENERGY DISTRIBUTIONS OF RECOIL IONS

Figures 4 and 5 show the energy distributions of scattered H^+ and H^- from the various targets used in the work, for 15-keV H^+ impact. For the heaviest target (Au) the peak flux occurs at 13 keV and, as target mass decreases, the energy of peak flux generally declines, the lowest being for C at 5 keV. Also recoil H^+ flux decreases generally with decreasing target atomic mass. The energy of the peak recoil flux is much higher than in the earlier studies of Verbeek *et al.*[1-6] for larger angle scattering ($\theta = 135°$). For example, for 15-keV H^+ scattered through 135° by Au, Verbeek *et al.*[4] find the peak H^+ flux at 6 keV, while for scattering at 30.4° we find the peak at 13 keV. Thus as the scattering angle decreases, the peak shifts to higher recoil energies. Our present spectra are very similar to those measured by Morita *et al.*,[8] also for small-angle scattering.

In Fig. 6 we show recoil energy distributions for H^+ on Nb at 5- and 15-keV incident energies. Note that here we have normalized both curves to unity at the peak and shown the flux as a function of E/E_0, where E_0 is incident projectile energy. We observe that as impact energy decreases the peak recoil energy approaches closer to the incident projectile energy; this behavior has been previously demonstrated by Eckstein *et al.*[5]

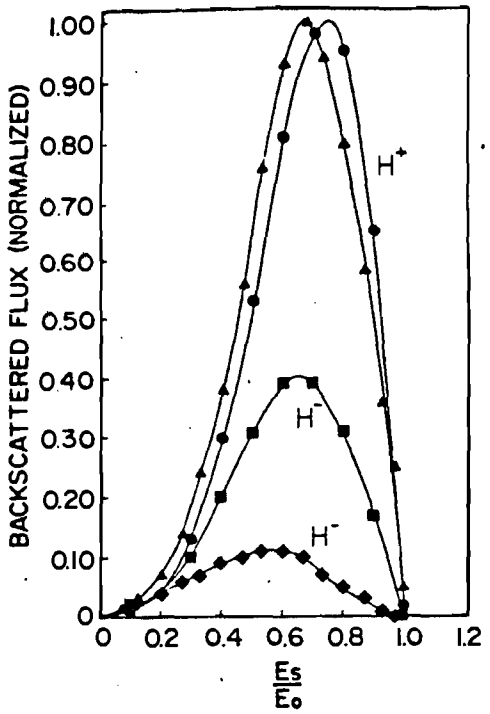

FIG. 6. Energy distribution of recoil H^+ and H^- for 15 keV (triangles and diamonds) and 5-keV H^+ (squares and circles) incident on Nb at 69° from the surface normal; scattering angle θ is 30.4° H^+ fluxes have both been normalized to unity at their peaks. For 5-keV impact the flux of H^+ at the peak is 117×10^{-7} (particles out) (particles in)$^{-1}$ (eV)$^{-1}$. For 15-keV impact the flux of H^+ at the peak is 70×10^{-7} (particles out) (particles in)$^{-1}$ (eV)$^{-1}$ (sr)$^{-1}$. The abscissa is in terms of recoil energy (E_s) divided by incident energy (E_0).

Computer simulations are available for predicting the energy distribution of backscattered particles. These simulations give the flux of all scattered particles (H^+, H^-, and H^0), while our measurements give only the flux of the charged components. Previous work by Behrisch *et al.*[22] has shown that the fraction of recoils which are positively charged does not vary appreciably with recoil direction and is a function only of a recoil energy. In the following section of this article we shall give further evidence that charge-state distribution is a function only of recoil energy. We have utilized the published measurements of positively charged fraction by Behrisch *et al.*[22] to convert the data of Fig. 4 to an estimate of total recoil flux energy distribution. In Fig. 7 we show this data for H^+ on Cu along with a prediction of energy spectrum by Haggmark[21] performed using the TRIM computer simulation. The simulation and experimental data agree very well in both the form of the energy spectrum as well as the magnitude of the flux.

VI. CHARGE-STATE FRACTIONS

The incident projectile is a positive ion, while most of the recoils are either neutral or H^-. It is not immediately clear by what process the projectile picks up one or more electrons. Brandt and Sizmann[23] argue that screening by the electron gas in a metal precludes formation of bound states. Cross[24] points out that for high projectile speeds the screening charge may lag behind the projectile at some Bohr radii, so binding in the Coulomb potential of the ion is not effected; this is not, however, true for speeds below a Bohr velocity which are appropriate to the present work. Thus we may conclude that the projectiles in the solid are stripped. It follows that the pick up of charge occurs only as the projectile finally emerges across the surface where the electron density is rapidly decreasing; screening then decreases and bound states are possible. Two general classes of mechanism might be envisaged for the charge pickup process. Firstly, one could argue that pickup occurs through a charge transfer event between the projectile and one of the atoms in the surface layer. The probability of such an event would be predicted in the form of a collision cross section which would depend only on the energy of the projectile at the collision event; thus the ratio of the H^- to H^+ fluxes should be a function only of recoil energy. As a second type of process one could consider the emerging particle as a potential well interacting with the extended potential well which describes the metal target; electrons from the conduction band might tunnel through the barrier giving rise to ion neutralization by the Auger process.[25] Formation of H^- by such processes has also been suggested.[26] For any mechanism involving penetration of the potential barrier between the surface and recoiling atom the probability for forming H^0 and H^- must be related to the time for which the emerging projectile interacts with the surface; thus the ratio between charge components should be related to the emerging projectile's velocity component normal to the surface.

Using data such as that presented in Figs. 4 and 5 one can calculate a ratio of H^- to H^+ flux as a function of recoil energy. Figure 8 shows the H^-/H^+ ratio for H^+ on gold at two different recoil angles. There is a general agreement. By contrast if we plot the same data as a function of recoil velocity component normal to the surface (in essence as a function of interaction time with the surface), there is no correspon-

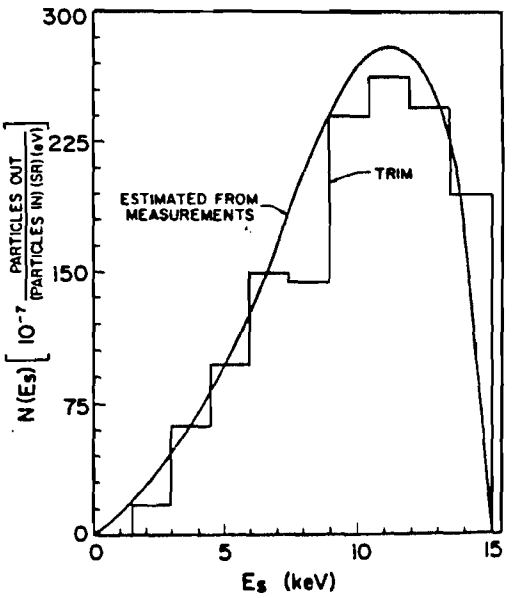

FIG. 7. Estimated recoil-flux energy spectrum of all species (H^+, H^0, and H^-) for the case of 15-keV H^+ on Cu incident at 69° from the surface normal; scattering angle θ is 30.4°. The experimental estimate is achieved from the H^+ energy spectrum shown in Fig. 4 by dividing by the charge state fraction as measured by Behrisch *et al.*[22] The histogram is a computer simulation by Haggmark[21] using the TRIM code.

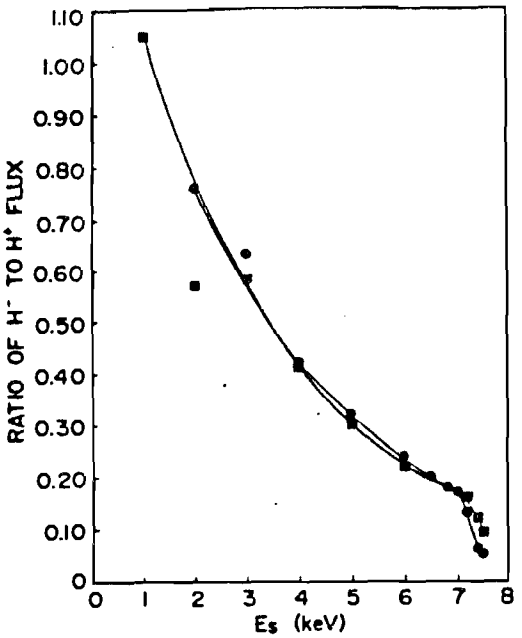

FIG. 8. Ratio of H^- flux to H^+ flux as a function of recoil energy for impact of 7.5-keV H^+ on gold. Square data points represent scattering at 30.4° (or 9.4° from the surface). Circular data points represent scattering at 24.4° (or 3.4° from the surface).

dence between data for different recoil directions. We therefore conclude that the process governing charge-state distribution is a biparticle collision mechanism dependent only on projectile energy at the surface. A similar conclusion has been arrived at by a number of other authors; these include Overbury *et al.*,[27] studying 1–2 2-keV H^+ impact on C, Tolk *et al.*,[28] studying 0.2–3.0-keV He^+ impact on lead, and also Kimura *et al.*,[29] studying 200-keV H^+ impact on stainless steel. Clearly the atomic configurations involved in the biparticle collisions will not be those of isolated atoms, but will be modified owing to the influence of the surrounding matrix.

If one accepts that the charge-state fractions are established by neutralization and stripping events as the projectile exits the last monolayer, one should be able to estimate charge-state fractions from known biparticle charge changing collision cross sections. We note, however, that cross sections for neutralization of H^+ in a gas phase target are typically of the order 2×10^{-15} cm^2 or above. (See, for example, data for Li, Na, and K targets at 10-keV energy and below.[30]) These numbers would predict total neutralization of the recoils and no ion fraction, while we detect as much as 20% of the recoils as being H^+. We should perhaps not be surprised at this result. Biparticle collision cross sections include significant contributions at large impact parameters and may quite well overestimate the cross sections applicable to a solid where the impact parameter will have a maximum value related to the interatomic spacing.

VII. STUDIES WITH D^+ PROJECTILES

A number of measurements have been made with D^+ projectiles and compared with those achieved with incident H^+ or D^+ at the same energy or at the same incident velocity. Shown in Fig. 9 are the recoil D^+ fluxes for 15 and 20-keV D^+ impact on gold, for a single impact and recoil angle. Also shown is the recoil H^+ spectrum for 7.5-, 10-, and 15-keV H^+ impact. The data for D^+ impact are not the same as those for equivelocity H^+ or for equienergy H^+. Thus the results for D^+ impact cannot be scaled to those for H^+ impact simply by placing them on the same velocity scale or on the same energy scale. Our analysis of charge state ratios (see Sec. VI above) suggests that the backscattered ion flux is governed by two factors. The multiple collisions within the solid governs the flux of projectiles recoiling back to the surface. Atomic collision events in the surface monolayer give rise to partial neutralization of the recoils and govern the charge-state distribution. Thus the flux S of recoil H^+ at recoil energy E_s due to proton impact at energy E_0 is given by

$$S_{H^+}(E_s,E_0) = F_H(E_s,E_0) f_H^+(E_s)\,, \qquad (1)$$

where $F_H(E_s,E_0)$ is the flux of all particles returning to the surface and $f_H^+(E_s)$ is the fraction which emerge as H^+ ions. Experimental measurements and computer simulations[14] show that for various light projectiles the total backscattering coefficient (integrated over all recoil energies, angles, and charge states) is approximately independent of projectile when data is plotted as a function of the reduced energy parameter ϵ suggested by Lindhard.[31]

$$\epsilon = 32.5EA_2/(Z_1^{2/3}+Z_2^{2/3})^{1/2}(A_1+A_2)Z_1Z_2\,. \qquad (2)$$

Here E is the projectile energy (keV) and Z_1,Z_2 are the atomic numbers of projectile and target, while A_1,A_2 are the atomic masses of projectile and target. For equal-energy protons and deuterons incident on a gold target the reduced energies are essentially the same. If we assume that the recoil flux at a specific recoil energy and angle is also a function only of ϵ,

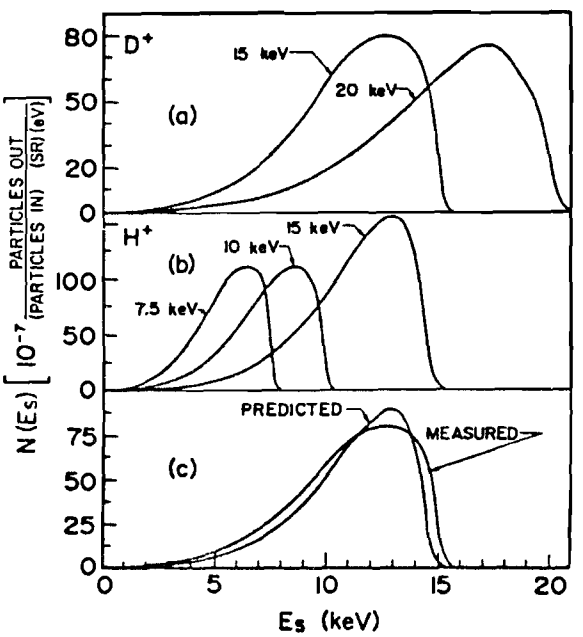

FIG. 9. Backscattered positive-ion energy spectra for H^+ and D^+ impact on Au at an angle of 69° from the surface normal. Recoils are at a 30.4° scattering angle. (a) shows data for 15- and 20-keV D^+ impact; (b) shows data for 7.5, 10, and 15-keV H^+ impact; (c) repeats the data for 15-keV D^+ impact and shows a "predicted" spectrum obtained by scaling from the 15-keV H^+ data of Fig. 9(b).

then the recoil energy spectra for equal-energy H^+ and D^+ impact should be essentially the same. Thus the recoil flux at recoil energy E_s for protons incident at some energy E_0, $F_H(E_s,E_0)$, is equal to the recoil flux $F_D(E_s,E_0)$ at a recoil energy E_s for D^+ impact at the same incident energy E_0. Now it is well known that the charge changing cross sections that we believe govern charge-state distribution of recoils are the same for equal *velocity* H^+ and D^+. Thus if the fraction of hydrogen recoils at energy E_s emerging as H^+ ions is $f_H^+(E_s)$, then the fraction of deuterium recoils at energy E_s which emerges as D^+ ions is $f_H^+(E_s/2)$, the value for hydrogen at $E_s/2$. From Eq. (1) then,

$$S_H \cdot (E_s,E_0) = F_H \cdot (E_s,E_0) f_H^+(E_s) ,$$

$$S_D \cdot (E_s,E_0) = F_D \cdot (E_s,E_0) f_D^+(E_s) ,$$

$$= F_H \cdot (E_s,E_0) f_H^+(E_s/2) ,$$

which gives us

$$S_D \cdot (E_s,E_0) = S_H \cdot (E_s,E_0) \frac{f_H^+(E_s/2)}{f_H^+(E_s)} . \qquad (3)$$

This provides a method for scaling hydrogen data to predict the result for deuterium. In Fig. 9(c) we show a predicted D^+ distribution for $E_0 = 15$ keV obtained by scaling the 15-keV H^+ data for Fig. 9(b) using ion fractions f^+ from the work of Behrisch *et al.*.[22] There is quite good agreement with the directly measured result reproduced also in Fig. 9(c). Apart from providing a useful method for scaling together the ion flux measurements for the different isotopes the success of the argument lends further weight to the conclusion that charge states are established by biparticle collision events which occur as the recoils exit the last monolayer.

Impact of a diatomic projectile on a solid target will not necessarily produce the same backscattering behavior as two independent atoms of one-half the molecule's energy (i.e., at the same velocity). Two factors are relevant. Presumably the molecule dissociates as the result of some excitation event that leaves the component nuclei in a repulsive configuration. Thus there is additional energy liberated in the center-of-mass frame of the molecule and this may significantly alter the observed energy distribution in the laboratory frame. Secondly, since the time taken for the molecular fragments to fly apart may be comparable with the time the fragments spend in the target, the path of one fragment will be influenced by the presence of the other. For example, in the study of ion transmission through foils it is well known that the angular distribution of dissociation fragments is related to electron density oscillations caused by one fragment influencing the passage of the second fragment moving a few Angstroms behind the first.[32] It is not immediately clear what magnitude should be ascribed to the repulsive potential of the two components, since this will involve screening by the free electrons in the solid.

We have performed some limited studies of H^+ and H^- energy distributions observed as a result of H_2^+ impact on gold and niobium. Typical examples are shown in Fig. 10, and are compared with the corresponding energy distribution for equivelocity H^+.

Following Heiland *et al.*[33] the energy of a fragment

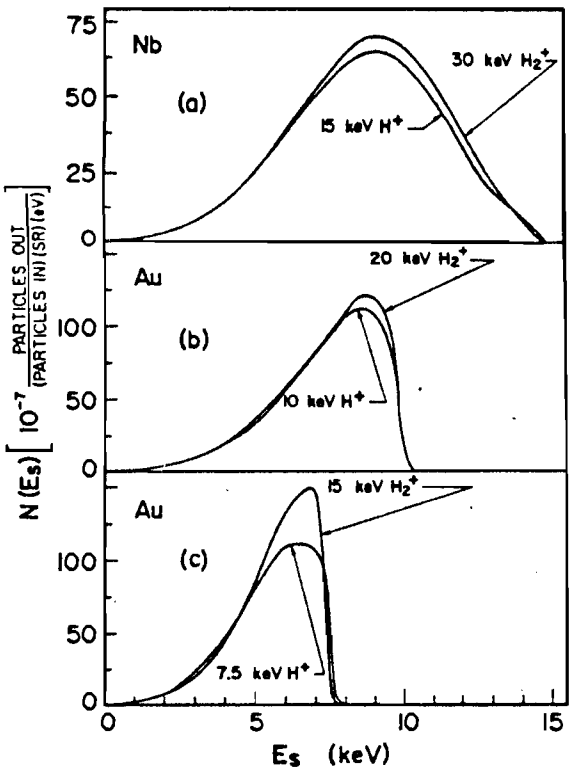

FIG. 10. Comparisons of energy distributions of recoil H^+ induced by H^+ and H_2^+ impact on Au and Nb at an angle of 69° from the surface normal with scattering through 30.4°. Each figure compares data for H^+ and H_2^+ projectiles at equal incident velocity.

scattered from the surface and originating from dissociation of a projectile of energy E_{beam} is given (in the laboratory frame of reference) by

$$E_{lab} = \tfrac{1}{2}E_{beam} + \tfrac{1}{2}E_{rep} \pm (E_{beam}E_{rep})^{1/2}\cos\phi . \qquad (4)$$

Here ϕ is the angle between the beam direction and the molecular axis and E_{rep} is the repulsive energy acting between the two fragments when dissociation occurs. Dissociation might occur by removal of the electron from the projectile resulting in two protons which will have a repulsive potential energy[33] of 13.6 eV; since the dissociation occurs on the surface we do not have to concern ourselves with screening.

For this situation we would calculate from Eq. 4 that the highest possible recoil energy for incident 15-keV H_2^+, occurring when dissociation arises at the surface, is a value of $E_{lab} = 7.96$ keV achieved when ϕ is zero. The data of Fig. 10(c) show clearly that no fragments of this energy are observed. A number of experiments have been performed for H_2^+ incident energies from 7.5 to 30 keV on gold and niobium with the general result that the maximum recoil energy of H^+ fragments is not significantly different from $\frac{1}{2}E_{beam}$. Heiland *et al.*[33] draw the same conclusion from their similar studies performed at energies between 0.2 and 2.0 keV. It must be concluded that dissociation occurs with little or no liberation of repulsive potential energy. This implies dissociation either by formation of a weakly repulsive excited H_2 or H_2^+ state, or simply by vibrational excitation of the molecule.

We would note that no undissociated recoil H_2^+ has been detected in these experiments. This indicates that colli-

sion events which direct the projectiles to the detector are sufficiently violent for dissociation to occur. Undissociated D_2^+ fragments were detected by Eckstein *et al.*[34] for D_3^+ on Au, but for low-energy impact (4.9 keV) and very-small-angle scattering (10°); even for these relatively gentle collisions the undissociated scattered D_2^+ flux was only 5% of the flux of dissociated D° fragments.

The detailed energy distributions of scattered H° due to H_2^+ impact when expressed as scattered flux per nucleon incident differ slightly from those due to equal velocity H°. The difference is significant only at the peak of the energy distribution and is of the order 10% for comparison between 10-keV H° and 20-keV H_2^+. While we can offer no quantitative explanation of this small difference, we would argue that a difference is not unexpected. Consider a 20-keV H_2^+ ion with an internuclear separation of 1.06 Å incident on gold and dissociating by a Coulomb repulsion involving, say, 5 eV of potential energy in the center-of-mass frame of the molecule. The internuclear separation of the fragments would increase to the interatomic spacing of target atoms (2.56 Å) in a time of about 7.4×10^{-15} sec. For this period the fragments are closer together than the atoms of the solid which they are penetrating and energy loss processes for one fragment might be significantly affected by the close presence of the other fragment. A 10-keV H° projectile traversing gold and emerging at 9 keV would have traversed a distance of about 105 Å according to the stopping power data of Andersen and Ziegler,[35] taking a time of about 7.1×10^{-15} sec. Thus the time taken for the fragments of a 20-keV H_2^+ projectile to separate to a distance equal to the interatomic spacing of the target (estimated here as 7.4×10^{-15} sec) is comparable with the total time spent in the target (estimated as 7.1×10^{-15} sec) by a fragment which emerges with 9-keV energy. This argument is simplistic and neglects such factors as screening by the free electrons of the solid, nevertheless it does suggest that for this example (20-keV H_2^+ incident and 9-keV H° recoils) the dissociation fragments interact with each other for a substantial fraction of the time spent in the solid. It is therefore not surprising that the scattering behavior for dissociation fragments differs from that for isolated atomic projectiles at the same incident velocity. As one goes towards lower recoil energies, the period for which the motion of the fragments is correlated becomes a smaller fraction of the total time spent in the target and one would expect any differences between the scattering of monoatomic H° and the scattering of dissociation fragments to become less significant. Indeed this agrees with the observations in Fig. 10 which shows negligible differences for recoil energies below 5 keV.

VIII. CONCLUSIONS

The mean energy of recoil H° for scattering through 30.4° in significantly higher than for previously published scattering experiments which involve larger angle scattering of about 135°. The energy spectra and observed recoil flux are in good agreement with a calculation for a copper target performed by the TRIM computer simulation. There is evidence that the charge state distribution of the recoils is established by charge transfer and ionization events occurring as the emerging projectile traverses the last atomic layer of the target. Energy spectra of recoil H° resulting from impact of molecular ions indicate that dissociation occurs either by excitation of a weakly repulsive H_2 or H_2^+ state or, alternatively, simply by vibrational excitation of the projectile. Dissociation does not occur through stripping of the electron, which would produce a strongly repulsive H°-H° configuration.

ACKNOWLEDGMENTS

Partial support of this work by the Magnetic Fusion Energy program of the Department of Energy is gratefully acknowledged. We are also very grateful to Dr. L. G. Haggmark of Sandia Laboratories, Livermore, for permission to publish his results from the TRIM computer simulation.

[1]P. Meischner and H. Verbeek, J. Nucl. Mater. 53, 276 (1974).
[2]H. Verbeek, J. Appl. Phys. 46, 2981 (1975).
[3]W. Eckstein, H. Verbeek, and S. Datz, Phys. Lett. 27, 527 (1975).
[4]H. Verbeek, W. Eckstein, and S. Datz, J. Appl. Phys. 47, 1785 (1976).
[5]W. Eckstein, F. E. P. Matsche, and H. Verbeek, J. Nucl. Mater. 63, 199 (1976).
[6]H. Verbeek, W. Eckstein, and R. S. Bhattacharya, J. Appl. Phys. 51, 1783 (1980).
[7]J. E. Robinson and D. P. Jackson, J. Nucl. Mater 76 and 77, 353 (1978).
[8]K. Morita, H. Akimune, and T. Suita, Jpn. J. Appl. Phys. 7, 916 (1968).
[9]G. M. McCracken and N. J. Freeman, J. Phys. B 2, 661 (1969).
[10]T. Ishitani and R. Shimizu, Jpn. J. Appl. Phys. 10, 821 (1971).
[11]O. B. Firsov, Soviet Phys. JETP 34, 773 (1972).
[12]U. Littmark and A. Gras-Marti, Appl. Phys. 16, 247 (1978).
[13]M. T. Robinson and I. M. Torrens, Phys. Rev. B 9, 5008 (1974).
[14]O. S. Oen and M. T. Robinson, Nucl. Instrum. Methods 132, 647 (1976).
[15]W. Eckstein, H. Verbeek, and J. P. Biersack, J. Appl. Phys. 51, 1194 (1980).
[16]R. L. Fitzwilson and E. W. Thomas, Phys. Rev. A 3, 1305 (1971), and Phys. Rev. A 6, 1054 (1972).
[17]R. L. Fitzwilson and E. W. Thomas, Rev. Sci. Instrum. 42, 1864 (1971).
[18]P. Sigmund, Phys. Rev. 184, 383 (1969).
[19]J. N. Fox, R. L. Fitzwilson, and E. W. Thomas, J. Phys. E 3, 36 (1970).
[20]J. A. Ray, C. F. Barnett, and B. Van Zyl, J. Appl. Phys. 50, 6516 (1979).
[21]L. G. Haggmark (private communication), performed using the TRIM code of Ref. 15.
[22]R. Behrisch, W. Eckstein, R. Meischner, B. M. V. Scherzer, and H. Verbeek, *Atomic Collisions in Solids* edited by S. Datz, B. R. Appleton, and C. D. Moak (Plenum, New York, 1973), Vol. I, p. 315.
[23]W. Brandt and R. Sizmann, Phys. Lett. 37 A, 115 (1971).
[24]M. C. Cross, Phys. Rev. B 15, 602 (1977).
[25]H. D. Hagstrum. Phys. rev. 96, 336 (1954).
[26]J. R. Hiskes, A. Karo, and M. Gardner, J. Appl. Phys. 47, 3888 (1976).
[27]S. H. Overbury, P. F. Dittner, and S. Datz, Nucl. Instrum. Meth. 170, 543 (1980).
[28]N. H. Tolk, J. C. Tully, J. Krauss, C. W. White, and S. H. Neff, Phys. Rev. Lett. 36, 747 (1976).
[29]K. Kimura, A. Itoh, and M. Mannami, Radiat. Eff. 41, 91 (1979).
[30]V. Gruebler, P. A. Schmelzbach, V. Konig, and P. Marmier, Helv. Phys. Acta 43, 254 (1970).
[31]J. Lindhard, V. Nielsen, and M. Scharff, Mater. Fys. Medd. Dan. Vid. Selks. 30, 10 (1968).
[32]Z. Vager and D. S. Gemmell, Phys. Rev. Lett. 37, 1352 (1976).
[33]W. Heiland, U. Beitat, and E. Taglauer, Phys. Rev. B 19, 1677 (1979).
[34]W. Eckstein, H. Verbeek, and S. Datz, Appl. Phys. Lett. 27, 527 (1975).
[35]H. H. Andersen and J. F. Ziegler, *Stopping Powers and Ranges* (Pergamon, New York, 1977), Vol. I.

Auger spectra induced by 100-keV Ar^+ impact on Be, Al, and Si

W. A. Metz, K. O. Legg, and E. W. Thomas
School of Physics, Georgia Tech, Atlanta, Georgia 30332

(Received 13 August 1979; accepted for publication 10 December 1979)

The Auger electron spectrum induced by the impact of 100-keV Ar^+ on metallic aluminum is shown to be consistent with the source of Auger electrons being ejected target particles. The principal spectral line has been identified as being due to ejected Al atoms with a single $2p$ vacancy. Subsidiary peaks are due to ejected atoms and Al^+ ions with one or two $2p$ vacancies. The ion-induced Auger spectrum of silicon is similar. By contrast the spectrum induced by Ar^+ impact on Be exhibits a rather broad peak characteristic of a K-shell vacancy and is similar to that induced by the impact of electrons. By considering the lifetime of the Be K-shell vacancy we conclude that the Auger decay occurs while the Be atoms are either in the solid or interacting with the surface.

PACS numbers: 79.20.Nc, 79.20.Fv, 32.80.Hd

I. INTRODUCTION

The impact of heavy ions on surfaces gives rise to intense emission of Auger electrons. Early descriptions of the Auger spectra were given by Louchet *et al.*[1] and by Grant *et al.*,[2] concentrating on spectra induced by Ar^+ impact on light target materials such as Be, Mg, Al, and Si. The ion-induced spectra are normally rather different from the corresponding electron-induced spectra; line shapes are changed, the main peak for the ion-induced spectrum is generally lower than that for electron impact, and the subsidiary structure is different in the two cases. The present work studies further the spectra induced by Ar^+ impact on Be, Al, and Si with the conclusion that for Al and Si the Auger electrons are predominantly due to sputtered Al and Si atoms with $2p$ vacancies.

Louchet *et al.*[1] realized at the outset that the mechanism by which incident ions induce vacancies is quite different from that by which electrons create vacancies. Electron-induced spectra occur by a Coulomb excitation of a core electron followed by an Auger decay while the atom remains in the target matrix. For heavy ion impact at the energy of the early experiments (generally 3–60-keV Ar^+) the cross sections for Coulomb excitation are too small to explain the observed ion-induced spectrum. Rather, one must invoke an electron promotion mechanism where impact of projectile A on target B leads to temporary formation of the molecule AB; the energy levels of the electrons are perturbed as the nuclei approach each other causing some levels to become degenerate and thereby permit an electron to transfer to a vacant level. As the atoms separate the energy levels return to those appropriate to the isolated atoms A and B but now with a vacancy in an inner shell. It is this vacancy which is filled by a subsequent Auger transition leading to emission of an Auger electron. The reader is referred to the comprehensive treatise by Barat and Lichten[3] for a discussion of how the correlation diagrams for the quasi-molecule AB may be constructed and interpreted to predict where vacancies will occur.

The present work studies Auger spectra induced by 20–200-keV Ar^+ impact on Be, Al, and Si. The promotion mechanism predicts[3] that vacancies will occur in the $2p$ shell of Al and Si; for Be the vacancies will be in the $1s$ shell. According to the promotion model, Ar^+ impact on targets of nuclear charge greater than that of the projectile should result in vacancy creation in the inner shells of the projectile not of the target; a study of such cases is to be presented in a subsequent paper.[4]

II. EXPERIMENTAL ARRANGEMENT

The layout of the experiment is shown in Fig. 1. A UHV chamber capable of base pressures below 10^{-10} Torr was linked via a differentially pumped beam line to a 20–200-keV ion implanter. Target samples were placed on a standard manipulator and positioned at the center of the chamber. A

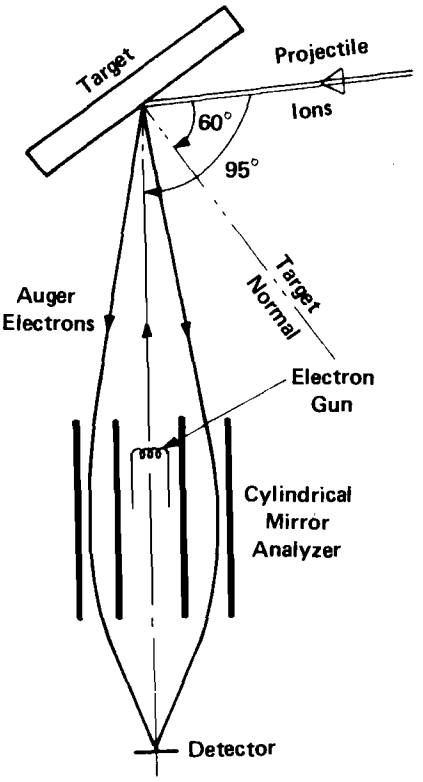

FIG. 1. Schematic diagram of the experimental arrangement (not to scale).

 0021-8979/80/052888-06$01.10

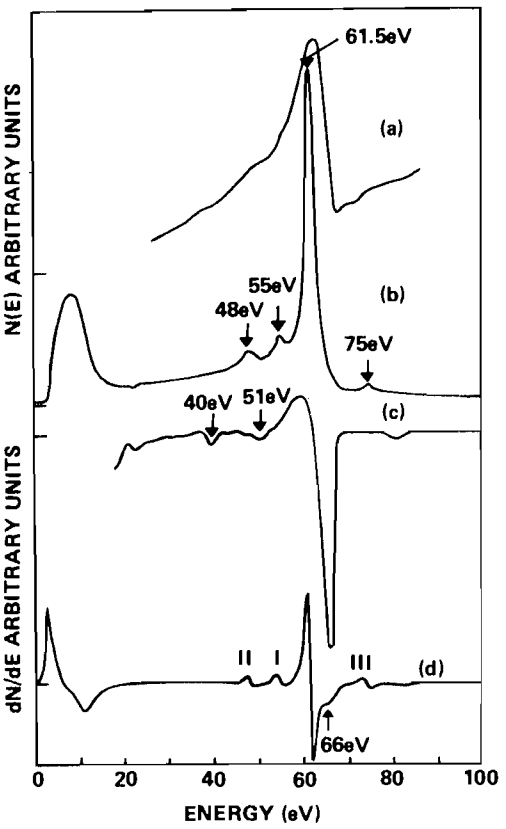

FIG. 2. Auger spectra induced by 3-keV electrons and 100-keV Ar^+ ions on aluminum. Spectra (a) and (b) are for electrons and ions, respectively, with the spectra taken in the integral mode. Spectra (c) and (d) are again for electron and ion impact, respectively, but taken in the derivative mode.

standard commercial cylindrical mirror analyzer (CMA) with an axial electron gun was placed so that it could be used both to record the electron-induced Auger spectrum of the target (utilizing the integral electron gun) as well as the ion-induced Auger spectrum (utilizing an ion beam from the accelerator). The ion beam was 95° from the CMA axis with the sample normal lying between, and coplanar with the two at an angle of 60° from the ion beam. The CMA detected electrons emitted into a 42° annulus about its axis. Ion beam currents were between 1 and 20 μA with a beam diameter of about 3 mm. The electron beam was 10 μA with a diameter of 0.1 mm. For the work described here the ion beam energy was generally 100 keV and the electron beam energy was 3 keV. Pressure in the target region varied from 7×10^{-10} to 6×10^{-9} Torr with the beam on; most of the residual gas was of the projectile species (Ar).

Samples of Be, Al, and Si were mechanically and chemically polished polycrystals cleaned *in situ* by 100-keV Ar^+ from the accelerator. After cleaning, the surfaces carried no more than 2% monolayer of C and 20% O contamination as determined by AES.[5] Further cleaning was found to have no significant effect on the results. Auger spectra were normally taken in the derivative mode commonly used in Auger measurements and built up over a period of several minutes using a multichannel analyzer to increase the signal/noise ratio. For a few target species we recorded also the integral Auger spectra, again using a multichannel analyzer to improve the signal/noise ratio. The inherent resolution limit of the CMA was about 0.3%, but resolution was limited in the differential mode by the 5-V rms modulation used.

III. THE OBSERVED AUGER SPECTRA

In Fig. 2 the spectra induced by Ar^+ and electron impact on aluminum are shown in both integral and derivative modes of recording. In Fig. 3 we display the integral spectra observed when the aluminum target is oxidized. The primary feature in the derivative spectra is an intense line at either 61.5 eV (for Ar^+ impact) or 67 eV (for e impact). The binding energy for the $L_{2,3}$ shell[6] is about 80.5 eV so that this major peak is undoubtedly due to a $2p$ vacancy. Additional subsidiary structure is seen at lower and higher energies most clearly in the derivative spectra. According to Guennou *et al.*,[7] the major peak in the electron-induced derivative spectrum (at 67 eV) is an L_{23} VV Auger transition (where V indicates valence electron) and the 51-eV subsidiary peak is due to L_{23} VV electrons that have excited a bulk plasmon; the 40-eV peak is identified as L_1L_{23} V transition.

It is instructive to examine the differences in detail between the ion- and electron-induced spectra of aluminum. The electron spectrum [Fig. 2(a)] shows a distinct tail towards lower energies which is related to energy loss by L_{23} VV electrons as they traverse the distance from their point of excitation to their escape from the surface; electrons excited below the surface emerge at lower energies than those excited at the surface. No such "loss tail" is seen on the ion-induced spectrum [Fig. 2(b)]. Raising the ambient pressure in the target chamber to 10^{-5} Torr with oxygen we observe significant changes to the electron-induced spectrum [see Fig. 3(a) in comparison with Fig. 2(a)]. This is caused by formation of a surface oxide and is related to changes in valence band structure. A similar test for the ion-induced spectrum showed no significant change in the Auger spectrum when compared with the spectrum taken in the absence of oxygen [see Fig. 3(b) compared with Fig. 2(b)]. We did check that simultaneous electron and ion bombardment in the presence of oxygen showed a spectrum composed of the superposition of Figs. 3(a) and 3(b). This confirms that the Ar^+ beam is not simply sputtering the oxygen from the surface to leave clean aluminum. Thus we conclude that the ion-induced spectrum from an oxide covered surface of aluminum is identical with that for clean aluminum and that the

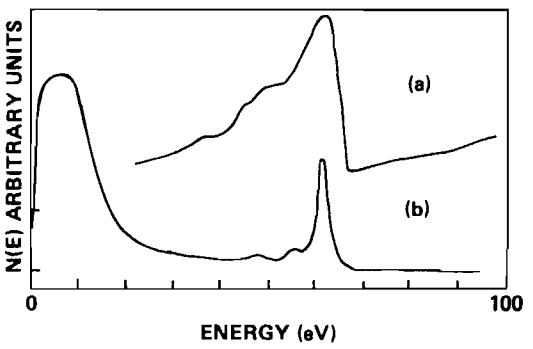

FIG. 3. Integral Auger spectra induced by impact of 3-keV electrons [spectrum (a)] and 100-keV Ar^+ ions [spectrum (b)] incident on oxidized aluminum.

ion-induced Auger spectrum does not involve the valence band of the solid. The 40-eV peak in the electron-induced spectrum [Fig. 2(c)] is not observed in the ion-induced spectrum. This peak is due to[7] a L_1 (i.e., $2s$) shell vacancy that will not be created by the promotion mechanism in an $Ar^+ + Al$ collision; thus its absence is expected. The 51-eV peak in the electron-induced spectrum is related to plasmon excitation[7] involving a 15–16-eV energy loss. In the ion-induced spectrum there is a peak 13.5 eV below the main feature but this is not at the correct energy for either a bulk or a surface plasmon in aluminum. Thus the ion-induced spectrum exhibits none of the characteristics expected when the Auger emission takes place while the excited atom is in the solid; there is no loss tail, no change when the surface is oxidized, and no peaks associated with excitation of plasmons. We would conclude that the Auger decay takes place when the excited atom is outside the surface. Consequently the electrons originate from atoms or ions ejected from the solid.

Previous work on the Auger spectrum induced by Ar^+ impact on Al has been performed by the group at Toulouse.[1,8–11] Their experimental arrangement differs significantly from the present system only in that it selects electrons ejected at 33° from the incident beam direction[8] rather than into the 42° annulus centered at 95° from the beam direction which was used in the present work. The observed spectra are generally the same as those shown in Figs. 2(b) and 2(d) except that the subsidiary lines at 48 and 55 eV are superimposed on a continuous background that amounts to about 30% of the 61.5-eV peak height; no such background is seen in the present work. The Toulouse group see a shoulder on the high-energy side of the 61.5-eV peak which they ascribe to an L_{23} VV transition involving the valence band electrons; that would require Auger transitions from atoms in the solid. No such shoulder is observed in the present integral spectra although an inflection is seen on the derivative spectrum [Fig. 2(d)] at 66 eV which almost corresponds to the position of the major downward peak in the electron-induced Auger spectrum [Fig. 2(c)].

Figure 4 shows the ion-induced spectra of silicon. The

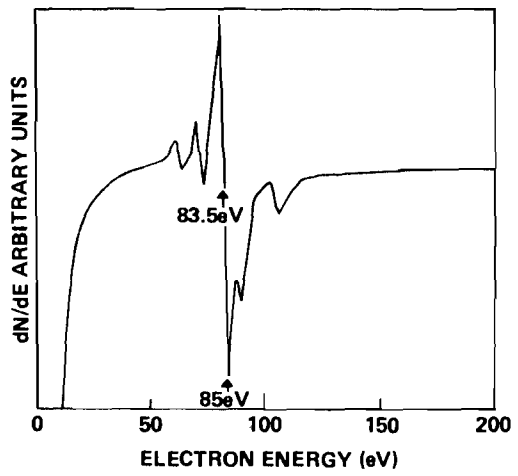

FIG. 4. Differential Auger spectrum induced by 100-keV Ar^+ impact on silicon.

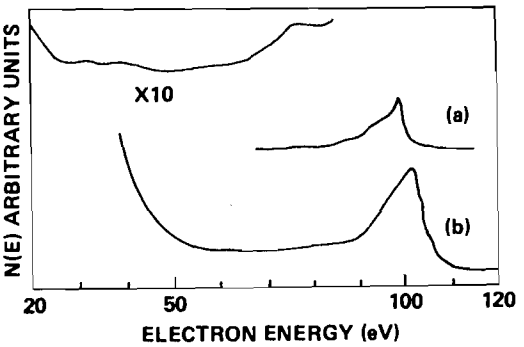

FIG. 5. Auger spectra induced by (a) 3-keV electrons and (b) 100-keV Ar^+ ions on beryllium. The spectra are taken in the integral mode.

general features are similar to those found for aluminum. The ion-induced spectrum shows a number of sharp lines whose form is consistent with the electron emission occurring from atoms or ions that have been ejected from the solid. Figure 5 shows electron- and ion-induced spectra for a beryllium target. Here the emission results from K-shell vacancies in Be and there appears to be a broad line.

IV. DISCUSSION

We shall concentrate first on the aluminum case. The vacancies are formed in the $L_{2,3}$ shell and the general form of the spectrum is consistent with the source of electrons being from atoms or ions ejected out of the surface. The $L_{2,3}$ vacancies can be created by electron promotion in $Ar^+ + Al$ collisions; vacancies will not be formed in the L_1 shell.[3] Al atoms recoiling in the collision cascade within the solid will collide with other Al atoms and if the collision energy is sufficiently high, this may also result in $L_{2,3}$ shell vacancy production through symmetric Al + Al collisions. Thus the vacancies can occur both by the collision of the projectile on the target and also by collisions of recoiling target atoms. The same spectrum is seen[12] for Ne^+ impact on Al where promotion of L_{23} electrons in the primary $Ne^+ + Al$ impact is not possible[3]; this suggests that at least part of the observed Auger spectrum is induced by collisions of recoiling target atoms. The promotion mechanism occurs only during a rather close approach of the participating nuclei which in turn means that the collisions are violent with considerable energy transfer to the target nuclei. Vrakking and Kroes[12] have studied the threshold energy for excitation of the Auger lines and concluded that at least 300 eV energy is required in the center of mass frame for $L_{2,3}$ shell promotions in both the Ar + Al and Al + Al collisions. Thus the vacancies are created in atoms moving in the laboratory frame with at least 600 eV of energy or a minimum speed v of 6.5×10^6 cm/sec; taking the lifetime of the $L_{2,3}$ vacancy τ as 1.33×10^{-13} sec,[13] the decay length of the $L_{2,3}$ vacancy is at least 86 Å (the product $v\tau$). By contrast the escape depth of an aluminum Auger electron is about 4.2 Å.[14] Thus atoms recoiling into the solid will in general emit their Auger electron at a depth from which it cannot escape. It follows that only when the excited Al atom recoils out of the target (i.e., is sputtered) will the Auger electron be detected. This conclusion is consistent with our analysis of the spectrum which also leads to

the conclusion that the Auger electrons come from particles that have been ejected from the solid.

We must now attempt to identify the states of excitation in the ejected particles. Reference to previous studies of gas-phase bi-particle collisions[15] show a complex Auger spectrum having eight or more lines that in no way resembles the spectra shown in Fig. 2; these gas-phase spectra are identified as being from ionized states of aluminum. We have therefore examined the possibility that the major feature of the ion-induced Auger spectrum of metallic Al is from sputtered Al atoms with a $2p$ shell vacancy. In the absence of a published value of the energy of the $2p^5\ 3s^2\ 3p^2$ configuration we have estimated a value as follows. The difference between $E(2p^5\ 3s^2\ 3p^2)$ and $E(2p^5\ 3s^2\ 3p)$ for Al should be approximately equal to the difference between $E(2p^6\ 3s^2\ 3p^2$ and $E(2p^6\ 3s^2\ 3p)$ of Si; this latter difference is simply the energy for removing one electron from Si and is given to be 8.15 eV in standard references.[16] Taking the energy of the $2p^5\ 3s^2\ 3p$ configuration to be 80.5 eV from the calculations of Shirley *et al.*,[6] we arrive at an energy of 72.35 eV for the $2p^5\ 3s^2\ 3p^2$ configuration of Al. We now calculate the energies for the following five transitions leading to filling of the $2p$ vacancy and ejection of an outer shell electron:

$$2p^5\ 3s^2\ 3p^2 \rightarrow 2p^6\ 3s^2 \quad E_{\text{Auger}} \quad 66.37\text{ eV} \quad (1a)$$
$$\rightarrow 2p^6\ 3s\ 3p(^3P^0) \quad E_{\text{Auger}} \quad 61.74\text{ eV} \quad (1b)$$
$$\rightarrow 2p^6\ 3s\ 3p(^1P^0) \quad E_{\text{Auger}} \quad 58.95\text{ eV} \quad (1c)$$
$$\rightarrow 2p^6\ 3p^2(^1D) \quad E_{\text{Auger}} \quad 55.78\text{ eV} \quad (1d)$$
$$\rightarrow 2p^6\ 3p^2(^3P) \quad E_{\text{Auger}} \quad 54.71\text{ eV}. \quad (1e)$$

In each case the energy of the final state is readily obtained from standard tables.[16] We observe that transitions (1b) and (1c) can explain the principal peak in Fig. 2(b) (at 61.5 eV), transitions (1d) and (1e) can explain the first subsidiary peak [designated I in Fig. 2(b)] and lying at 55 eV; furthermore, transition (1a) agrees exactly with the shoulder to the main peak which is most clearly exhibited at 66 eV in the derivative spectrum [Fig. 2(d)]. It has previously been argued that this latter shoulder is in fact due to Auger electrons from the valence band of the solid[2]; the above argument provides an alternative explanation consistent with our picture of deexcitation outside the solid.

We have also examined the possibility that Al^+ with a $2p$ vacancy contributes to the spectrum through the two transitions

$$2p^5\ 3s^2\ 3p \rightarrow 2p^6\ 3s \quad E_{\text{Auger}} \quad 55.7\text{ eV} \quad (2a)$$
$$\rightarrow 2p^6\ 3p \quad E_{\text{Auger}} \quad 49.0\text{ eV}. \quad (2b)$$

The energy of the parent state is taken from the theoretical binding energies of Shirley *et al.*[6] and the energies of the daughter states from Moore.[16] Transition (2b) can explain peak II in Fig. 2(b) and transition (2a) may contribute to peak I. Finally the high-energy structure [designated III in Fig. 2(d)] exhibited at 75 eV has been identified by Viel *et al.*[9] as being due to decay of ejected particles with two inner shell $2p$ vacancies.

While we have not discussed all possible configuration of ejected atoms and ions it is clear that the observed spectrum can be properly ascribed to ejected target particles. The observed spectrum can be completely explained as being due to ejected Al atoms and Al^+ ions with one or two $2p$ vacancies. The breadth of the lines (approximately 2.3 eV FWHM) is perhaps a Doppler broadening due to the energy of the emerging particles. A recoil energy of 300 eV would produce a broadening of the order 2.5 eV.[15,17]

The Auger spectrum of Si exhibits the same general form as that of Al. We can again predict Auger electron energies for decay of neutral Si with a $2p$ vacancy and Si^+ with a $2p$ vacancy. The excited Si state has a configuration $2p^5\ 3s^2\ 3p^3$. Its energy can be estimated as 98.3 eV using the relationship that $E(2p^5\ 3s^2\ 3p^3) - E(2p^5\ 3s^2\ 3p^2)$ for Si is approximately the same as $E(2p^6\ 3s\ 3p^3) - E(2p^6\ 3s^2\ 3p^2)$ for P; the energies of the levels can be taken from Shirley *et al.*[6] and from Moore.[16] The energy of the $E(2p^5\ 3s^2\ 3p^2)$ state of Si^+ is 106.5 eV from Shirley *et al.*[6] Again using Moore[16] to estimate energies of the final states we arrive at the transitions

$$2p^5\ 3s^2\ 3p^3 \rightarrow 2p^6\ 3s^2\ 3p\ (^2P^0) \quad E_{\text{Auger}} \quad 90.15\text{ eV} \quad (3a)$$
$$\rightarrow 2p^6\ 3s\ 3p^2\ (^4P) \quad E_{\text{Auger}} \quad 84.70\text{ eV} \quad (3b)$$
$$\rightarrow 2p^6\ 3s\ 3p^2\ (^2D) \quad E_{\text{Auger}} \quad 83.30\text{ eV} \quad (3c)$$
$$\rightarrow 2p^6\ 3s\ 3p^2\ (^2S) \quad E_{\text{Auger}} \quad 80.65\text{ eV} \quad (3d)$$
$$\rightarrow 2p^6\ 3s\ 3p^2\ (^2P) \quad E_{\text{Auger}} \quad 79.71\text{ eV} \quad (3e)$$
$$\rightarrow 2p^6\ 3p^3\ (^4S^0) \quad E_{\text{Auger}} \quad 74.75\text{ eV} \quad (3f)$$
$$2p^5\ 3s^2\ 3p^2 \rightarrow 2p^6\ 3s^2\ (^1S) \quad E_{\text{Auger}} \quad 82.01\text{ eV} \quad (4a)$$
$$\rightarrow 2p^6\ 3s\ 3p\ (^3P^0) \quad E_{\text{Auger}} \quad 75.47\text{ eV} \quad (4b)$$
$$\rightarrow 2p^6\ 3s\ 3p\ (^1P^0) \quad E_{\text{Auger}} \quad 71.74\text{ eV} \quad (4c)$$
$$\rightarrow 2p^6\ 3p^2\ (^1D) \quad E_{\text{Auger}} \quad 66.90\text{ eV} \quad (4d)$$
$$\rightarrow 2p^6\ 3p^2\ (^3P) \quad E_{\text{Auger}} \quad 65.94\text{ eV} \quad (4e)$$
$$\rightarrow 2p^6\ 3p^2\ (^1S) \quad E_{\text{Auger}} \quad 63.00\text{ eV} \quad (4f)$$

There are obviously far more lines here than there are peaks in Fig. 4 but many lines are sufficiently close that they would be unresolved due to broadening by the Doppler effect. We note particularly that transition (3b)–(3e) fall in the region of the main peak and that transition (3a) falls exactly at the first subsidiary peak to the high-energy side of the main peak (at 90 eV). Transitions (4b)–(4f) lie in the region of the subsidiary peaks I and II. The high-energy peak III can be identified as decay of Si atoms with two $2p$ vacancies. Consequently the spectrum from silicon can be completely explained as being due to ejected Si and Si^+ with one and two $2p$ vacancies; this is the same explanation as we invoke for aluminum.

The Be spectrum (Fig. 5) must of course be related to the formation of K-shell vacancies. The discussion of correlation diagrams by Barat and Lichten[3] shows how the K-shell vacancy can occur by a $3d\,\sigma$ promotion. This beyllium spectrum differs notably from that of aluminum in the breadth of the main Auger line; it is approximately 10 eV wide (FWHM) compared with the 2.3-eV width of the major peak from Al. If we arbitrarily assume that the recoil energy of beryllium atoms with the K-shell vacancy is 300 eV and that the lifetime of the K-shell vacancy is about 10^{-14} sec (the value calculated by McGuire[18] for boron) then the distance moved during the lifetime of the K-shell vacancy is only some 8 Å. It follows then that if the Be atom recoils out of the target then the majority of decays will occur while the ejected atom is still interacting with the surface. Thus the Auger line shape will reflect distortion of the energy levels by the

surface leading to a line broadening towards lower Auger energies as discussed by Dorozhkin *et al.*[19] Furthermore, the escape depth for 101-eV electrons from Be is about 3.76 Å[14] and therefore is quite comparable with the decay length for K-shell vacancies of 300-eV Be. It follows then that Be atoms or ions recoiling into the target from surface collisions will emit their Auger electrons while close enough to the surface that such electrons can escape and be detected. Consequently a large proportion of the Auger electrons may be emerging from atoms in the matrix or atoms interacting with the surface; this would lead to an Auger line shape similar to that excited in the solid by impact of electrons. Detailed identification of the emitting states is not possible because of the extreme width of the observed line. We note however, that the peak intensity occurs at 101 eV which coincides exactly with decay of a $1s\ 2s^2\ 2p$ neutral atom state as observed in gas-phase collisions.[20] Moreover, we do not observe a line at 96 eV which is expected from Be^+ ions with a single K-shell vacancy.[20] Thus the observed spectrum is consistent with the source of electrons being Be atoms with single K-shell vacancies.

Recently Vrakking and Kroes,[12] following earlier suggestions by Hennequin and Viaris de Lesegno,[21] have argued that the main line of the ion-induced Auger spectrum comes from free recoiling target atoms deep within the solid in the highly disturbed region of the collision cascade. The free electron density is said to be reduced by a factor of 3 from the value for an unperturbed solid causing a decrease in plasmon energy. We believe that this model by Vrakking and Kroes is not consistent with the observed spectra. If excitation of plasmons is invoked to explain the small peaks on the ion-induced spectra then one would expect that changes to free electron density by oxidation or by alloying with other metals should inevitably cause shifts and shape changes to the peaks. We observe no significant change to the aluminum spectrum when the surface is oxidized and Viel *et al.*[22] observe no change to the aluminum lines when they are excited in an aluminum-magnesium alloy; this implies that the subsidiary peaks are not related to electron density and are therefore not plasmon losses. The model of Vrakking and Kroes[12] would seem to explain only peak I as a plasmon loss. Peak II is also referred to as a loss peak but its origin is not explained. The Vrakking and Kroes model requires that the electrons emerge from depths of 30 Å or more (for 5-kV Ar^+ impact), more than five times the normally accepted escape depth for the aluminum Auger electrons. It is well known[23] that the cross section for electron ionization of atoms is always of the order 10^{-16} cm^2 or higher. Thus any electrons emerging from deep in the solid will have almost unit probability of ionizing an atom in this disturbed region of the collision cascade and therefore will emerge with an energy loss equal to the relevant ionization potential of the target atom. For Al we should expect a peak at 5.98 beV below the main peak; our observed peak I [Fig. 2(b)] lies 6.5 eV lower. Furthermore when the surface is oxidized there should be an additional peak related to ionization of oxygen at an energy loss of 13.61 eV; while peak II [Fig. 3(b)] lies 13.0 to 13.5 eV below the main feature it is present even when the surface is not oxidized and does not change its relative height on oxidation. Study of the spectra for silicon and beryllium targets leads to the same conclusion that there are no structures representing energy loss by ionization, which should be an inevitable consequence of the model by Vrakking and Kroes.[12] All observed structures for the aluminum and silicon targets can be completely explained as coming from free ejected atoms and ions that have one or two inner shell vacancies.

Recently Wittmaack[24] has studied the Auger spectrum of Si induced by 2–30-keV noble gas ion bombardment. The conclusions are generally the same as those of the present work in that the major features are identified as being due to sputtered target atoms with single L-shell vacancies, and the subsidiary features are not loss peaks (as suggested by Vrakking and Kroes) but are the result of the same type of excitation process as the principal line. Wittmaack attempts to identify the lines using transition energies calculated[25] for solid Si. We regard this as an incorrect approach since the origin of the lines is said to be free atoms sputtered from the target. The calculated line positions presented in the present paper are based on energies for free atoms and are therefore consistent with the supposed origin of the line. The spectra published by Wittmaack are taken with a 1-V peak-to-peak modulation and show a certain fine structure which is not observed in the present work where the modulation was 5 V peak to peak.

V. CONCLUSION

The Auger spectra induced by ion impact on Be, Al, and Si exhibit a line spectrum characteristic of the target species. For the case of Be the spectrum is due to K-shell vacancies and closely resembles that observed due to electron impact on solids. Consideration of the K-shell lifetime and possible recoil speeds leads us to conclude that the Auger electron is emitted while the parent atom is either in the solid or at least still interacting with the surface of the solid. Hence it is not surprising that the observed spectrum resembles that induced by electron impact where the emitting species is certainly in the solid matrix. By contrast, the ion-induced spectra of Al and Si do not show the features expected if the parent atom interacts with the solid matrix during emission. We conclude that the Auger electrons arise from atoms that have been sputtered from the surface and undergo their decay as free atoms remote from the surface. The spectrum from Al can be completely explained by reference to published energy level information. The major peak is due to decay of ejected Al atoms with a single $2p$ vacancy. Subsidiary structure is due to Al atoms with two $2p$ vacancies and to Al^+ ions with a single $2p$ vacancy. The spectrum from Si is similar. We find no evidence to support the contention of Vrakking and Kroes[12] that the Auger lines from Al arise from recoiling Al atoms within the collision cascade of the solid.

ACKNOWLEDGMENTS

This work was supported in part by the Condensed Matter Division of the NSF and also in part by the Magnetic Fusion Energy Division of the Department of Energy.

[1]F. Louchet, L. Viel, C. Benazeth, B. Fagot, and N. Colombie, Radiat. Eff. **14**, 123 (1972).
[2]J.T. Grant, M.P. Hooker, R.W. Springer, and T.W. Haas, J. Vac. Sci. Technol. **12**, 481 (1975).
[3]M. Barat and W. Lichten, Phys. Rev. A**6**, 211 (1972).
[4]K.O. Legg, W.A. Metz, and E.W. Thomas (unpublished).
[5]K.O. Legg, F. Jona, D.W. Jepsen, and P.W. Marcus, J. Phys. C **10**, 937 (1977).
[6]D.A. Shirley, R.L. Martin, S.P. Kowalczyk, F.R. McFeeley, and L. Ley, Phys. Rev. B **15**, 544 (1977).
[7]H. Guennou, G. Dufour, and C. Bonnelle, Surf. Sci. **41**, 547 (1974).
[8]N. Benazeth, J. Agusti, C. Benazeth, J. Mischler, and L. Viel, Nucl. Instrum. Methods **132**, 477 (1976).
[9]L. Viel, C. Benazeth, and N. Benazeth, Surf. Sci. **54**, 635 (1976).
[10]C. Benazeth, N. Benazeth, and L. Viel, Surf. Sci. **65**, 165 (1977).
[11]J. Mischler, M. Negre, N. Benazeth, D. Spanjaard, C. Gaubert, and D. Aberdam, Surf. Sci. **82**, 453 (1979).
[12]J.J. Vrakking and A. Kroes, Surf. Sci. **84**, 153 (1979).
[13]E.J. McGuire, Phys. Rev. A**3**, 587 (1971).
[14]D.R. Penn, J. Electron Spectros. Relat. Phenom. **9**, 29 (1976).
[15]P. Dahl, M. Rodbro, G. Herman, B. Fastrup, and M.E. Rudd, J. Phys. B**9**, 1581 (1976).
[16]C.E. Moore, Natl. Bur. Std. Circ. (U.S.) **467** (1949).
[17]C. Benazeth, N. Benazeth, and L. Viel, Surf. Sci. **78**, 625 (1978).
[18]E.J. McGuire, Phys. Rev. **185**, 1 (1969).
[19]A.A. Dorozhkin, A.A. Petrov, and N.N. Petrov, Sov. Phys. Solid State **20**, 1660 (1979).
[20]P. Bisgaard, R. Bruch, P. Dahl, B. Fastrup, and M. Rodbro, Phys. Scr. **17**, 49 (1978).
[21]J.F. Hennequin and P. Viaris de Lesegno, Surf. Sci. **42**, 50 (1974).
[22]L. Viel, C. Benazeth, and N. Benazeth, Surf. Sci. **54**, 635 (1976).
[23]L.J. Kieffer, At. Data **1**, 19 (1969).
[24]K. Wittmaack, Surf. Sci. **85**, 69 (1979).
[25]W.A. Coghlan and R.E. Clausing, At. Data **5**, 338 (1973).

Appendix v

Listing of Publications

Title	Authors	Journal/Status	Percentage Union Carbide Support
Trapping and Re-emission of 0.125 t0 1 keV Deuterium in Stainless Steel	E. W. Thomas	J. Appl. Phys. 51, 1176 (1980)	10%
Time Resolved Metal Impurity Fluxes in the DITE Tokamak.	E. W. Thomas J. Partridge J. Vince	J. Nucl. Mat. 89, 182 (1980)	10%
Ion Induced Auger Spectroscopy.	E. W. Thomas K. O. Legg W. A. Metz	Nucl. Instr. Methods 168, 379 (1980)	50%
Auger Spectra Induced by Ion Impact on Metals.	K. O. Legg W. P. Metz E. W. Thomas	Nucl., Instr. Methods 170, 561 (1980)	50%
The Auger Spectra Induced by 100 keV Ar^+ Impact on Be, Aℓ and Si.	W. A. Metz K. O. Legg E. W. Thomas	J. Appl. Phys 51, 2888 (1980)	50%
Scattering of 5 and 15 keV H^+ from Surfaces	J. E. Harriss E. W. Thomas	Nucl. Instr. and Methods. 170, 513 (1980)	80%
Scattering of 5 to 30 keV Hydrogen from Surfaces	J. E. Harriss R. Young E. W. Thomas	J. Appl. Phys. 51, 5344 (1980)	80%

(OVER...)

Title	Authors	Journal/Status	Percentage Union Carbide Support
Small Angle Scattering of Hydrogen from Surfaces.	J. E. Harriss R. Young E. W. Thomas	J. Nucl. Mat. (To be publd)	80%
Oxygen Desorption from Transition Metals by Hydrogen Ion Bonbardment.	E. W. Thomas R. Whaley K. O. Legg.	In preparation	80%

PROGRESS REPORT NO. 2

ORNL/Sub-7802/X05/2

INTERACTION OF ENERGETIC HYDROGEN WITH SURFACES

by

E. W. Thomas
K. O. Legg
R. P. Young
L. Riddle

Prepared for

OAK RIDGE NATIONAL LABORATORY
OAK RIDGE, TENNESSEE 37830

Operated by

UNION CARBIDE CORPORATION

For the

DEPARTMENT OF ENERGY

Contract No. W-7405-eng-26
Sub Contract No. -7802

30 September 1981

GEORGIA INSTITUTE OF TECHNOLOGY
School of Physics
Atlanta, Georgia 30332

1981

INTERACTION OF ENERGETIC HYDROGEN WITH SURFACES

PROGRESS REPORT NO. 2

Covering the Period

November 1, 1980 to September 30, 1981

by

E. W. Thomas

K. O. Legg

R. P. Young

L. Riddle

Report Prepared by:

The Georgia Institute of Technology

School of Physics

Atlanta, Georgia 30332

Under subcontract number 7802 for

Oak Ridge National Laboratory

Oak Ridge, Tennessee 37830

operated by

Union Carbide Corporation

for the

Department of Energy

Contract No. W-7405-eng-26

30 September 1981

TABLE OF CONTENTS

I. Title

Interaction of Energetic Hydrogen with Surfaces.

II. Contract Number

This report covers work performed on particle-surface interactions under a contract between Union Carbide Corp with the Georgia Tech Research Institute. The work is covered by Project Authorization No. X05 under Basic Ordering Agreement No. 7802 (under DOE Prime No. W-7405-eng-26).

The work is an extension of studies performed earlier under contract AT-(40-1)-2591 for the U. S. Department of Energy. This direct contract was terminated on 29 February 1980 and superceded on 1 March 1980 by the contract with Union Carbide.

This report covers the period 1 November 1980 to 30 September 1981.

III. Abstract

The program is devoted to studies of particle-surface collision phenomena relevant to plasma-wall interactions in plasma devices. We report measurements of time resolved Balmer-alpha emission that show relative behavior of recycling at various points in the machine. Surprisingly, recycling in the limiter region is only slightly (50 to 100%) higher than that elsewhere except when the west beam line injector is fired,when recycling at the limiter is four times that elsewhere. We report some further analysis of an experiment to monitor recycling by following the ratio of H to D as the Tokamak working gas is changed from H to D and from D to H. There is some indication that recycling behavior is not uniform at all parts of the wall's surface. Final results of an experiment on hydrogen backscattering from surfaces are reported along with preliminary data from a new experiment to measure retention, re-emission and permeation of ion implanted hydrogen.

Finally, we describe briefly progress on construction of a new experimental arrangement that will permit time resolved measurement of impurity flux to the wall.

IV. Discussion of Progress

During the present reporting period we have been engaged in a variety of studies. These include three laboratory based experiments performed at Georgia Tech. and three diagnostic experiments based on the ISX-B Tokamak at Oak Ridge. Of the six separate projects two are finished and published, one is finished and being analyzed while the remaining three are still under way. To describe these activities we have prepared a number of fairly detailed discussions which are attached to this report as appendixes. Here we shall restrict ourselves to brief summaries of the highlights of the work and refer the reader to the Appendixes for details.

A. Hydrogen Recycling; H_α Emission

Balmer alpha emission from the plasma edge is thought to be from hydrogen leaving the device wall and being excited by electron impact as it enters the plasma edge. Thus the Balmer alpha emission intensity detected at a point in the device represents local recycling of hydrogen from the wall at the point of observation. It is planned to place six H_α detectors at various points in ISX-B to search for asymmetries in recycling.

To date two such detectors have been placed on ISX-B, one at the limiter sector (# 14) and one at a general position (sector # 8). A detailed report on the preliminary observations is given as Appendix I.

The general observations are that re-cycling from the limiter section is only 50 to 100% larger than that in the general position (sector 8). When the west beam line is fired the recycling at the limiter becomes 400%

larger than at the general position. Firing the east beam line has no significant effect on signals from either position. The signals are strongly affected by the gas puff cycle and correlate closely with machine instabilities particularly excursions in the horizontal shift monitor. Some of the raw data is reproduced in Appendix I. We are gathering further amounts of data and are attempting to develop some model of these observations.

B. Hydrogen Recycling in ISX-B; H/D Changeover

One may study hydrogen recycling in a Tokamak by operating first on one isotope (say D) then changing to another (say H) and observing the density of the first isotope in subsequent discharges using the second as a filling. We preformed such an experiment on ISX-B using separately detected optical emission from the Balmer alpha lines of H and D to provide the measurement of plasma composition. The experiment is detailed in Appendix II and led to the conclusion that some 60% of the machine's working fuel comes from the wall and not from the filling gas. It now appears that this conclusion may be erroneous; the interpretation of the data is under review. It has always been appreciated that detection of Balmer alpha radiation provides only a local measurement of hydrogen flux emerging from the wall and entering the plasma. It was, however, assumed that plasma and wall rapidly acquired the same relative populations of hydrogen isotopes so that the signal represented also the relative concentration of H and D in the machine. While this appears to be true for observations in the mid-plane of ISX it is not the case for observations in a vertical direction where the signals represent re-emission from the top and bottom surfaces. There is the implication that hydrogen recycling exhibits poloidal asymmetry. We are considering the possibility of performing a direct experimental test of this contention.

C. Ion Induced Desorption of Oxygen

We performed a brief series of experiments to study removal of adsorbed oxygen by impact of hydrogen ions. For 50 to 200 keV H^+ removing adsorbed oxygen from Ti and Fe the process is a simple sputtering mechanism with a cross section of around 10^{-18} cm^2. For H_2^+ (and H_3^+) impact we observed very sharp increases of cross section by one to two orders of magnitude over those exhibited by H^+. These rises undoubtedly represent a threshold for commencement of some inelastic desorption mechanism. Comparison with electron induced desorption suggests that the process is electron stimulated desorption by excitation of an inner shell vacancy with the electron being obtained by stripping from the projectile. Protons do not have an available electron so proton impact does not induce the effect. The full details of the experiment are contained in Appendix III which is a preprint of a paper that is about to be published.

The effect is of some intrinsic interest and represents the first observation of ion induced desorption proceeding by a quantum process. In the event that neutral beam injectors are operated at 100 to 200 keV then we would predict rather large impurity loads due to this effect where the beams strike surfaces.

This particular project is now terminated and all significant data are accepted for publication.

D. Scattering of Hydrogen from Surfaces

We have produced a final publication on our experiments to study backscattering of H^+ and D^+ from surfaces for incident energies around 1.8 to 15 keV. We conclude that distribution of the reflected particles among the various possible charge states is governed by bi-particle collisions at the

surface and is not related to band structure. Energy distributions are in good agreement with calculations by the TRIM computer simulation code. These data are the first that confirm TRIM for near grazing incidence and emergence.

Full details of the work are contained in Appendix IV which is a reprint of a recent publication. This project is completed and terminated.

E. Reflection, Re-emission and Permeation of Deuterium in Metals

We have recently completed fabrication of a new system to study interaction of hydrogen with metals. A deuterium beam is incident on a target and the rate of deuterium re-emergence from the sample measured by the rise of deuterium pressure in a chamber located in front of the target. On commencing bombardment the pressure rise represents only reflection. The pressure then increases with dose as implanted deuterium diffuses to the surface and re-emerges (or re-emits). Finally, the signal reaches a plateau indicating that the target is saturated and that re-emission is occurring at the same rate as implantation. One can also study the permeation of deuterium through to the back surface by monitoring the pressure rise in a chamber behind the sample. We would anticipate no initial permeation when bombardment is commenced but this will build up to a constant value as the target becomes saturated. Our initial studies show the expected behavior and we are able to measure reflection, re-emission from the front (bombarded) surface and permeation through to the back (unbombarded) surface. Initial results are in good agreement with the work of others where comparisons are possible.

Full details of the experiment and results obtained to date are given in Appendix V. This experiment continues.

F. Time Resolved Fluxes of Impurities

A well established technique for monitoring impurity fluxes to the plasma edge is to rotate a cylindrical collector behind a slit so that incident material is deposited as a streak. The probe may then be removed for analysis by any one of the conventional surface analysis techniques so that deposit density may be measured quantitatively and impurity flux estimated. We are constructing such a device for addition to the sample transport system of ISX-B. Details of the progress to date are contained in Appendix VI. Experiments are scheduled to commence early in 1982 after the end of the ISX shut-down.

IV. Related Activities

Dr. Thomas, the Project Director, has been working on an IAEA project to produce a compendium of data suitable for use by plasma modellers. The project was initiated by Dr. Langley of the IAEA and will culminate with a report to be published in Nuclear Fusion. Dr. Thomas' particular contribution was a review of data on secondary electron emission initiated by impact of electrons and ions on solids. Apart from review and data collection the project required attendance at a one week workshop held at the IAEA in Vienna. Work on this project is essentially complete.

Dr. Thomas will also submit a contribution to a workshop on Atomic Data for plasma-wall interaction modelling to be held in Nagoya, Japan, in December 1981.

V. Conferences and Travel

During the period covered by this report Dr. Thomas attended the following two conferences.

(a) "International Conference on Atomic Collisions in Solids," Lyons, France, July 1981.

(b) "Workshop on Atomic Data for Modelling Plasma-Wall Interactions," IAEA Vienna, Austria, July 1981.

Dr. Thomas also visited the Culham Laboratory of the UKAEA and DOE headquarters. Numerous visits were made by Drs. Thomas, Dr. Legg, Mr. Young and Mr. Riddle to Oak Ridge for the purpose of performing experiments on ISX-B.

VI. Personnel

Professor E. W. Thomas has been Project Director and Principal Investigator devoting approximately 27.5% of his full time to this project.

Dr. K. O. Legg, Research Scientist, occupies the position of Co-Principal Investigator, and devoted approximately 30% of his full time to this project.

Mr. R. P. Young has been the principal graduate student on this work during the present reporting period drawing 50% of full time support. Mr. Larry Riddle worked on the project as a graduate research assistant at no cost to the project.

VII. Appendixes

I. Interim Report of Data from H_α Monitors.

II. A Re-cycling Experiment on the ISX-B Tokamak.

III. An Inelastic Mechanism for Ion Induced Desorption of Oxygen from Titanium and Iron. (A pre-print of a paper to be published in J. Nucl. Materials.)

IV. Small Angle Scattering of Hydrogen from Surfaces. (A reprint of a paper in J. Nucl. Materials, 93 and 94, 524 (1980).)

V. Reflection, Re-emission and Permeation of Deuterium in Metals.

VI. Time Resolved Probe for Detecting Contaminants in the Plasma Edge.

APPENDIX I

Interim Report of Data from H_α Monitors

E. W. Thomas and R. P. Young

Two detectors sensitive to the Balmer alpha line of hydrogen were placed on ISX-B on 24 July 1981. One was placed in sector 14 (limiter sector) and the other in sector 8. Both look vertically through the machine and are well collimated detecting photons from atoms in a 2.54 cm diameter cylindrical region centered along the device axis. The signal is presumably caused by hydrogen entering the plasma edge and being excited by electrons. In principal, the signals are related to the hydrogen emerging from the wall as a result of recycling processes and our detectors are monitoring such recycling at the top and bottom surfaces of ISX-B, both of which lie in their field of view. Both detectors are positioned at approximately the middle of the torus so they are not receiving signals from the inner and outer walls. The detectors have equal sensitivities and absolute values of detection sensitivity are known approximately. The detector in the limiter region has been provided with a neutral density filter to prevent saturation due to the high signals in this region; the attenuation factor has been taken into account in the following discussions.

The detectors have been in place since 24 June and records of their output are available for 24 June, 24 to 31 July and for 3, 4, 5 August. The detector in sector 8 is placed to provide an indication of behavior at a general point in the machine while the detector in sector 14 is to provide behavior in the specific region of the limiter. More detectors are being fabricated to provide a broad view of toroidal asymmetries. The following discussion is designed to provide an interim report on observations to date.

General Behavior

Figs. 1, 2 and 3 show typical results on successive shots 39494, 39495 and 39496, respectively. The full line is the detector in sector 8; its scale is to the left. The dashed line is the detector in sector 14 (the limiter sector); its scale is to the right and should be multiplied by ten to correct for the neutral density filter in that position. Both detectors have a small zero offset that should be subtracted; this is shown on all figures. In all cases the signal starts low, rises at about 100 m sec, equilibrates to a new level and in some cases shows a further later rise (see the limiter signal at 200 m sec in Fig. 3). The various sharp spikes correlate with indications of machine instability. In particular, the largest spikes at 190 m sec in Fig. 1, 260 m sec in Fig. 2 and 215 m sec in Fig. 3 all coincide in time with a large, short duration, negative excursion in the horizontal in - out shift monitor. We note that the excursion occurs on both traces. In general, the signal from the limiter region (dashed line) after multiplication by ten (to correct for the neutral density filter) is about a factor of 1.5 to 2 times greater than the signal from sector 8.

Ratio of Signals from Sectors 14 and 8

A major reason for performing these experiments is to search for Toroidal asymmetries in recycling and this can be qualitatively probed by recording the ratio of the H_α signals from the two detectors. In Fig. 4 we show this ratio of the limiter signal (sector 14) and the signal from the non-specific location (sector 8) for shots 39494, 5 and 6 (the records of Figs. 1, 2 and 3). Also indicated are facsimilies of the gas puff (essentially the same for all three shots) and the neutral beam current. (No beams for shot 39494, EBL only for 39495 and both beams used for 39496.)

For much of the discharge period the ratio is 1.5 to 2.0 implying that recycling at the limiter is only slightly greater than that at a general wall position. An unusual, but quite repetitive feature seen here and in many other cases is a rise to 2.5 or 3.0 at about 60 m sec corresponding apparently to a minimum in the gas puff rate. Shot 39495 involved neutral injection from the East beam line but gives essentially the same ratio as 39494 which involves no injection; reference to Figs. 1 and 2 shows that the absolute magnitude of the signals are also the same in both shots. Shot 39496 involves injection from both beam lines and displays a substantial rise in the limiter signal and a small rise in the sector 8 signal (see Fig. 3) with the result of an increase in the ratio to about 4.5 (see Fig. 4). Thus firing the west beam line enhances signal at both points with the signal from the limiter being 4.5 times that in sector 8. Since the rise in signals is somewhat slower than the rise in beam current we would argue that it is not simply due to excited atoms in the injected beam passing the viewing field of the detector. Firing the East beam line has no effect on signals.

It is instructive also to relate the magnitudes of signals to gas puff. Both detectors show a small rise in signal at about 50 m sec (Figs. 1, 2, 3) slightly after the crest of the first peak in the gas puff (Fig. 4). Both detectors also show a rise at about 100 m sec which correlates with the second major puff peak at 100 m sec; the new level is then maintained. These characteristics are independent of neutral beams since they occur in shot 39494 (no beams - Fig. 1) shot 39495 (EBL only - Fig. 2) and 39496 (both beam lines, Fig. 3). Thus the rises in signals are correlated with gas puff. Note, however, that the ratios of signals remain essentially constant (except for the features at 60 and 180 m sec mentioned above).

In general terms these characteristics are displayed in most of the records examined. One discrepancy is, however, worthy of note. In some of the early records the ratio of signals (limiter ÷ sector 8) was higher. For discharge 37636 the ratio was about 5 and relatively unchanging throughout the discharge. For discharges around 37662 the ratio became as high as ten (at 120 m sec) but this may have been unusual; there are, in fact, no records beyond 120 m sec in this case because the detectors both saturated. The discharges of this day (6/24/81) were characterized by very high gas puffs kept fairly constant until the end of the discharge. For shot 37636 the puff was about 25 torr-L/s and constant; for 37662 it was off scale and therefore exceeded 50 torr-L/s. It would appear that the high signal ratios (and indeed signal strengths) were related to the long high gas puff.

Absolute Magnitudes

A rough calibration of detection sensitivity has been made showing that 2000 units on the trace scale corresponds to a photon flux of 1.5×10^{12} photons sec^{-1}. We have attempted to interpret this with the following simple model.

Let us suppose that the hydrogen is recycling from the wall and has a number density N_H (atoms cm^{-3}) velocity V_H (cm sec^{-1}). It penetrates into the edge of the plasma where it encounters electrons of density N_e (electrons cm^{-3}) with an average velocity V_e (cm sec^{-1}) and are excited to the n = 3 level with a cross section σ. Since $V_H << V_e$ the hydrogen is essentially at rest and the excitation rate is simply $N_H N_e V_e \sigma$. Of the excited states only a certain fraction F emit the Balmer α line (the rest emit Lyman β) so the photon emission rate N_ν photons cm^{-3} sec^{-1} is given by

$$N_\nu = F N_H N_e V_e \qquad (1)$$

The observed signal is equal to the product of this emission times the effective volume from which detection occurs V, the detector solid angle ω, detection sensitivity S so:—

$$\text{Signal} = N_\nu VS\omega = (F\ N_H\ N_e\ V_e\ \sigma)\ VS\omega \qquad (2)$$

Let us make the following estimates:

$N_e = 2.5 \times 10^{12}$ cm^{-3} (Private communication by Peter Mioduszewski - for edge of ohmically heated plasma in ISX).

$T_e = 40$ eV (ditto).

$V_e = 3.8 \times 10^{8}$ cm/sec.

$\sigma = 0.23\ \pi\ a_o^2$

$\equiv 2.02 \times 10^{-17}$ cm^2 (Theoretical estimate B. L. Moiseiwitch and S. J. Smith, Rev. Mod. Phys. 40, #2 (1968)).

$F \approx 1/10$ (Assuming excitation is mainly to the 3p state).

$S = \left(\frac{1.5 \times 10^{12}}{2000}\right)^{-1}$ (Photons sec^{-1} per scale division)$^{-1}$.

$\omega = 0.013$ (Detector has a 2.54 cm circular aperture and is assumed to be 20 cm from the top plasma edge. We neglect any contribution from the bottom of the plasma since the effective solid angle will be much smaller.)

$V \approx 4.0$ cm^3 (The effective area of the cylindrical pipe-like region from which emissions are collected times the thickness of the plasma edge which we arbitrarily assume to be 1 cm).

Signal = 250 scale units (Taken from the sector 8 trace on Fig. 3 at 150 m sec and reasonably representative also of Figs. 1 and 2).

Inserting all these factors we can estimate the one remaining factor - N_H, the density of hydrogen. We obtain

$$N_H \approx 1.9 \times 10^9 \text{ H atoms cm}^{-3}$$

Now if these H atoms are emerging from the wall with say 5 eV of energy, then their flux is 5.7×10^{15} H atoms cm^{-2} sec^{-1}. If the source of H is a displacement type of re-emission mechanism (with one H atom ejected for every H atom or ion incident on the wall) and the wall is at a saturated or equilibrium situation then the flux of atoms onto the wall is also 5.7×10^{15} cm^2 sec^{-1}. J. Roberto states (private communication) that the integrated flux of hydrogen to a probe at the limiter radius is about 10^{15} H atoms cm^{-2} per shot of 200 m sec or a flux of about 5×10^{15} H atoms cm^{-2} sec^{-1}.

The apparent agreement between our estimate of flux to the wall (5.7×10^{15} cm^{-2} sec^{-1}) and Roberto's measurement (5×10^{15} cm^{-2} sec^{-1}) is quite certainly fortuitous. The only conclusion we would wish to draw from this is that our measured signals are not inconsistent with the simple model expressed by Equation 1.

Relationship to Ne

If Equation 1 is indeed applicable to the prediction of the photon signal then signal should be proportional to electron density. Dividing signal by electron density one should achieve a parameter proportional to hydrogen density and hence flux (assuming V_e and V_H do not change). We have no measure of N_e in the plasma edge but presumably this is at least proportional to N_e measured in the body of the plasma by the 2 mm microwave.

In Table I we show the observed photon signal from sector 8, our reading of N_e from the 2 mm records, and the ratio of the two signals for shot 39496

and 39501. Setting aside sharp fluctuations what we see is that the ratio (and therefore presumably the hydrogen flux) is roughly constant to 100 m sec and then increases by 50%; thus the rise occurs at around the major peak of the gass puff.

Summary

(1) Both detectors show a general rise throughout the discharge.

(2) Rises in both signals correlate to increases in gas puff.

(3) The signal in the limiter region shows a major rise on firing the West Beam line; the rise in sector 8 is smaller. Firing the East Beam line has no effect on these signals.

(4) The ratio of limiter to sector 8 signals is typically 1.5 to 2.0 for conditions of 8/3,4,5/81 rising to 4.5 when west beam line is fired. The same ratio is five for conditions of 6/24/81 when high constant gas puffs were used; a ratio of almost ten seen at one or two points on that day is non typical.

(5) The signal levels are approximately what would be expected if the flux emerging from the wall was equal to the flux incident on the wall (which has been measured previously).

(6) The result of dividing signal level by N_e is presumably proportional to recycled flux. This ratio is constant for small gas puffs early in the discharge and rises when the gas puff is increased.

(7) Erratic signals correlate with machine instabilities particularly with negative excursions in the horizontal shift monitor.

Table I.

Ratio of H_α Signal to Electron Density

t m sec	H_α signal (arby units)	N_e (arby units)	$\frac{H_\alpha \text{ signal}}{N_e}$ (arby units)
Shot 39496			
0	-	-	-
25	80	0.1	800
50	80	1.0	80
75	60	0.5	120
100	160	2.0	80
125	320	3.5	91
150	500	4.0	125
175	200	5.0	140
200	870	5.0	174
Shot 39501			
0	-	-	-
25	30	0.1	300
50	40	1.0	40
75	30	0.7	43
100	80	2.0	40
125	230	3.2	72
150	270	4.0	67.5
175	330	5.0	66
200	400	7.0	57
225	780	8.5	92

Figure Captions

Figure 1. H_α signal traces from shot 39494. Sector 8 is the continuous line and has the scale to the left with the effective zero of signal as indicated. Sector 14 (limiter) is the dashed line with the scale and zero to the right; this scale must be multiplied by ten to account for a neutral density filter in this detector.

Figure 2. H_α signal traces from shot 39495. For details see caption to Fig. 1.

Figure 3. H_α signal traces from shot 39496. For details see caption to Fig. 1.

Figure 4. Top three traces show the ratio of signals from sector 14 to signal from sector 8 for shots 39494, 39495, 5 and 6 corrected for zero offset and for filter characteristics. At the bottom is a facsimile of the gas puff trace (same for all three shots) the East Beam line current (fired on shots 39495 and 39496) and the West Beam line current (fired on shot 39496 only).

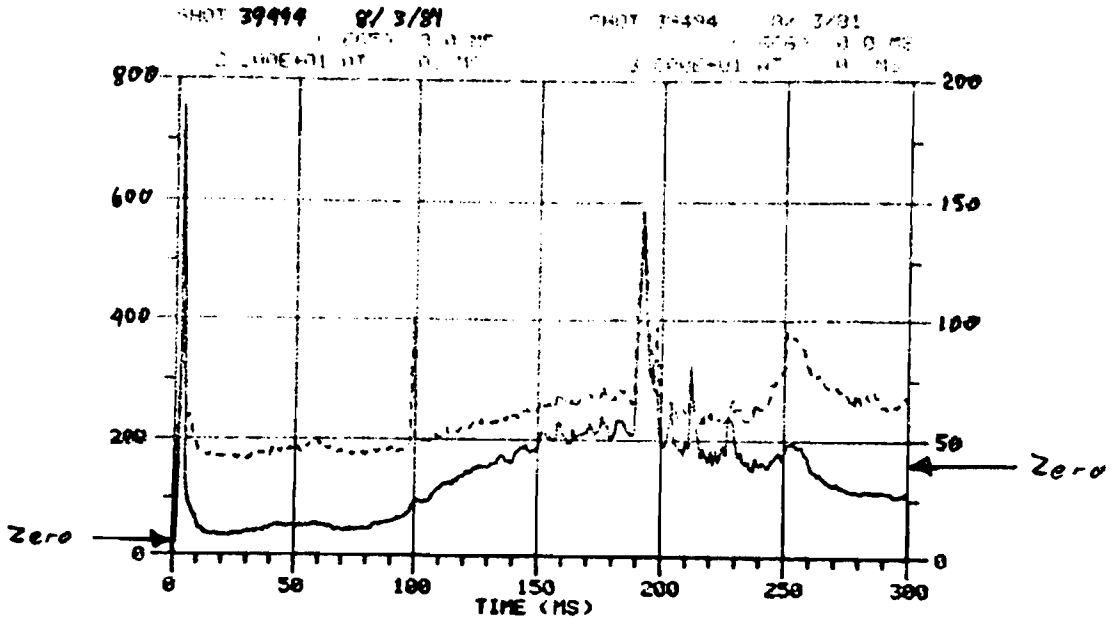
SHOT 39494 8/ 3/81
800
600
400
200
0
200
150
100
50
0
Zero
Zero
0
50
100
150
200
250
300
TIME (MS)

Fig 1

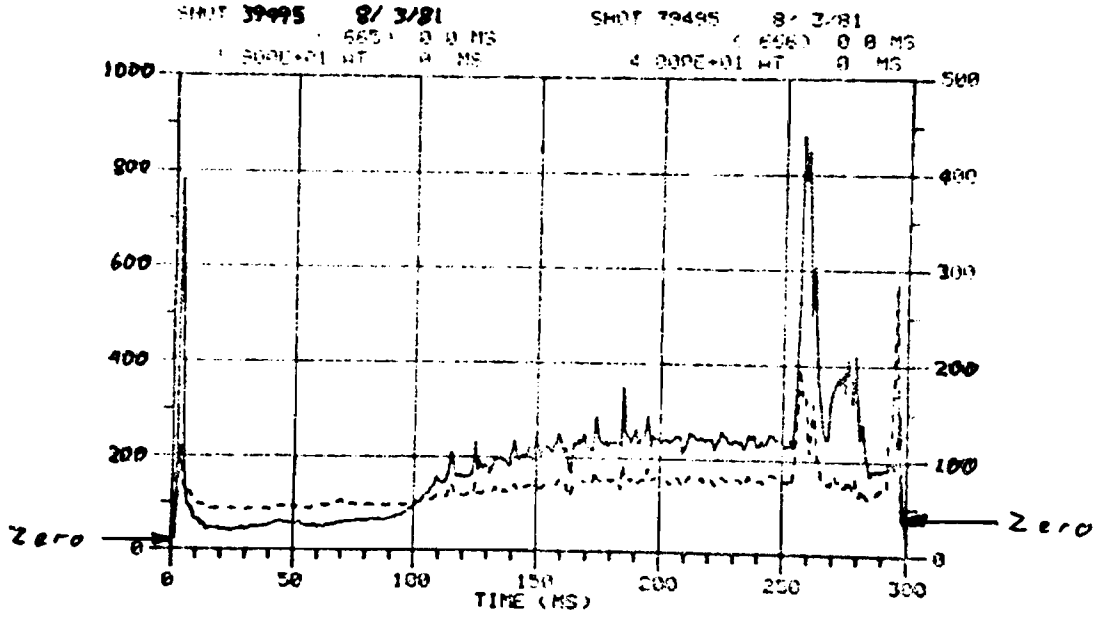
SHOT 39495 8/ 3/81
1000
800
600
400
200
0
500
400
300
200
100
0
Zero
Zero
0
50
100
150
200
250
300
TIME (MS)

Fig 2

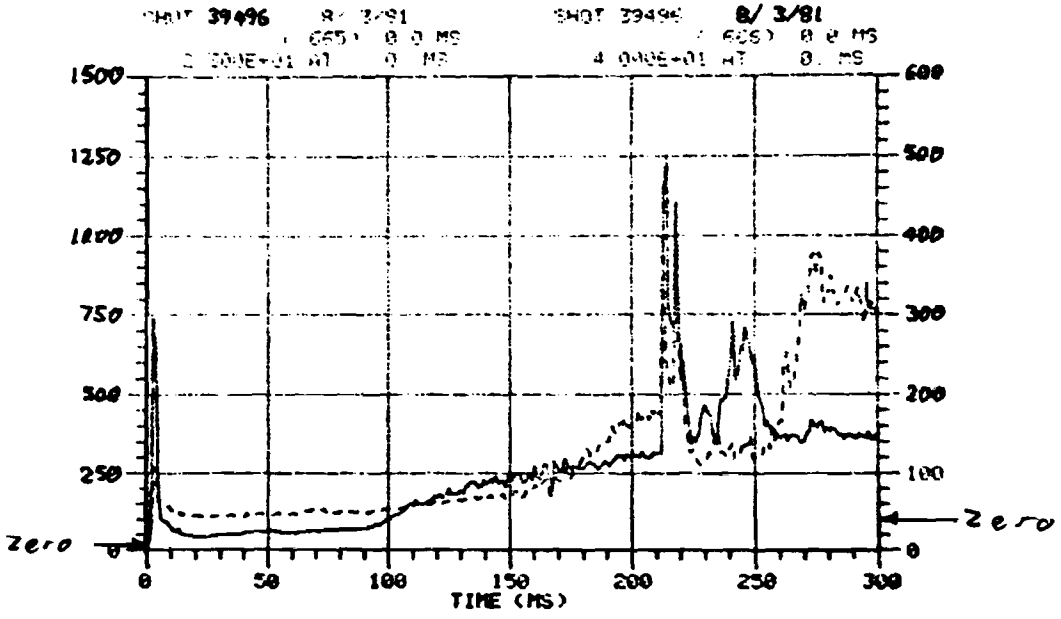
SHOT 39496 8/ 3/81
SHOT 39496 8/ 3/81
1500
1250
1000
750
500
250
zero
0
600
500
400
300
200
100
0
zero
0
50
100
150
200
250
300
TIME (MS)

Fig 3

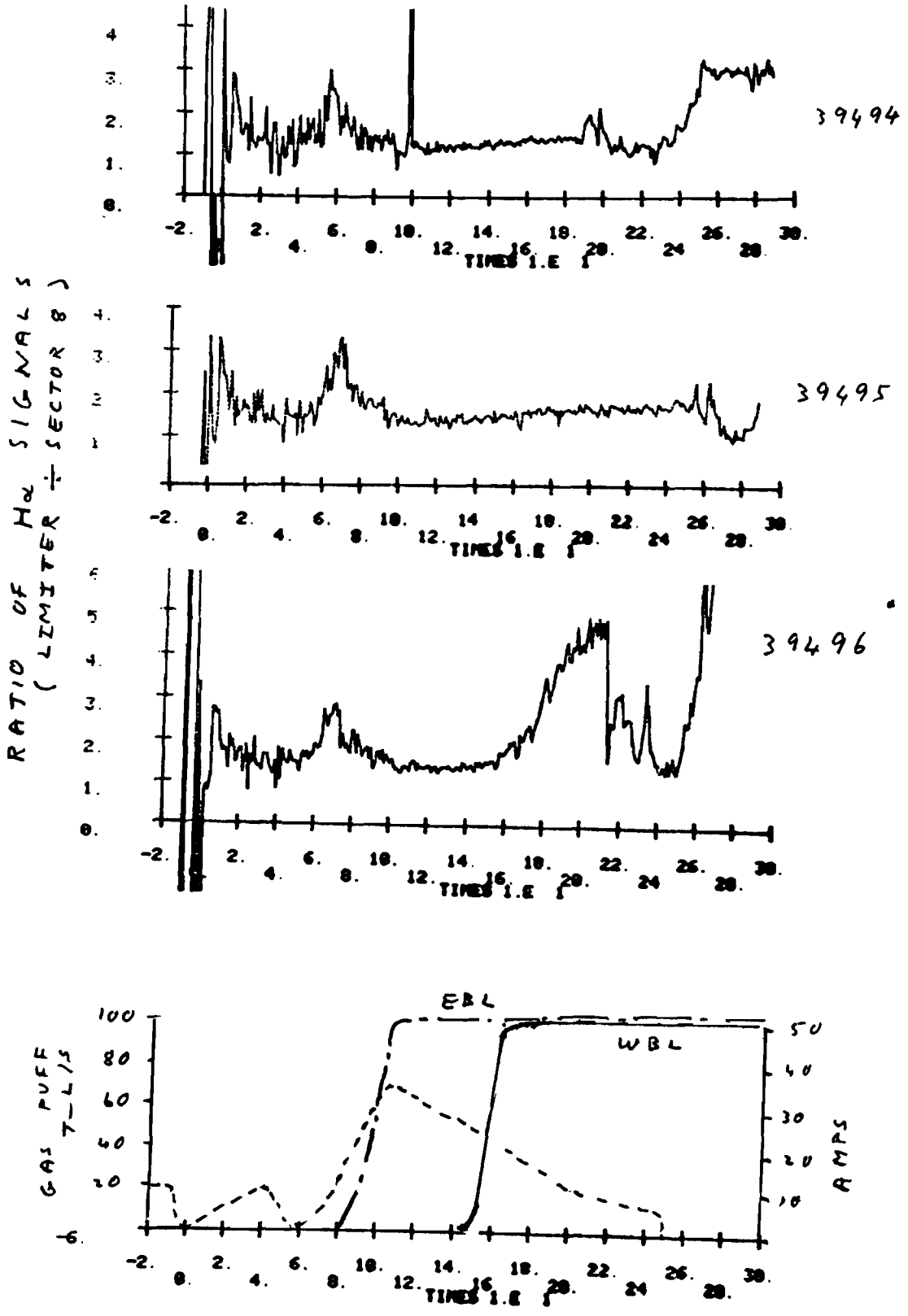
RATIO OF Hα SIGNALS
(LIMITER ÷ SECTOR 8)
39494
39495
39496
TIMES I.E
EBL
WBL
GAS PUFF
T-L/S
AMPS

Fig 4.

APPENDIX II

A Re-cycling Experiment in the ISX-B Tokamak

by

R. P. Young, R. S. Whaley, and E. W. Thomas

School of Physics

Georgia Institute of Technology

Atlanta, Ga. 30332

Abstract. The isotopic composition of the ISX-B plasma is studied as the working gas is changed from D_2 to H_2 and back again by monitoring the intensities of the Balmer alpha lines of these two isotopes. It is found that it takes some four ohmically heated discharges to change the plasma composition to the new isotope. We conclude that some 60% of the hydrogen taking part in a discharge of ISX-B is in fact from the walls.

INTRODUCTION

In present day Tokamaks the particle confinement time is typically ten times less than the duration of the tokamak discharge so that the hydrogen in the plasma is replaced many times by the processes known generally as recycling. Ions, or charge exchange neutrals, exiting the confinement region and impacting on the device wall will in part be reflected and in part be retained in or on the wall. After repeated device operation the wall surface will become saturated with hydrogen so that atoms arriving in subsequent discharges must displace atoms already present. An effective method for studying retention and displacement is to monitor the H and D components in a plasma as one changes the operating gas from (say) D_2 to H_2. In the first discharge in the new gas (H_2) any contribution of the other isotope must be due to deuterium from previous operation retained in (or on) the vessel wall. The use of such H/D changeover experiments to study recycling was pioneered by McCracken *et al.* [1] in the study of the DITE Tokamak, and have also been performed on TFR [2] and on Alcator [3]. Our objective here is to perform a similar study on the ISX-B machine.

In order to monitor the relative contribution of H and D to device operation we detect optical radiation from the Balmer alpha lines of H and D, which are separated by 0.176 nm. Resolution is by a Fabry Perot interferometer [4] operating at an interference order of about 1830. Detection is by a photomultiplier. By repetitive scanning of the Fabry Perot Interferometer one may obtain, during one discharge, a number of sequential records of relative H and D concentration. The interferometer was arranged to view vertically downward along a chord of the ISX-B plasma at a major radius of about 93 cm. The experimental arrangement was very straighforward and is shown on Fig. 1. A discharge lamp operating on a mixture of H_2 and D_2 was

incorporated to permit periodic checking of the Fabry Perot resolution and retuning of the resonant cavity. A 10 Å wide filter was used to filter out emissions at other wavelengths.

RESULTS

The present series of experiments were performed with ohmically heated discharges where plasma currents were typically 160 kA, ion temperatures about 1 keV and particle densities about 10^{22} m^{-3}. Gas filling was carried out by a piezo-electric valve open for 50 ms before the start of the discharge followed by continuous gas puffing during the discharge. Before experiments were commenced the machine was discharge cleaned using a tokamak type discharge for a period of 10 hours.

Figure 2 shows a typical trace from the detector using a discharge in deuterium after extensive deuterium operation. Shown also is a trace of the ramp voltage driving the Fabry Perot at 50 msec per sweep with a 10 msec flyback. In each scan we traverse the D_α line twice. The trace shows the signal decreasing to a fairly constant value in the region 70 to 140 msec with a rapid (and non reproducible) rise at the end where MHD instability occurs. The measurements to be presented later were taken at about 120 msec where the discharge is stable. In operation with both H and D present the trace has an additional peak due to H between the two D peaks in a scan. Widths of the peaks are due mainly to instrumental effects and are similar for H and D; we therefore took the signal to be simply proportional to peak height. We shall present our data as a ratio of signals T; this is equal to the height of the D peak divided by the sum of the H and D peak heights.

In Fig. 3 we show the variation of our optical signal as a gas changeover occurs.

Prior to taking the data of Fig. 3a the Tokamak had been operated for 38 discharges on D_2; shot 1 was the first of a series of discharge in H_2 gas and clearly the deuterium signal remains very significant. Due to noise in the signal we estimate that these data points are reliable only to $\pm$ 20% and it is therefore not clear whether the deuterium signal eventually decays completely to zero. However, it is clear that the deuterium signal has largely disappeared after 4 discharges. In Fig. 3b we show the reverse change where the device has been operated for 28 discharges on hydrogen and the filling gas is changed to deuterium. Again after four discharges the signal is due entirely to the new filling gas. Thus the data qualitatively indicate changeover is essentially complete in four discharges.

DISCUSSION

McCracken et al. [1] argue that the optical signal is proportional to the flux of hydrogen emerging from the wall and entering the plasma edge. This flux will include an energetic component representing ions and charge exchange neutrals reflected from the wall. It will include also near-thermal energy atoms ejected from the wall by the impact of the ions and by charge exchange neutrals from the plasma; these ejected atoms will have been implanted into the wall at an earlier stage in the discharge or during previous discharges. McCracken et al. [1], argue that the optical signal from D (or from H) is proportional to the flux F of atoms entering the plasma from the wall. We shall assume this also to be true here so that the measured intensity ratio T, shown in Fig. 3, is related to optical intensity I and entering flux F by the equations

$$T = \frac{I_D}{I_H + I_D} = \frac{F_D}{F_H + F_D} \qquad (1)$$

where the subscripts H and D indicate the respective contributions from these two isotopes.

The data of Fig. 3a shows clearly that at 120 m sec into the first discharge after changeover some 60% of the hydrogen entering the edge is D and therefore is hydrogen retained on or in the wall as a result of earlier discharges in deuterium. Fig. 3a shows a similar result for the changeover from H to D operation. For other machines the percentage of hydrogen from the wall retained isotope was 60% to 70% in DITE [1], 70% in ALCATOR [3] and 20% to 30% in TFR [2]. Figs. 3a and 3b further show that the changeover to the new working gas is 80% to 90% complete after four discharges. By comparison changeover to a similar level took 15 discharges in DITE [1], 10 discharges in ALCATOR [3], and about two discharges in TFR. It is not at all clear whether it is valid to compare these various results from different Tokamaks since the observations are under different conditions, with different types of machines. However in a spirit of academic comparison we show in Fig. 4 data for a change from H to D operation from three machines using our own data from Fig 3b, data from DITE [Fig. 4b of Refc. 1] and from TFR [Fig. 5 of Refc. 2].

These present experiments give us no information on the mechanism whereby the hydrogen is retained in or on the wall. Certainly hydrogen incident at some energy is implanted and trapped in the manner discussed (among others) by Thomas [5]. There may also be conventional adsorption on the surface. Since trapping in stainless steel will give rise to a retention of 10^{20} atoms m^{-2} or more [5] and adsorption gives rise to a retention equivalent to a monolayer, say 2×10^{19} atoms m^{-2}, trapping probably represents the majority of the retained hydrogen. We would argue that trapping and de-trapping are probably the mechanisms of principal importance; this was the position taken by McCracken et al. [1] in analysing experiments on DITE.

One should recognize two distinct parts of the device wall that will undergo substantially different recycling behaviour. There is in each machine a limiter which suffers a high bombardment flux. With the trapped hydrogen density in stainless steel being about 10^{20} atoms m^{-2} at room temperature [5] and the bombardment flux to the limiter of the order 10^{23} m^{-2} sec^{-1} [6] it is clear that the hydrogen trapped after one discharge will be entirely liberated early in the next discharge. There is secondly the toroidal wall which suffers a much lower bombardment flux and which may require a number of successive discharges to cause a complete isotopic exchange. Thus the first discharge will show a complete exchange in the limiter and successive discharges will show a slower exchange in the toroidal wall. The data in Fig. 5 from TFR and from DITE seem to be consistent with such a behaviour with a large change on the first shot followed by a slower component. Allowing for the error bars on the present data for ISX such a two component changeover may be also occuring here.

CONCLUSION

The data show unambiguously that some 60% of the observed hydrogen signal is from atoms that were retained in the wall from previous discharges and only 40% is due to the filling gas. Thus the wall is a major source of fuel as it is for DITE [1] and for TFR [2] and for ALCATOR [3]. Isotopic changeover is largely completed after 4 discharges, roughly consistent with TFR and much faster than on DITE.

ACKNOWLEDGEMENTS

We are grateful to Drs. J. Roberto, R. Zure and R. Isler, and also to the ISX-B operations team, for their considerable assistance in performing these studies. The work was, in part, supported under sub-contract with the Oak-Ridge National Laboratory, operated by Union Carbide for the Department of Energy (Contract No. W-7405-eng-26).

REFERENCES

[1] G. M. McCracken, S. J. Fielding, S. K. Erents, A. Pospieszczyk and P. E. Stott, Nuclear Fusion 18 (1978) 35.

[2] P. Platz, J. Nucl. Mater. 93&94, 173 (1980).

[3] E. S. Marmar, J. Nucl. Mater. 76&77, 59 (1978).

[4] Burleigh Instruments Inc., East Rochester, N.Y. Model RC 40.

[5] E. W. Thomas, J. Appl. Phys. 51, (1980), 1176.

[6] H. C. Howe, J. Nucl. Mater. 93&94, 17 (1980).

Figure Captions

1. Schematic diagram of the detection system showing mirror M, Fabry Perot F. P. ; Lens L. ; Pinhole P. and photomultiplier detector PM. A discharge lamp L, containing a mixture of D_2 and H_2 was used intermittently for checking resolution and could be viewed via the half silvered mirror HSM. The filter F was used to reduce background signals.

2. Facsimile of trace showing intensity as a function of time in shot 28871 on a D_2 filling after extended operation on D_2 and before the changeover experiment was commenced. Shown also is the ramp voltage driving the Fabry Perot at 50m sec per sweep with a 10m sec flyback. Each peak is a scan of the Balmer alpha line of D. Peaks b_1 and b_2 occur in one sweep as do peaks c_1 and c_2. Peaks a and d occur at respectively the end and beginning of scans. Peak d occurs during MHD instability. During changeover the H signal shows up as an additional peak between the D peaks on each sweep.

3. The ratio, T, of D line intensity to the sum of H and D line intensities as a function of shot number. Fig. (a) is for operation with an H_2 filling gas after 38 discharges in D_2; the discharge designated n=0 is the last discharge in D_2 and is shot number 28874 of the ISX-B operating sequence. Fig. (b) is for operation with a D_2 filling gas after 28 discharges in H_2; the discharge designated n=0 is the last discharge in D_2 and is shot number 28903 of the ISX-B operating sequence.

4. The ratio T of D line intensity to the sum of H and D line intensities as a function of shot number for a change from H_2 to D_2 operation. The circles are the present data from Fig. 3b; the squares are for TFR [Fig 5, refc. 2] and the crosses for DITE [Fig. 4b, refc. 1].

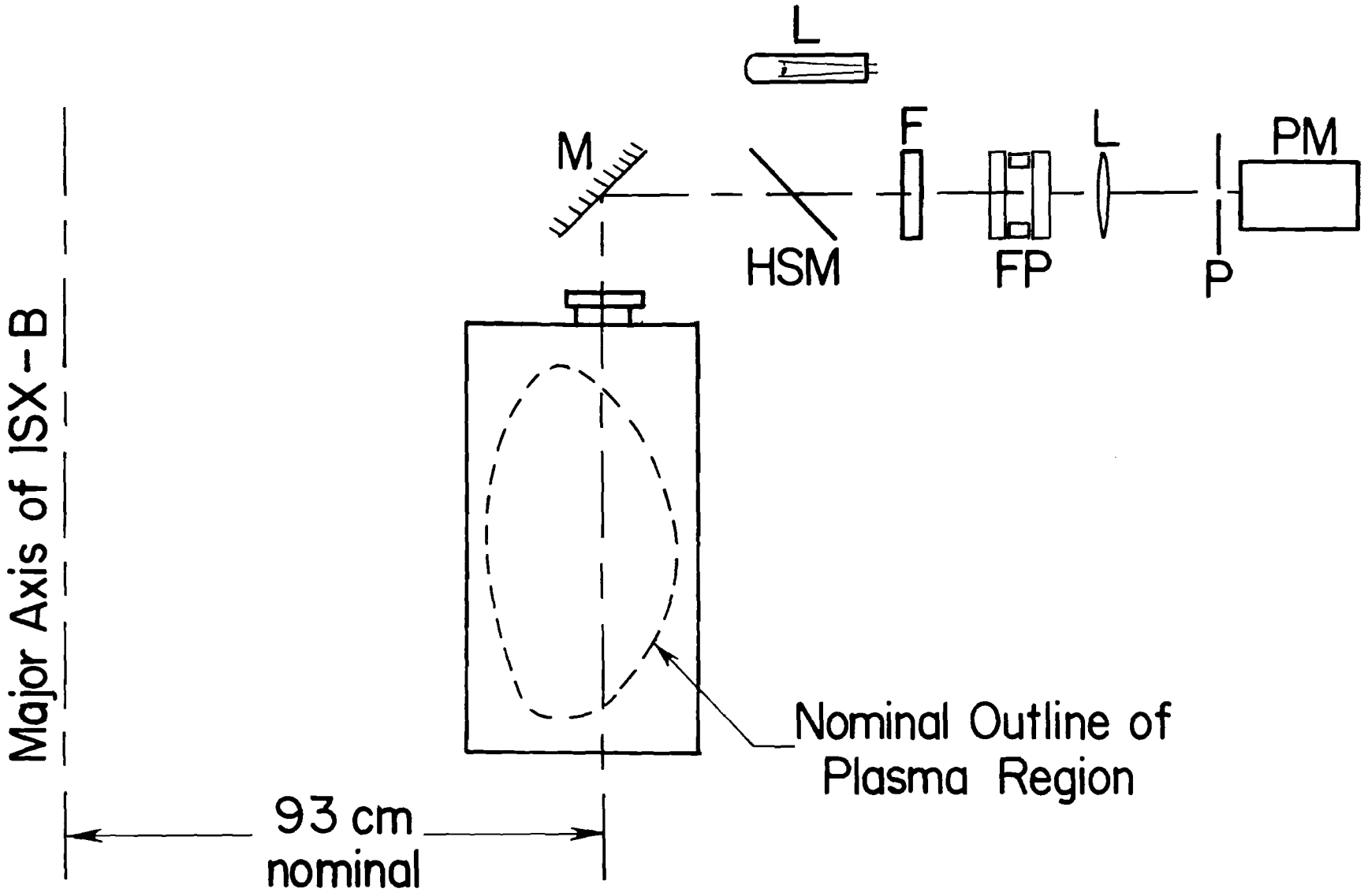
L
M
F
L
PM
HSM
FP
P
Major Axis of ISX-B
Nominal Outline of
Plasma Region
93 cm
nominal

Figure 1

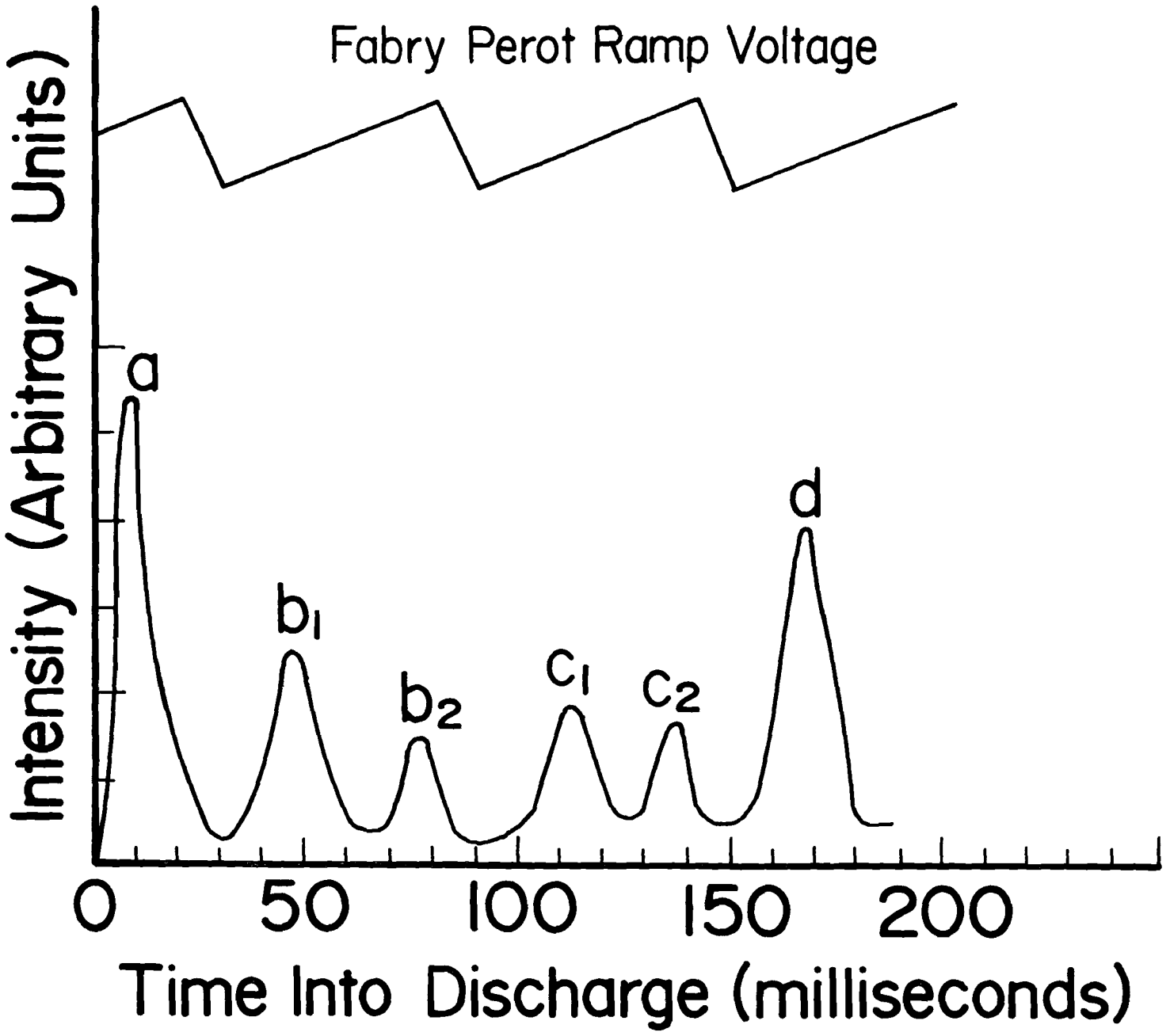
Fabry Perot Ramp Voltage
Intensity (Arbitrary Units)
a
b1
b2
c1
c2
d
0
50
100
150
200
Time Into Discharge (milliseconds)

Figure 2

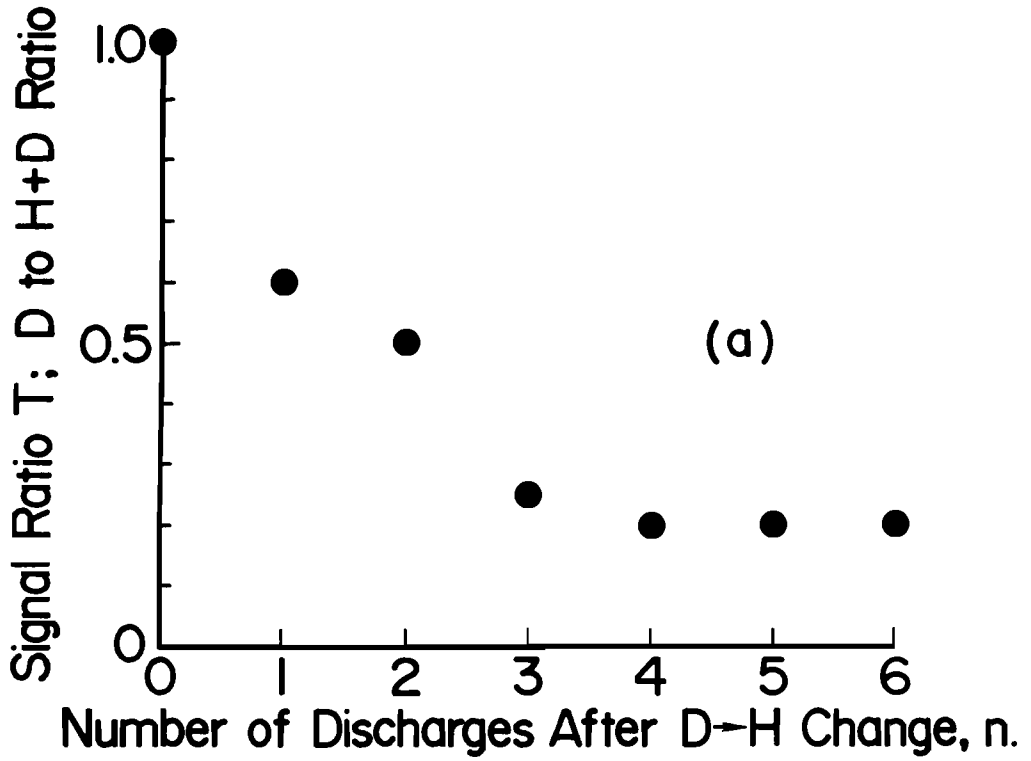
Signal Ratio T; D to H+D Ratio
1.0
0.5
0
(a)
0
1
2
3
4
5
6
Number of Discharges After D→H Change, n.

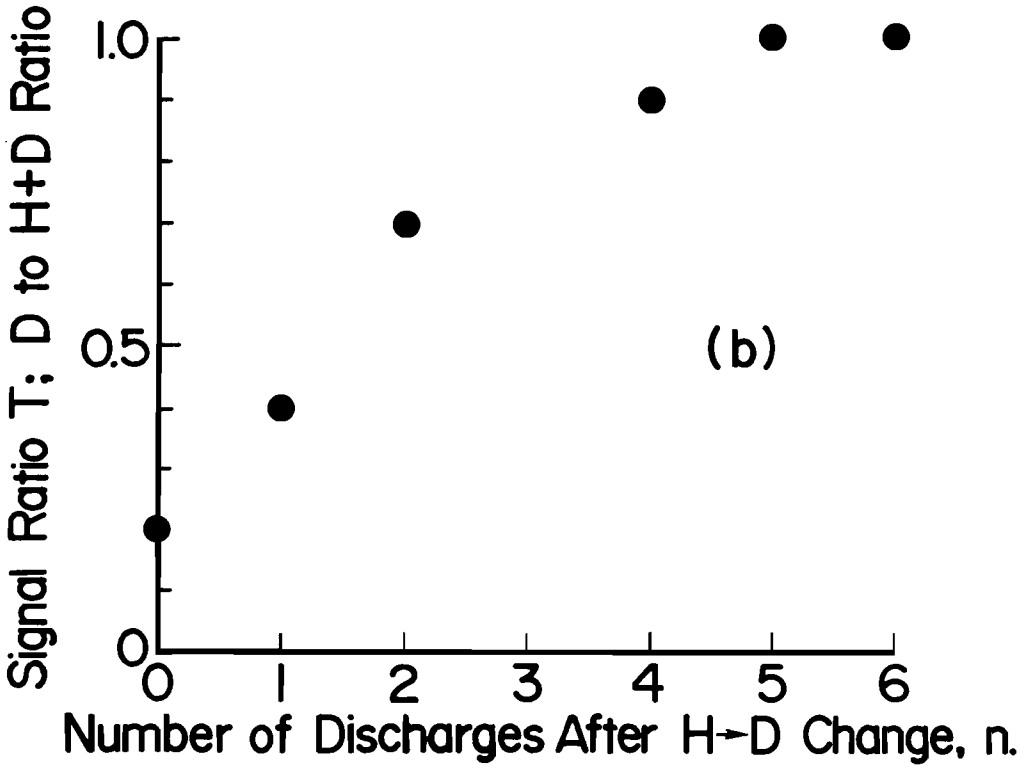
Signal Ratio T; D to H+D Ratio
1.0
0.5
0
(b)
0
1
2
3
4
5
6
Number of Discharges After H→D Change, n.

Figure 3

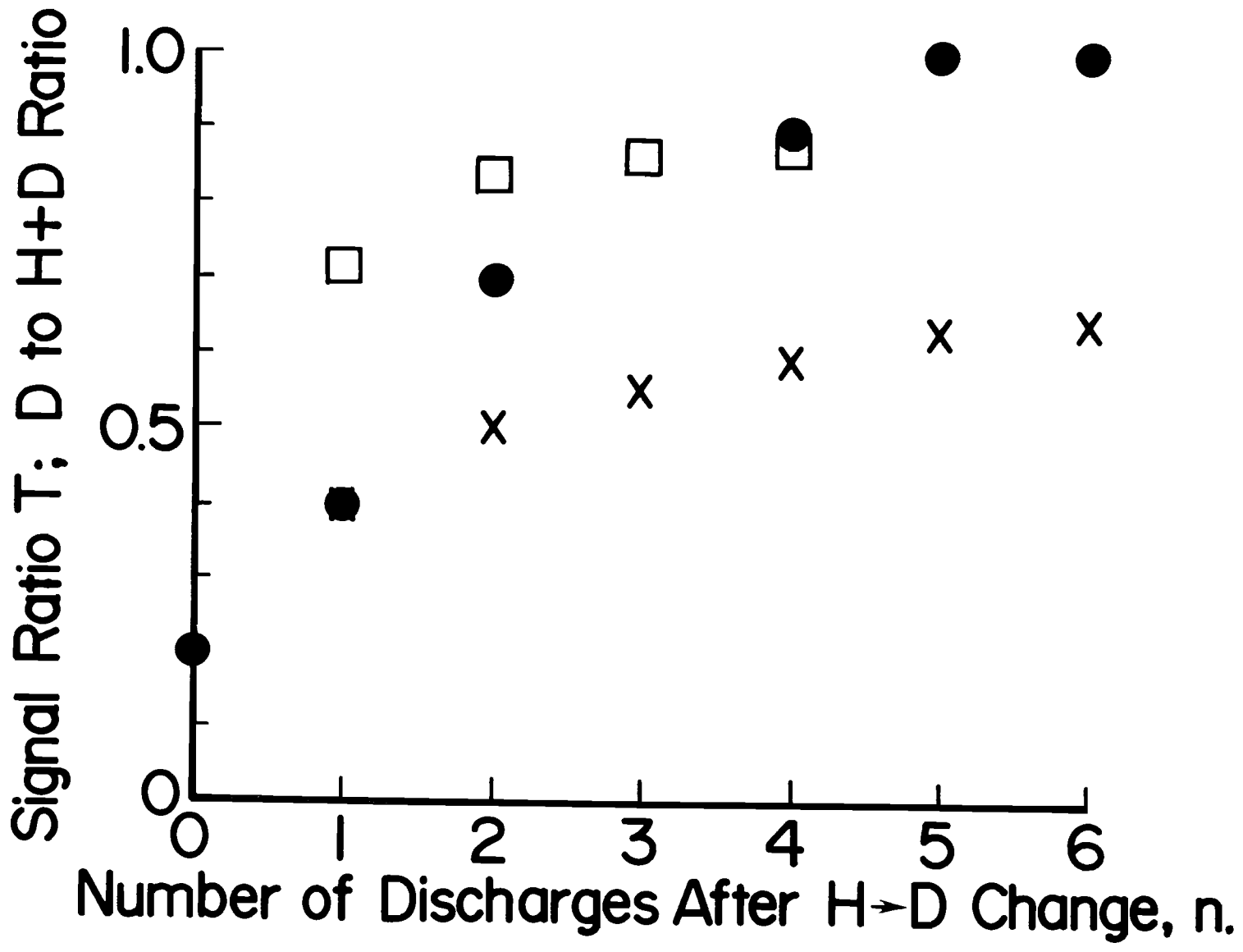
Signal Ratio T; D to H+D Ratio
1.0
0.5
0
0
1
2
3
4
5
6
Number of Discharges After H→D Change, n.

Figure 4

APPENDIX III

An Inelastic Mechanism for Ion Induced Desorption of Oxygen from Titanium and Iron

K. O. Legg, R. Whaley and E. W. Thomas

School of Physics

Georgia Institute of Technology

Atlanta, GA 30332

Abstract

Measurements are reported of the cross sections for desorption or sputtering of oxygen from polycrystalline Ti, and Fe by H^+, H_2^+ and H_3^+ in the energy range 20 keV to 200 keV. At low energies the desorption cross sections are a few times 10^{-18} cm^2 and are believed due to a conventional sputtering mechanism involving kinematic transfer of energy. At energies above 40 keV/proton for Fe and 80 keV/proton for Ti the cross sections for desorption by molecular ions show a sharp rise indicating onset of some new inelastic desorption mechanism. We propose that this mechanism is electron stimulated desorption initiated by electrons stripped from the projectiles and having the same speed as the projectile.

Introduction

Sputtering from solids has usually been modelled in terms of dynamical interactions between the incoming particle and the lattice or in terms of the creation of thermal spikes. Removal of atoms adsorbed on a surface should occur also by these same mechanisms. However removal of adsorbed species by electron impact (electron stimulated desorption or ESD) or by photon impact (photon stimulated desorption or PSD) cannot, at low energies, be due to a kinematic process and must instead be due to some sort of inelastic excitation mechanism. Typically ESD shows a sharp threshold energy indicating that a specific excitation process is involved in the desorption. The earliest picture of ESD formulated by Menzel and Gomer [1] and by Redhead [2] supposes that an incident electron excites a bonding (valence) electron into a non-bonding or antibonding state. The surface species is then assumed to be in a repulsive potential which causes it to be ejected. On this model ESD would exhibit a definite threshold related to the energy required to excite the bonding electron. While this picture may be adequate for a covalently bonded situation it does not explain desorption of ionically bonded species where several electrons must be removed before the adsorbate finds itself in a repulsive situation. Knotek and Feibelman [3,4,5] discuss ESD of ionically bonded species and it is useful to consider as an example their consideration of O^+ desorption from TiO_2. One would expect the oxygen to be bonded as O^{2-} so that three electrons must be removed to liberate O^+; this cannot occur by the Menzel, Gomer, Redhead [1,2] model. Knotek and Feibelman provide convincing evidence that ESD from TiO_2 occurs by the electrons creating a 3p hole in the Ti which cannot be filled by intra-atomic Auger transition because the titanium is in a Ti^{4+} configuration with no outer shell electrons; instead there is an inter atomic Auger transition involving removal of electrons from the O^{2-} leaving it

as O or O^+ and permitting desorption. Knotek and Feibelman also suggest that desorption can be initiated by inner shell excitation of the bonded species (e.g. the 2s shell of O) followed by intra-atomic Auger decay reducing the number of electrons associated with the oxygen and again placing it in a repulsive situation in the form O^o or O^+. They point out that for desorption from TiO_2 the energy involved in inner shell excitation of the oxygen is insufficient to give rise to desorption as O^+ but might cause desorption as neutral O. Clearly the position of the ESD threshold should show whether the inner shell excitation is of the substrate or of the adsorbate, and is a major factor in confirming the applicability of the mechanism.

The purpose of the present experiment is to explore whether ion induced desorption might also occur by an inelastic excitation mechanism. We study the total oxygen sputtering (or desorption) cross section as a function of ion energy between 20 and 200 keV for removing oxygen from titanium and iron by impact of H^+, H_2^+, and H_3^+. To enhance the possibility of detecting inelastic processes we use light ions (the three molecular ions of hydrogen) rather than heavy ions (e.g. Ar^+) where conventional sputtering by kinematic energy transfer might dominate.

Experiment

The experiment arrangement has been described previously in the context of other experiments [6] and will not be discussed in detail. The targets are placed in a u-h-v chamber where they can be bombarded by an ion beam from an accelerator, incident at an angle of 60^o from the surface normal. A conventional cylindrical mirror Auger spectrometer views the target at 95^o to the beam direction and is used to monitor the composition of the surface. The targets were electropolished polycrystalline high purity Ti and Fe cleaned prior to use by low energy argon ion bombardment. Typically the Auger spectrum

of the nominally clean target showed a C and O contamination level of less than 10% of a monolayer. About one monolayer of oxygen was adsorbed at room temperature and at a pressure of 10^{-6} Torr. The approximate coverage was determined by continuous Auger monitoring and comparing the O-KLL peak height with the data of Palmberg [7]. The oxygen was then pumped out and the target bombarded by a broad H^+, H_2^+, or H_3^+ beam centered about the Auger electron gun beam. The ion current density at the electron impact point was measured with a small aperture faraday cup. During sputtering, the O-KLL Auger signal was continuously monitored using 3 keV electron excitation. In order to check readsorption rates and to ensure that there was negligible electron beam desorption, the same experiment was run with no ion beam. It should be noted that, because only the oxygen remaining on the surface was measured, only the total desorption cross section was determined.

For sputtering with readsorption from the ambient the surface coverage at time t is given by the differential equation

$$\frac{dN}{dt} = - \frac{J}{e} \sigma N + \alpha P s(N^o - N) \qquad (1)$$

where N is the number density of adsorbed atoms (cm^{-2}) at time t and N^o is the number density for a monolayer coverage. J is current density and e electronic charge so J/e is the number of incident ions cm^{-2} sec^{-1}. The first term therefore represents collisional removal of adsorbed oxygen with a sputtering or desorption cross section σ. The second term represents replacement of oxygen from the ambient gas with s being average sticking coefficient, P the partial pressure of oxygen in the background gas and α being a constant of proportionality ($\alpha = 1/\sqrt{2\pi m\ kT}$ in ideal gas theory). The formulation assumes that there are $N^o - N$ adsorption sites vacant at any one time

and the sticking coefficient for these sites is s; for the N sites already occupied the sticking coefficient is zero and thus only one monolayer of oxide can be formed. Integrating, one arrives at the density as a function of time

$$N(t) = \left[N(0) - \frac{N^o \, \alpha Ps}{\frac{J}{e}\sigma + \alpha Ps} \right] \exp - \left(\frac{J}{e}\sigma + \alpha Ps \right) t + N^o \frac{\alpha Ps}{\frac{J}{e}\sigma + \alpha Ps} \qquad (2)$$

where N(0) is the coverage at time t = 0 when the oxygen atmosphere has been removed and bombardment by the ion beam is commenced. As $t \to \infty$

$$N(t) \to N(\infty) = N^o \frac{\alpha Ps}{\frac{J}{e}\sigma + \alpha Ps} \qquad (3)$$

We find that the O-KLL line shape does not change significantly during sputtering so we take the peak to peak height in the derivative spectrum as being proportional to adsorbate surface density N(t). Plotting $\ln[N(t) - N(\infty)]$ vs. t yields a straight line of slope $-\left(\frac{J}{e}\sigma + \alpha Ps \right)$. We determine αPs from the rate of rise of N(t) with time when the ion beam is removed, and with our measured value of J (typically about 30μ A cm^{-2}) we can evaluate the desorption cross section σ. With the relatively low sputtering rates involved in this work the equilibrium coverage N(∞) is attained at about half a monolayer so that the measured cross section is relevant only to the removal of the first one half monolayer. The inaccuracies in measuring N(∞) and in the experimental determination of current density J are the major factors contributing to the large scatter of the data points.

In Fig. 1 we show the cross sections for desorbing oxygen from Ti and Fe. For a projectile H_n^+ the measured desorption cross sections have been divided by n to give cross section per incident proton; the data are presented as a function of incident energy $\frac{\cdot}{\cdot}$ n, or energy per proton.

Discussion

The cross sections for removal of adsorbed oxygen by impact of H_2^+ and H_3^+ on iron (Fig. 1) show a remarkable increase of more than an order of magnitude in the energy range 40 to 50 keV/nucleon. This effect is peculiar to the impact of molecular ions as incident H^+ shows a very low and energy invariant cross section. Similar features are exhibited by the cross section for removing oxygen from titanium although here the increase is only a factor of four and occurs at the somewhat higher energy of 80 keV/nucleon. To the best of our knowledge there is only one previous direct measurement of oxygen removal by hydrogen ions, performed by ourselves [8], with an indirect optical technique. This previous work gives cross sections of about 1.6 to 3.5 x 10^{-18} cm^2/proton for removing 0 from Mo by 6.7 to 20 keV/proton H^+, H_2^+ and H_3^+; these figures are quite comparable with the present data at low energies.

Conventional sputtering theories involve consideration of kinematic energy transfer from the projectile to the target atoms either by direct projectile-target atom collisions or as the result of the collision cascade. Such calculations have been performed by Taglauer et al., [9] for removal of S from Ni by H^+ and give cross sections of 2 to 6 x 10^{-16} cm^2 (depending on the model used) at 2.0 keV decreasing towards higher impact energies. Sputtering of bulk metals by H^+ at energies below 10 keV has been studied extensively and fits a kinematic energy transfer model [10]. A typical sputtering coefficient (e.g., for Fe [10]) for 10 keV H^+ impact is 10^{-3} which implies a sputtering cross section of the order 10^{-18} cm^2 and is roughly comparable with the low energy data in Fig. 1. None of the sputtering models involving kinematic energy transfer are capable of predicting rapid cross section rises

such as those shown in Fig. 1.

We would argue that the low cross sections exhibited for sputtering by H^+ indicate that for this species one is observing only the effect of kinematic energy transfer. The cross section values are very similar to what one would expect from extrapolation of low energy sputtering data for homogeneous solids where kinematic energy transfer is certainly a satisfactory explanation of the ejection mechanism; the cross section exhibits the expected (slow) decrease with increasing energy. If this is accepted then the present data for H_2^+ and H_3^+ impact at lower energies (E < 40 keV/proton for Fe and E < 80 keV/proton for Ti) could be explained also as due to kinematic energy transfer.

The rapid cross section rises exhibited on Fig. 1 must indicate the onset of some other ejection mechanism. The rapidity of the onset would strongly imply an inelastic process with a definite threshold. For guidance in the explanation of the high cross sections we must turn to the allied fields of electron and photon stimulated desorption where removal of oxygen is related to inelastic excitation mechanisms.

Let us first examine the possibility that ionization of an inner shell electron by direct ion impact is the precursor to desorption. The threshold for ion-induced excitation of an inner shell will be at an ion energy equal to the required excitation energy. For excitation of L or M shell electrons from the adsorbate or substrate species in the present experiments the threshold should be below 1 keV and cannot explain the sharp rise seen here at 40 or 80 keV. Moreover, an H_2^+ molecular ion should act simply as two hydrogen atoms or ions and there would not be the extreme difference between H^+ and H_2^+ that we observe here. We must conclude that excitation of inner shells by the projectile is not the origin of the large desorption cross sections seen for H_2^+ although it might possibly represent a small underlying contribution at all energies.

Let us focus now on the difference between H^+ and H_2^+. When a projectile traverses a solid one finds at the exit point not only the heavy ion but also a considerable flux of electrons with a velocity distribution centered on the speed of the ion. In part these electrons arise from charge exchange to the continuum states of the projectile. For H_2^+ there is a second component [11] comprising electrons stripped from the projectile. A general discussion of mechanisms leading to the production of electrons with speeds close to that of the ion is provided by Meckback and Baragiola [11]. A very significant observation is that the flux of electrons for H_2^+ impact can be 17 times greater than for H^+ impact at the same speed [12] due to the efficient stripping mechanism. It is therefore clear that when H^+ and H_2^+ are incident on a solid there is in addition to the ion core also a flux of energetic electrons having a speed distribution peaked at the speed of the ion. If stripped projectile electrons are responsible for initiating desorption then one should expect desorption by H_2^+ impact to be far more efficient than by H^+ since there are more electrons associated with the molecule; this is, of course, in accord with the present data.

Let us now examine the desorption mechanism under the assumption that electrons are stripped from the projectile as it traverses the first monolayer and that these electrons moving with the same speed as the projectile cause electron stimulated desorption. One would hope to find that the rising cross sections, exhibited on Fig. 1, occurs at the same projectile velocity as one would expect electron stimulated desorption to exhibit a threshold. We shall consider the situation on the assumption that the oxygen is ionically bonded so that desorption should be in accordance with the Knotek and Feibelman model [3,4,5] which invokes inner shell ionization followed by Auger decay. The binding energy of the oxygen 2s electron in a solid is given as about 24 eV in the catalogue of Coghlan and Clausing [13] and observed by Knotek and Feibelman [4]

to lie at about 20 eV in a variety of ionic solids. Thus the threshold for ESD by excitation of the 2s oxygen shell would be 20 to 24 eV. Hydrogen projectiles of energy 44 to 63.5 keV/nucleon would carry with them electrons of energy 20 to 24 eV. In Fig. 1 the onset of the large cross section for removal of oxygen from Fe occurs at an H_2^+ ions energy of about 44 keV/nucleon. Thus, the onset of the large desorption cross section occurs at a projectile energy where the projectile electrons are energetically able to excite the 2s shell of oxygen on the surface. We should also examine the magnitude of the desorption cross section. If electrons stripped from the H_2^+ projectile are the principal contributors to desorption then we expect one electron to every two protons. If indeed the electrons are causing desorption, via inner shell ionization, then the data of Fig. 1 implies an electron ionization cross section for 2s electrons in bound O of about 2×10^{-16} cm^2. While large this is not necessarily unreasonable as the total cross section for ionization of isolated atomic oxygen is estimated to be 5×10^{-17} cm^2 at 20 eV [14]. It is not clear at this point why a threshold at 44 keV is not also observed for desorption of oxygen from Ti. One would also anticipate, at a somewhat higher energy, the onset of a second desorption mechanism when the convoy electrons are able to ionize the 3p electrons of the substrate nuclei leading to interatomic Auger events leaving the adsorbate in a repulsive state. For Fe the binding energy of the 3p electrons is 56 eV [13] which could be excited by stripped projectile electrons associated with 102 keV/nucleon H_2^+; this is outside our present energy range. For ESD of O^+ from bulk TiO_2 by excitation of 3p electrons in Ti, the threshold is found experimentally to be 34 eV [3,4] which in our model would require electrons associated with 62 keV/proton projectiles; this energy is somewhat below the point where the onset is observed. We would note, however, that the ESD data of Knotek and Feibelman for bulk TiO_2 actually exhibits not only a 34 eV threshold but also an equally large structure at about 44 eV that has the appearance of a threshold for a second mechanism. That apparent threshold at 44 eV would require electrons associated with 80 keV/nucleon projectiles which is about where we observe the increase in cross section.

In summary, if the stripped projectile electrons are responsible for inner shell excitation which, in turn, leads to desorption then the rise in desorption from Fe is completely consistent with excitation of the 2s electron in the oxygen and the rise in desorption from Ti is approximately where one expects excitation of the 3p level of titanium. There are, however, two problems with this explanation. On the one hand one would have expected O to desorb from Ti by excitation of the 2s level in oxygen leading to a threshold at about 44 keV, the same as for desorption from Fe. Secondly the threshold for desorption via excitation of the 3p level in Ti is expected to be at 62 keV/proton while we observe it slightly higher at 70 to 80 keV/proton. These two apparent discrepancies do not necessarily cast doubt on our proposal that electrons are responsible, they may simply indicate inadequacies in our understanding of the ESD process. We must point out that the ESD work that we have used for comparison is in fact for ejection of O^+ ions from the surface of bulk oxides (such as TiO_2) not the total removal of adsorbed oxygen from the surface of the bulk metal that we are studying here.

We have some direct evidence of differences between bonding in the bulk oxide and adsorbed oxygen situations. One may study the energy loss spectrum for electrons scattered from a surface with adsorbed oxygen; peaks in the loss spectrum should represent energies at which interband transitions and plasmon creation occur. For bulk TiO_2 Knotek and Feibelman [3,4] find a loss peak at 32 eV which they identify as due to excitation of the Ti 3p electron leading to the conclusion that ESD should have a threshold at 32 eV; this is in fact the impact energy at which O^+ ESD commences. In our own work with adsorbed oxygen on a Ti substrate the loss curve shows a strong peak at 44 eV which dissapears when oxygen is removed.

This peak has in fact been seen by others and explained as due either to excitation of a chemically shifted 3p electron of Ti [15] or excitation of a momentum conservation interband transition in the manner suggested by Viatskin [16]. Whatever the explanation, if indeed the peak represents excitation of a 3p electron in Ti one would expect an electron stimulated desorption threshold at 44 eV and a threshold for desorption by stripped projectile electrons at a hydrogen projectile energy of 80 keV/proton. In fact the ESD data for TiO_2 by Knotek and Feibelman show a significant structure at 44 eV electron energy and the present ion induced desorption of adsorbed oxygen from Ti shows its rise at about 80 keV/proton. A similar situation exists in photon stimulated desorption of O^+ from V_2O_5 [17] where the threshold is at the energy for exciting 3p electrons but there is a second very large structure at 50 eV; this second structure occurs at the same energy as a peak in the electron energy loss spectra of V_2O_3 [18] which is ascribed to a momentum conservation interband transition. Irrespective of whether the explanation of these energy loss peaks in correct it is clear that they are related to structure in ESD and PSD studies and that their relative importance may depend on whether the oxygen is present as an adsorbate or in the bulk oxide phase.

Conclusions

The cross sections for removal of adsorbed oxygen from Ti and Fe by impact of H^+, H_2^+, and H_3^+ are of the order 10^{-18} cm^2/proton for low energy (20-40 keV/proton) impact and the removal mechanism presumably involves kinematic energy transfer from the projectile to the target. As energy is increased the cross section exhibits a sharp rise (at 40 to 50 keV/proton for Fe and circa 80 keV/proton for Ti) for removal by molecular ions (H_2^+ and H_3^+) but no significant change for the monatomic species (H^+). The sharp rise cannot be explained on the basis of kinematic energy transfer mechanisms and must represent onset of desorption by an inelastic event.

We postulate that the new process is electron stimulated desorption initiated by electrons stripped from the projectile and having a speed distribution peaked sharply at the speed of the projectile. The flux of such electrons will be quite large for molecular ion impact where they arise primarily from stripping with a small contribution from charge transfer to the continuum; for the H^+ projectile they arise only from charge transfer and will be of a much lower flux. On this basis we identify the sharp increase of cross section for removal of adsorbed oxygen from iron as due to ionization of the 2s shell of O by stripped projectile electrons followed by Auger processes leaving it in a repulsive state. The enhanced removal of O from Ti is identified as due to ionization, by stripped projectile electrons, of the 3p shell in Ti followed by interatomic Auger transitions involving electrons from the oxygen leaving it in a repulsive configuration.

Acknowledgements

This work was supported in part by subcontract from the Oak Ridge National Laboratory, operated by Union Carbide for the Department of Energy under Contract No. W-7405-eng-26.

References

1. D. Menzel and R. Gomer, J. Chem. Phys. 41, (1964) 3311.

2. P. A. Redhead, Can. J. Phys. 42, (1964) 886.

3. P. J. Feibelman and M. L. Knotek, Phys. Rev. B 18, (1978) 6531.

4. M. L. Knotek and P. J. Feibelman, Phys. Rev. Letts. 40, (1978) 964.

5. M. L. Knotek and P. J. Feibelman, Surf. Sci. 90, (1979) 78.

6. W. A. Metz, K. O. Legg and E. W. Thomas, J. Appl. Phys. 51, (1980) 2888.

7. L. E. Davis et al., "Handbook of Auger Spectroscopy" 2nd. Ed., Physical Electronics Industries, Inc., Eden Prarie, Minnesota (1976).

8. E. O. Rausch, M. W. Murray, H. Inouye and E. W. Thomas, J. Appl. Phys. 48, (1977) 4347.

9. E. Taglauer, U. Beitat, G. Marin and W. Heiland, J. Nucl. Mater. 63, (1976) 193.

10. Experimental data for Fe and a useful bibliography of sputtering data is to be found in the paper of R. Behrisch, G. Maderlechner, B. M. U. Scherzer and M. T. Robinson, Appl. Phys. 18, (1979) 391.

11. W. Meckback and R. A. Baragiola, "Processes of Charge Exchange Into the Continuum of Ionic Projectiles Interacting with Gases and Solids", in "Inelastic Ion-Surface Collisions", (Ed. N. H. Tolk, J. C. Tully, W. Heiland and C. W. White), Academic Press, N.Y., 1976 .

12. M. M. Duncan and M. G. Menendez, Phys. Lett. 56A, (1976) 177.

13. W. A. Coghlan and R. E. Clausing, Atomic Data 5, (1973) 317.

14. E. J. McGuire, Phys. Rev. A 16, (1977) 73.

15. J. Frandon, B. Brousseau and F. Pradel, J. Physique 39 (1978) 839.

16. A. Ia. Viatskin, Zh. Tekh. Fiz. 28 (1958) 2217. [Sov. Phys.- Tech. Phys. 3, (1958) 2038].

17. J. F. Van der Veen, F. J. Himpsel, D. E. Eastman and P. Heimann, Sol. Stat. Comms. 36 (1980) 99.

18. F. J. Szalkowski, P. A. Bertrand and G. A. Somorjai, Phys. Rev. B 9 (1974) 3369.

Figure Caption

Figure 1. Cross sections for desorption of oxygen adsorbed on Ti and Fe. Circles are for the Fe substrate; open circles for H_2^+ impact; closed circles for H_3^+ impact; half filled circles for H^+ impact. The crosses are for H_2^+ impact on Ti. Data is shown as the cross section per proton as a function of energy per proton. The lines are meant only to guide the eye and do not represent measurements.

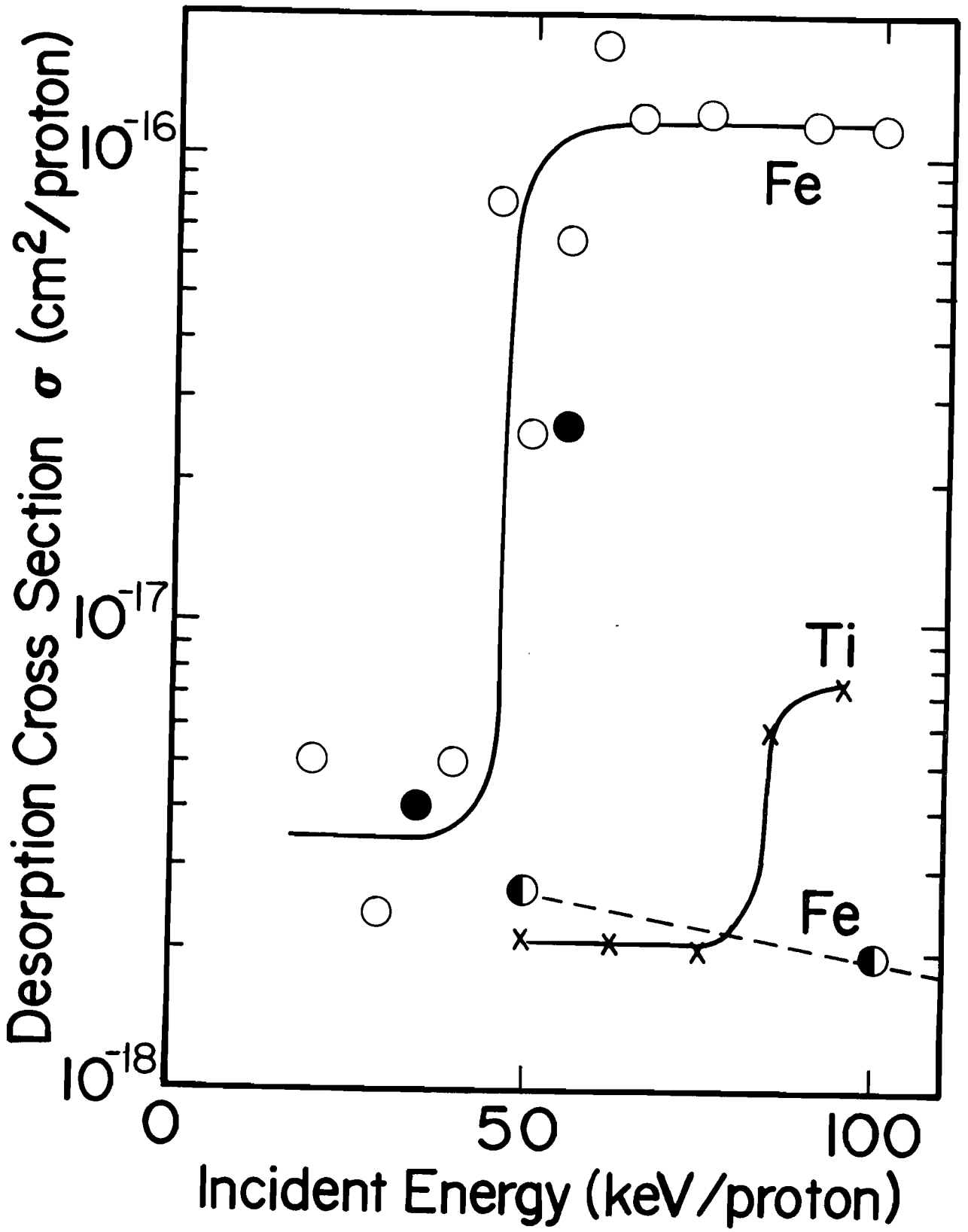
Desorption Cross Section σ (cm²/proton)
10⁻¹⁶
10⁻¹⁷
10⁻¹⁸
Fe
Ti
Fe
0
50
100
Incident Energy (keV/proton)

Figure 1

APPENDIX IV

SMALL ANGLE SCATTERING OF HYDROGEN FROM SURFACES*

E.W. THOMAS, R. YOUNG and J.E. HARRISS†
School of Physics, Georgia Tech, Atlanta, Georgia 30332, USA

Scattering of H^+ or H^- and H^0 as a result of H^+, and D^+ impact has been studied for targets of Be, C, Cu, Nb, Au, and stainless steel. Projectiles are incident at 69° from the surface normal and scattered particles are studied at near grazing emergence angles. Charge state distribution of the scattered particles is a function only of recoil energy and not impact energy nor of emergence direction. This indicates that the charge states are governed by bi-particle collision events rather than interactions with band structure of the surface. Comparison with previous experiments shows that as the incidence angle increases the average recoil energy gets larger. As an indication of absolute magnitudes we find that for 15 keV H^+ incident on Au at 69° from the surface normal, there are 0.081 protons, and 0.0072 H^-, and 0.263 neutral hydrogen atoms scattered per incident proton and per steradian at an angle of 9.4° from the surface.

1. Introduction

A knowledge of how hydrogen scatters from a surface is important in the modelling of hydrogen recycling from the first wall and from the limiter. Extensive measurements of reflection from polycrystalline metals have been performed by the Garching group [1–6] using 1–15 keV projectiles incident at between 0 and 45° from the surface normal; scattering at 135° from the initial direction is recorded. This geometry represents a large angle scattering event. The published information on small angle scattering seems to be limited to the work by Morita et al. [7]. Monte-Carlo type computer simulations by the MARLOWE [8, 9] and TRIM [10] codes are consistent with experimental measurements of total backscattering, and scattering through large angles. Hydrogen impacts on the first wall of a fusion device with a wide range of incidence angle. The peak flux of charge exchange neutrals is estimated to be at 50° from the wall normal [11]; impact of ions on the limiter may be at even larger angles. There is a need to provide additional studies of scattering where the angle of deviation is small and the trajectories of both incident and emergent particles make small angles with respect to the surface.

* Supported in part by the Magnetic Fusion Energy Program of the Department of Energy.

† Present address: Rockwell International, Newport Beach, CA 92660, USA.

The present experiments involve H^+ and D^+ projectiles incident in the energy range 1–15 keV at an angle of 69° from the surface normal. Scattered particles are observed at angles from 90 to 65° from the surface normal representing deviations of 21–46° from the incident direction. Targets were mechanically polished high purity polycrystalline Be, C, Cu, Nb, and Au as well as a specimen of commercial type 302 stainless steel. In view of space limitations we shall present only representative data here; a more complete report is in preparation [12].

The experimental arrangement is a modification of equipment used earlier to study scattering of hydrogen in gases [13, 14]. An ion beam from an rf source is mass-analyzed, collimated, and directed onto the target; current density was about 1 $\mu A/cm^2$. A pair of collimating apertures selects particles scattered at some angle θ with respect to the incident trajectory; the solid angle of the collector system was 1.75×10^{-4} sr. The total flux of scattered ions (integrated over all recoil energies) was recorded as a current on a Faraday cup. The total flux of scattered neutral atoms was recorded by the secondary electron emission from the base of a Faraday cup in the manner of Fitzwilson and Thomas [14]. Energy spectra of scattered H^+ and H^- were determined by electrostatic analysis with detection by a channel electron multiplier operated in a pulse-counting mode. The spectra were assigned an absolute magnitude by nor-

Journal of Nuclear Materials 93 & 94 (1980) 524–528 © *North-Holland Publishing Company*

malizing to the total scattered ion flux determined by the current measurements. Placement of the detection systems on an arm pivoted about the point of beam impact permitted measurements to be repeated at various scattering angles θ.

The vacuum environment was provided by sorbent trapped diffusion pumps supplemented by titanium sublimation. Base pressure was around 10^{-9} Torr. Targets were subjected to a preliminary bombardment with 3.5 keV Ne^+ to clean the surface. The energy spectrum of the scattered Ne^+ showed peaks corresponding to scattering from the various atomic masses of the surface and its contaminants; this spectrum permitted a qualitative evaluation of surface cleanliness and showed impurity concentration of C and O to be less than 5% of a monolayer.

Most of the data presented here represents a variation of scattered flux with recoil energy or recoil direction. The relative magnitudes of different data points are quite accurate and are reliable to ±5% or better. However, the absolute magnitudes assigned to different data sets involve various absolute calibration steps and are less reliable. We estimate that the absolute magnitudes assigned to scattered ions (H^+ and H^-) are accurate to only ±20%. The absolute magnitude assigned to the total scattered flux (H^+, H^0, and H^- integrated over all recoil energies) is accurate only to ±50%; the major limitation is the assessment of detection sensitivity for recoil H^0, which is the predominant species in the recoil flux.

2. Energy distribution of recoil ions

Fig. 1 shows the energy distribution of scattered H^+ for impact of protons of various energies on a gold target; the projectiles are scattered through an angle of 30.4°. For all impact energies the peak flux of the particles occurs at 80% or more of the impact energy. By contrast in the previous work of Verbeek et al. [1-6] involving scattering through 135° the peak flux is at 40% or less of the impact energy. Thus, as one moves towards near grazing angles of incidence and

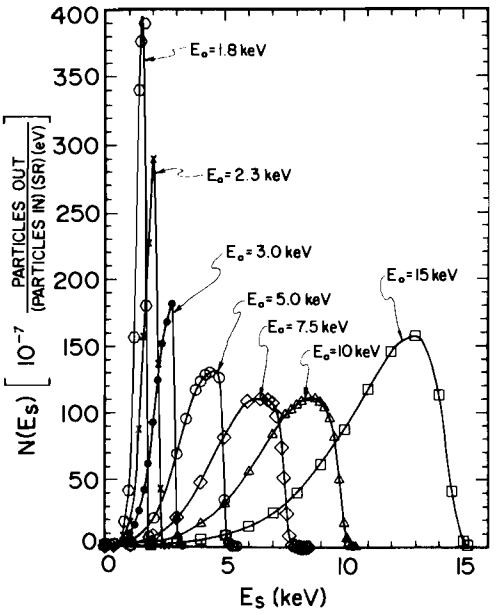

Fig. 1. Energy distributions of recoil H^+ incident on Au at 69° from the surface normal; scattering angle is 30.4°.

emergence the average energy loss in scattering decreases.

The data of fig. 1 give the energy spectra of H^+ only; recoil H^- have also been recorded but are not shown here. It is well known that the majority of the scattered particles are in fact neutral particles so that the data shown here represent only a small fraction of the backscattered flux of particles. In order to provide a rough estimate of the energy spectrum of all scattered particles together we have taken our spectra of scattered H^+ and divided the scattering coefficient by the fraction of particles in the positive charge state as measured by Behrisch et al. [15]. This procedure would seem to be justified since the charge state distribution of the scattered particles is a function only of recoil energy and is not dependent on recoil direction or impact energy (see the work of Behrisch et al. [15] and our own results in the following section). Such an estimate of the energy spectrum for all scattered particles together for the case of H^+ impact on Cu is shown in fig. 2. Included there is a prediction of the recoil energy spectrum performed by Haggmark [16] using the

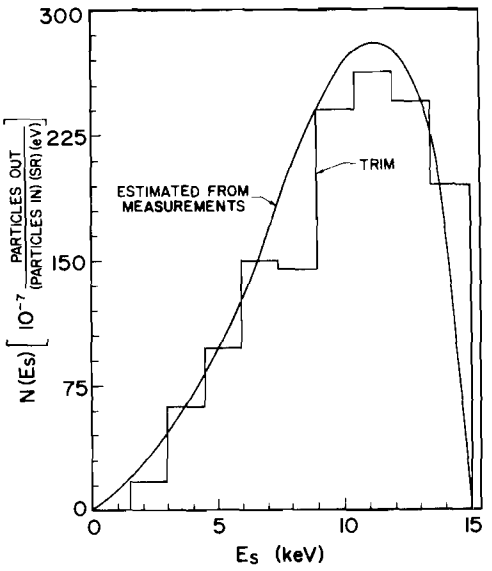

Fig. 2. Estimated recoil flux of all species (H^+, H^0, and H^-) for the case of 15 keV H^+ on Cu incident at 69° from the surface normal; scattering angle θ is 30.4°. The experimental estimate is achieved from a measured H^+ recoil spectrum divided by the charge state fraction as measured by Behrisch et al. [15]. The histogram is a computer simulation by Haggmark [16] using the TRIM code.

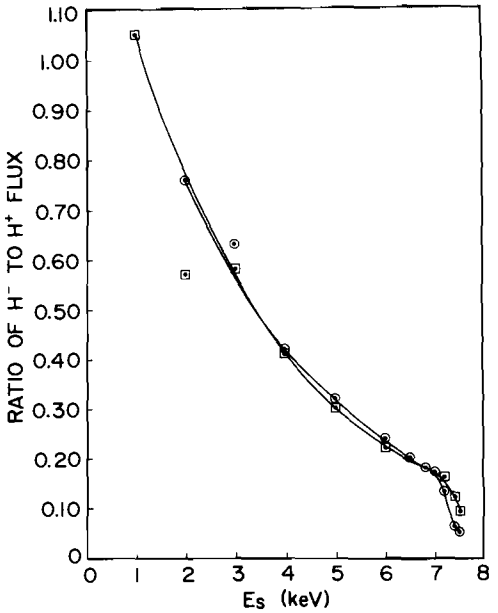

Fig. 3. Ratio of H^- flux to H^+ as a function of recoil energy for impact of 7.5 keV H^+ on gold. Square data points represent scattering through 30.4° (or 9.4° from the surface). Circular data points represent scattering at 24.4° (or 3.4° from the surface).

TRIM code. Agreement is excellent providing confirmation of the code for small angle scattering at near grazing angles of incidence and emergence.

3. Charge state fractions

The incident projectile is an ion while most of the scattered particles are neutral and a small fraction are H^-. It is generally argued [17] that screening by the electrons in the solid precludes the formation of bound states of the projectile while it is still in the solid. H^0 and H^- formation should then occur as the projectile leaves the surface. It is not clear what mechanism is involved in the transfer of charge to the projectile. One class of possible mechanisms involves the interaction of the emerging recoil with the free electrons in the extended potential well formed by the solid. Neutralization might occur by an Auger [18] process. For any such mechanism involving penetration of the potential barrier between target and recoil the probability of transfer will be related to the projectile's interaction time with the surface; the probability will therefore by a function of recoil velocity component normal to the surface. A second type of mechanism would be a conventional charge transfer event in a bi-particle collision between the emergent projectile and a surface atom. In this case the probability of H^0 and H^- formation would be related to the energy of collision which will be essentially the same as the emergent particle's energy. In fig. 3 we show the ratio of H^- to H^+ fluxes as a function of recoil energy for two different recoil directions. The data are essentially the same, suggesting that the electron pick-up is related to the recoil energy and not to the recoil velocity component normal to the surface. We conclude that the electron transfer event occurs in a bi-particle collision at the surface; this conclusion is consistent with other recent studies of neutralization on scattering of hydrogen and helium from surfaces [19, 20].

4. Angular distribution of total flux

The total scattered flux (H^+, H^0, and H^-) integrated over all recoil energies has been measured as a function of recoil angle. Fig. 4 shows that data for a variety of targets bombarded by 15 keV H^+ at 69° from the surface normal. Scattered flux parallel to the surface (a scattering angle of 21° in fig. 4) is zero and flux rises rapidly to peak at between 29° (for Be) and 36° (for Nb). The angle for specular scattering is 42°. Thus, the recoil flux peaks closer to the surface than the specular reflection angle. Beyond the peak, the scattered flux falls off slowly with scattering angle. Also shown in fig. 4 is the result of a computer simulation using the TRIM code for the case of copper. The simulation has been reduced by 20% to normalize it to the data at 35°. The absolute accuracy of these data is only 50%, thus a 20% difference between the TRIM code and experiment is not significant. In general the computation and experiment are in fair agreement although there are small systematic differences between the form of the angular variation.

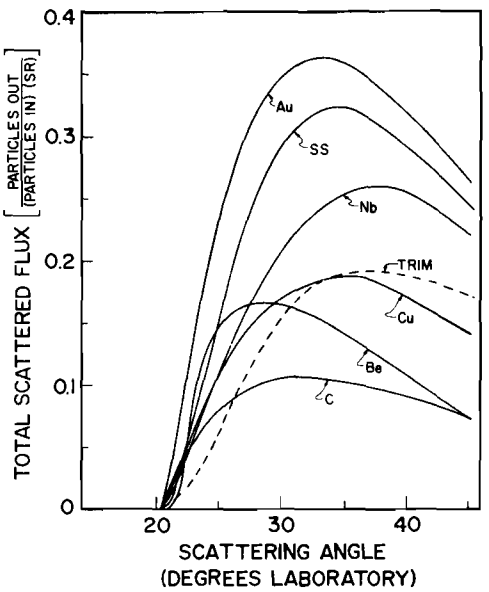

Fig. 4. Angular distributions of total recoil flux (H^+, H^0, and H^- together) for 15 keV H^+ incident at 69° from the surface normal; targets are Be, C, Cu, Nb, Au and stainless steel (type 302) as indicated. Also shown is a result for a copper target from the TRIM computer simulations [16]; it is normalized to experiment at 35°.

5. Scattering with incident D^+

A limited study was also performed of backscattering induced by D^+ impact. The energy distribution of scattered D^+ cannot be scaled to those for H^+ impact simply by placing them on the same velocity scale or on the same energy scale. An adequate scaling was achieved by the following procedure. It was first assumed that the flux of all scattered particles (positive negative and neutral particles together) for D^+ impact had the same energy distribution as for equal energy H^+ impact; there is ample evidence that total backscattering for D^+ and H^+ impact at equal energies are approximately the same [9]. We further assume that the partition of scattered particles among the different charge states is the same for scattered H^+ and D^+ of equal velocity. On this basis the two data sets can be scaled together.

References

[1] P. Meischner and H. Verbeek, J. Nucl. Mater. 53 (1974) 276.
[2] H. Verbeek, J. Appl. Phys. 46 (1975) 2987.
[3] W. Eckstein, H. Verbeek and S. Datz, Appl. Phys. Letters 27 (1975) 527.
[4] H. Verbeek, W. Eckstein and S. Datz, J. Appl. Phys. 47 (1976) 1785.
[5] W. Eckstein, F.E.P. Matsche and H. Verbeek, J. Nucl. Mater. 63 (1976) 199.
[6] H. Verbeek, W. Eckstein and R.S. Battacharya, J. Appl. Phys. 51 (1980) 1783.
[7] K. Morita, H. Akimune and T. Suita, Jap. J. Appl. Phys. 7 (1968) 916.
[8] M.T. Robinson and I.M. Thorens, Phys. Rev. B9 (1974) 5008.
[9] O.S. Oen and M.T. Robinson, Nucl. Instrum. Methods 132 (1976) 647.
[10] W.E. Eckstein, H. Verbeek and J.P. Biersack, J. Appl. Phys. 51 (1980) 1194.
[11] S.A. Cohen, Princeton University Plasma Physics Laboratory, MATT-1171 (1975).
[12] J.E. Harriss, R. Young and E.W. Thomas, J. Appl. Phys., to be published.

[13] R.L. Fitzwilson and E.W. Thomas, Phys. Rev. 3 (1971) 1305; Phys. Rev. A6 (1972) 1054.
[14] R.L. Fitzwilson and E.W. Thomas, Rev. Sci. Instrum. 42 (1971) 1864.
[15] R. Behrisch, W. Eckstein, P. Meischner, B.M.V. Scherzer and H. Verbeek, Atomic Collisions in Solids, Vol. I, Eds. S. Datz, B.R. Appleton and C.D. Moak, (Plenum, New York, 1973) p. 315.
[16] L.G. Haggmark, private communication. Performed using the TRIM Code of ref. [10].
[17] W. Brandt and R. Sizmann, Phys. Lett. 37A (1971) 115.
[18] H.D. Hagstrum, Phys. Rev. 96 (1954) 336.
[19] K. Kimura, A. Kyoshima, A. Itoh and M. Mannami, Radiation Effects 41 (1979) 91.
[20] N.H. Tolk, J.C. Tully, J. Krauss, C.W. White and S.H. Neff, Phys. Rev. Letters 36 (1976) 747.

Appendix V

Reflection, Re-emission and Permeation of Deuterium in Metals

When a metal foil is bombarded with a deuterium ion beam a certain fraction of the beam is reflected and the remainder slows down to near thermal energies in the solid representing an ion implanted component. These implanted atoms may suffer one of three fates. They may be permanently retained on a trapping site. They may return to the bombarded surface by a diffusion process, recombine to form D_2 molecules, and emerge into space or they may diffuse to the rear surface of the sample, recombine to form D_2 and emerge into space. The particles reflected and re-emitted from the front and back surfaces may in principle be detected by the rise of D_2 pressure in the surrounding vacuum chamber. The trapped deuterium may be studied by elevating the target temperature to cause desorption and monitoring the pressure rise in the surrounding chamber as a function of target temperature. The objective of the experiment is to study reflection, retention, re-emission from the front surface and permeation followed by re-emission from the back surface. The general experimental procedures are well established and have been used previously by one of us (EWT, refc. 1) in the study of re-emission and reflection from stainless steel. The significant and unusual aspect of the present work is the study of re-emission from the back (unbombarded) surface of the sample. There is some evidence that the mechanisms for re-emission from front and back surfaces are not the same. This suggests that either diffusion or recombination is in some way affected by the damage caused on the front

1. E. W. Thomas, J. Appl. Phys. 51, 1176 (1980).

surface (but not on the back) during implantation. In addition we are planning to perform new experiments on re-emission and reflection from the front surface to increase the available data base in these areas. The present status of the experiment is that the equipment fabrication has been recently completed and preliminary results have been obtained.

Experimental Arrangement

The recently constructed equipment is shown in the figure. The system consists of an enclosed chamber within a vacuum chamber and a partial pressure analyzer for detecting pressure rises of selected mass species. The inner chamber is electrically isolated from the outer chamber by means of insulators and a ceramic break. The target holder is attached to an XYZ manipulator by a stainless steel tube. By means of this manipulator the target holder can be put in contact with either of the bellows inside the inner chamber. When the target holder is against the bellows on the right in the figure, any pressure rise due to the ion beam is associated with processes occuring on the front surface while molecules associated with processes on the back surface are pumped through the small hole in the inner chamber wall and down to the ion pump. When the target is against the bellows on the left, the opposite is true. A beam cup is used to define the ion beam prior to entering the inner chamber. In addition, the target can be cooled to near liquid nitrogen temperatures or ohmically heated to around 400^{o}C. A typical experiment to study the pressure rise, say from the front surface using an energetic D^{+} ion beam, would proceed as follows:

a) the partial pressure analyzer is tuned to monitor the mass 4 (D_2) pressure,

b) the target is heated above 250^{o}C to drive out any trapped D,

c) the target is then brought to the desired temperature for the experiment and placed against the right bellows,

d) the ion beam is then allowed to strike the sample and a pressure rise is recorded as a function of time on a chart recorder,

e) several minutes after saturation of the target the ion beam is removed from the sample and the decay of the pressure signal is recorded until a steady state is obtained.

Preliminary Results

Reflection coefficients determined from preliminary data show excellent agreement with published results when the target was first heated to drive out any D and poor agreement when this procedure was not followed. For example, a 5 keV D^+ ion beam striking a stainless steel foil which was previously treated to remove the trapped D yielded a reflection coefficient of 0.17 compared with the value 0.12 by Thomas.[1] On the other hand, a 20 keV D^+ ion beam striking this surface when it has previously been bombarded and not had the D driven out gives a reflection coefficient of 0.13 compared to 0.04 by Thomas.[1]

It is also possible to monitor the amount of deuterium retained (or trapped) as the difference between the fluence incident and the deuterium emitted or reflected. For 5 keV D^+ impact the retained fluence of deuterium in a room temperature target is estimated to be 7.8×10^{15} D/cm^2. This is some two orders of magnitude lower than the fluence retained in a target at liquid nitrogen temperature. No previous measurements are available for comparison but this retained fluence representing one retained D atom for every metal atom in the projectile range certainly exceeds the solubility expected for hydrogen in steel.

The pressure signal from the back side of the sample is about an order

of magnitude smaller than from the front side. This cannot be explained simply by the different distances the atoms must diffuse to get to the surface. For 20 keV D^+ impinging on stainless steel (actually Fe) the range is about 1400 Å or 1.4×10^{-7} m. The target is .025 mm or 2.5×10^{-5} m thick so that the atoms must diffuse a distance two orders of magnitude greater to get to the back surface as that required to get to the front surface. The diffusion to the back surface is certainly being driven by the radiation, but it would appear that other factors must also be contributing to enhance diffusion to the back surface.

Conclusion

These very preliminary results are in general agreement with previous work and indicate that the equipment is operating satisfactorily.

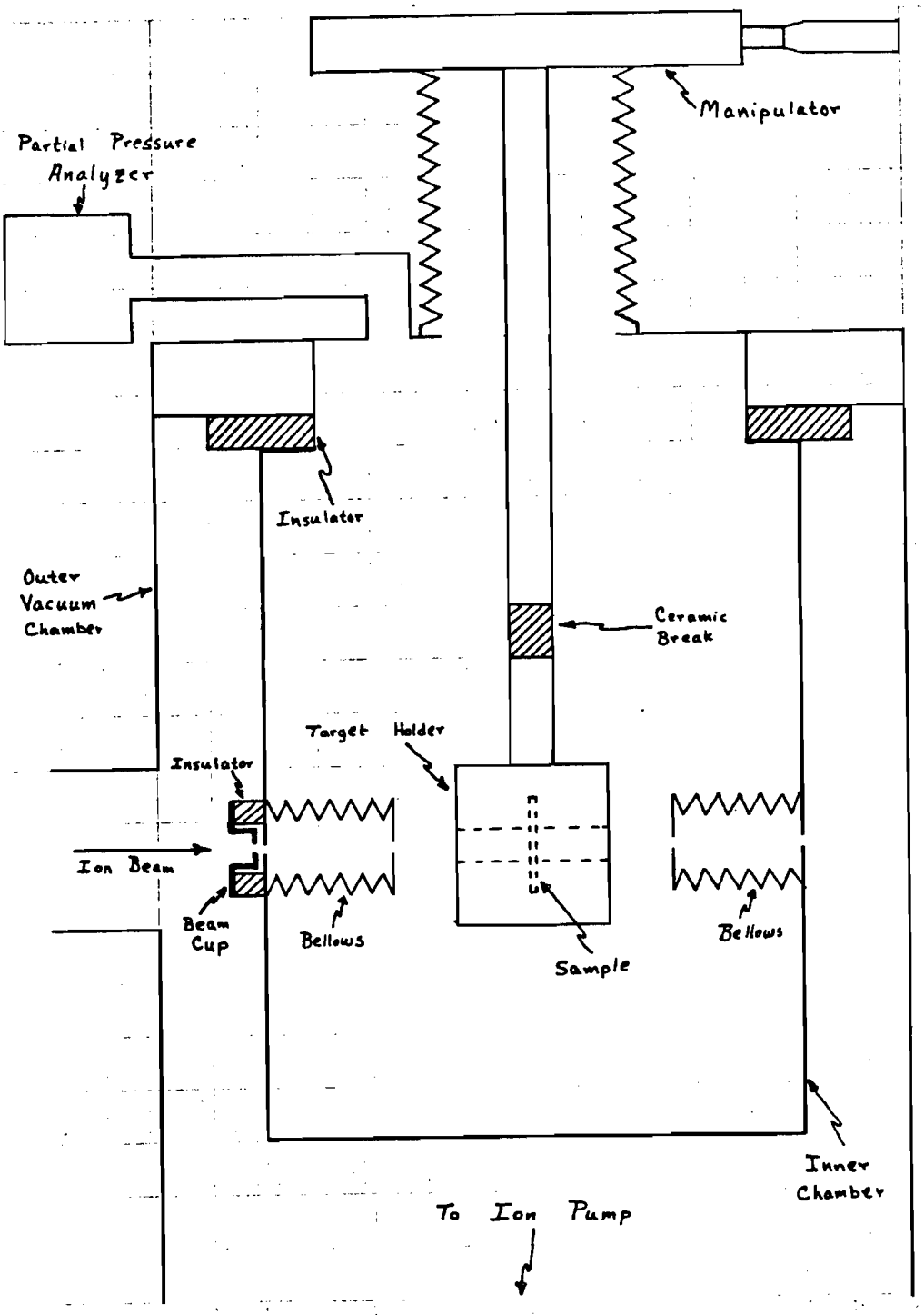
Manipulator
Partial Pressure Analyzer
Insulator
Outer Vacuum Chamber
Ceramic Break
Target Holder
Insulator
Ion Beam
Beam Cup
Bellows
Sample
Bellows
Inner Chamber
To Ion Pump

Appendix VI

Time Resolved Probe for Detecting Contaminants in the Plasma Edge

A well established technique for detecting contaminants in the plasma edge is to expose a spinning wheel or disc to the plasma edge and collect a streak of deposited material which may be subsequently analyzed to give an indication of the flux and composition of materials in the plasma edge. We are fabricating such a system for ISX-B.

Surface analytical diagnostic samples are introduced to the plasma on a carriage which runs down an evacuated tube linking the Tokamak to a surface analysis chamber. The carriage consists of two parts: one which runs down the track and stops outside the first wall, where electrical and mechanical connections can be made, and the other, which moves forward along the first, carrying experiments into the plasma region.

We have developed and built a time-resolved analyzer for this carriage. This consists of a drum which rotates behind a slit and can be placed near the plasma edge. Since the rotation is timed to the beginning of the Tokamak shot material deposited from the plasma onto the drum will form a streak around its circumference. After one or several shots the drum will be withdrawn into the surface analysis chamber, where the streak will be analyzed by Auger spectroscopy. This will allow measurements of the time dependence of plasma contaminants such as Fe, Ti and C.

The detailed construction of this analyzer is illustrated in Fig. 1, which shows the analyzer before assembly to the carriage. The right-angle gear assembly is attached to the fixed part of the carriage so that it is engaged by the drive shaft at the same time as the electrical connections are

made. This drive shaft is attached by a pin-and-slot drive to a rotary feedthrough driven by a stepping motor outside the vacuum chamber. The sample is mounted on a bracket slung from the movable part of the carriage and is driven by a series of shafts with a pin-and slot drive to transfer the rotation while allowing linear motion of the sample with respect to the gears. Samples may be changed in vacuo at the surface analysis station using an existing manipulator which picks them up and places them on a UHV manipulator for Auger studies and cleaning. A screwdriver coupling and shaft location detente allow the samples to be taken on and off the bracket, while an electrical connection (not shown here) allows ion current measurements to be made during rotation. Samples up to 3" in diameter and 1 1/2" long can be accomodated.

This system will be used to monitor plasma impurities, with special attention being paid to the clean-up period at the beginning of operation following the next scheduled shutdown. The samples will be run behind two slits, one very close to the probe surface for accurate time-resolved measurements, the other about 4 mm away for measurements of ion velocities using the spread in the line derived from ions spiralling about the magnetic field lines (Thomas et al.[1]). Erosion rates will also be studied by depositing a thin film on the probe and sputter profiling through it or using Rutherford backscattering to measure its thickness after exposure.

---

1. E. W. Thomas, J. Partridge, and J. Vince, J. Nucl. Materials 89 182 (1980).

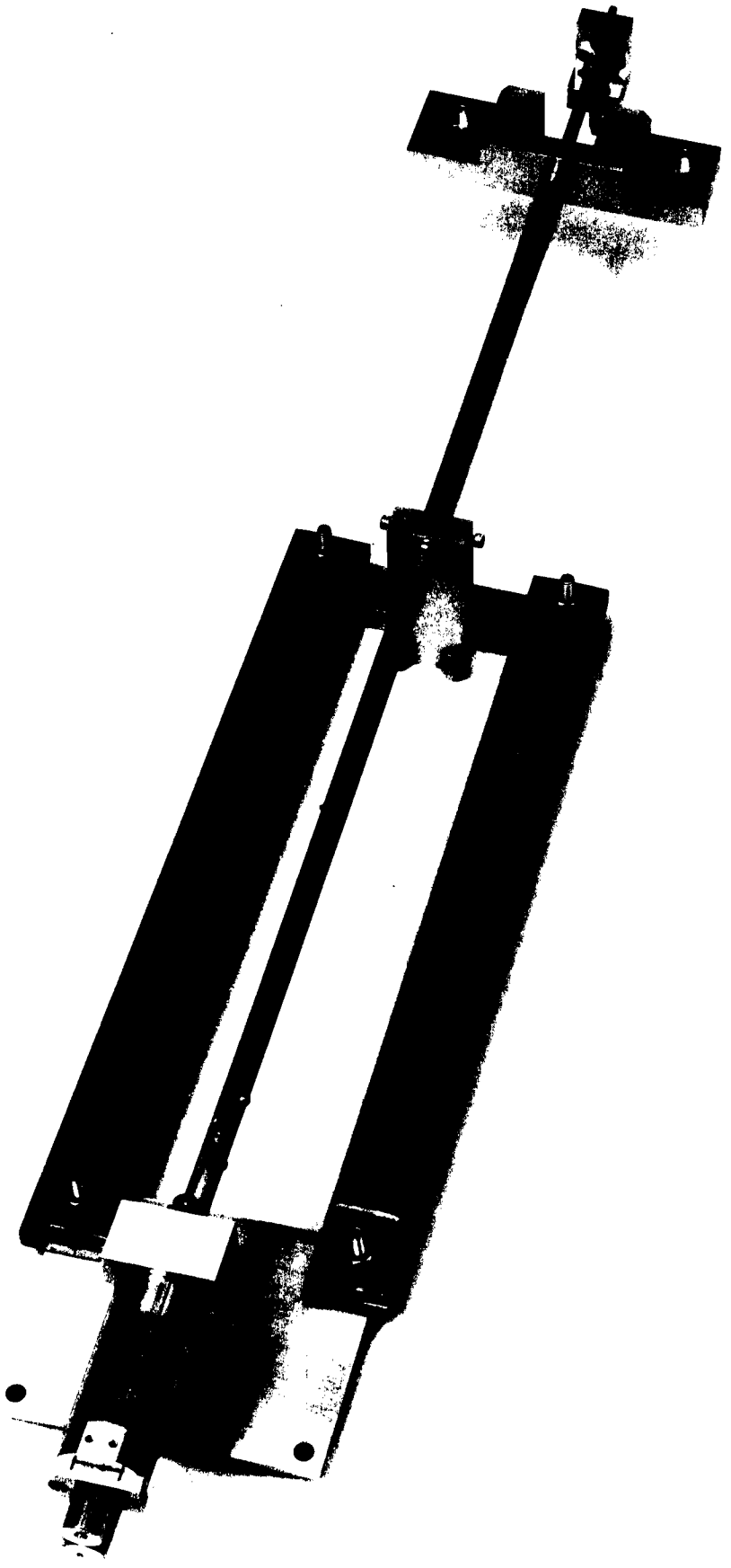

AVI-3